INTEGRATION OF PLUG-IN HYBRID ELECTRIC VEHICLE WITH THE GRID USING VEHICLE-TO-HOME AND HOME-TO-VEHICLE CAPABILITIES

Florence Berthold

A Thesis

in

The Department

of

Electrical & Computer Engineering

and

Energy Environment

Presented in Partial Fulfilment of the Requirements

For the Degree of

Doctor of Philosophy (Electrical and Computer Engineering) at

Concordia University

Montréal, Québec, Canada

And

University of Technology of Belfort-Montbéliard

September 2014

CONCORDIA UNIVERSITY
SCHOOL OF GRADUATE STUDIES

This is to certify that the thesis prepared

By: Florence Berthold

Entitled: Integration of Plug-In Hybrid Electric Vehicle with the Grid Using Vehicle-to-Home and Home-to-Vehicle Capabilities

and submitted in partial fulfillment of the requirements for the degree of

Doctor of Philosophy (Electrical and Computer Engineering)

complies with the regulations of the University and meets the accepted standards with respect to originality and quality.

Signed by the final examining committee:

_____ Chair
Dr. C. Schaeffer

_____
Dr. M. El Hachemi Benbouzid

_____ External to Program
Dr. A. Athienitis

_____ Examiner
Dr. S. Hashtrudi Zad

_____ Examiner
Dr. P. Pillay

_____ Thesis Co-Supervisor
Dr. S. Williamson

_____ Thesis Co-Supervisor
Dr. D. Bouquain

_____ Thesis Co-Supervisor
Dr. A. Miraoui

Approved by: _____
Dr. A.R. Sebak , Graduate Program Director

September 26, 2014 _____
Dr. A. Asif, Dean
Faculty of Engineering and Computer Science

In memory of Dr. Benjamin Blunier

ABSTRACT

The challenge for the next few years is to reduce CO_2 emissions, which are the cause of global climate warming. CO_2 emissions are mainly due to thermal engines used in transportation. To decrease this emission, a viable solution lies in using non-polluting electric vehicles recharged by low CO_2 emission energy sources.

New transportation penetration has effected on energy production. Energy production has already reached peaks. At the same time, load demand has drastically increased. Hence, it has become imperative to increase daily energy production. It is well-known that world energy production is mainly produced thermal pollutant power plants, except in Québec, where energy is produced by hydro power plants.

The more recent electricity utility trend is that electric, and plug-in hybrid electric vehicles (EV, PHEV) could allow storage and/or production of energy. EV/PHEV batteries can supply the electric motor of the vehicle, and act as an energy storage that assists the grid to supply household loads. This power flow is called *vehicle-to-grid*, V2G. In this dissertation, the V2G power flow is specifically called *vehicle-to-home*, V2H. That is battery is used during peak. Moreover, the EV battery is charged during the night, when energy production is low and cheap. This important aspect of Vehicle-to-Home (V2H) is that the vehicle battery is not connected to the grid, but is a part of a house micro-grid.

This dissertation presents an offline optimization technique, which includes different energy flows, between the home, EV/PHEV, and a renewable energy source (such as photovoltaic - PV and/or wind) which forms the micro-grid. This optimization has been realized through the dynamic programming algorithm. The optimization objective is to minimize energy cost, including fuel cost, electricity cost, and renewable energy cost.

Two fuzzy logic controllers, one located in the vehicle and the second one in the house, have been designed, tested by simulation (online simulation) and validated by experiments.

The research analyses two seasonal case studies: one in winter and the other one in summer. In the winter case, a cost reduction of 40 % for the offline simulation, 27 % for the online simulation and 29 % for the experiment is realized whereas in the summer case a cost reduction of 62 % for the offline simulation, 60 % for the online simulation and 64 % for the experiment is presented.

RÉSUMÉ

Le challenge de ces prochaines années est de réduire le plus possible les emissions de CO_2 qui la première cause du réchauffement climatique. L'émission de CO_2 est principalement due à l'utilisation du moteur thermique dans le milieu du transport. Pour diminuer cette émission, la solution réside à utiliser des véhicules électriques qui sont non polluants et rechargés par des sources émettant le moins possible de CO_2. Mais cela impliquerait une production supplémentaire d'énergie. Aujourd'hui l'énergie électrique est produite principalement par des centrales thermiques au niveau mondial, des centrales nucléaires en France et des centrales hydrauliques au Québec. Les pics d'utilisations et de productions restant une problématique posant encore beaucoup de problèmes.

Une utilisation croissante de véhicules électriques ou hybrides rechargeables permettrait de pouvoir disposer de systèmes de stockage d'énergie, permettant à la fois d'alimenter le moteur électrique du véhicule ou d'aider le réseau électriques. Ce flux est appelé *Vehicle-to-Grid* ou plus précisément dans le travail présenté ici, ce flux s'appelle *Vehicle-to-Home*. Alimenter la maison via la batterie du véhicule, permet de diminuer le pic de consommation du foyer. De plus, la batterie du véhicule peut être chargée durant la nuit lorsque la production d'énergie est au plus bas et la moins cher.

Ce document présente une optimisation *offline* du système qui inclut les différents flux d'énergie. Cette optimisation a été réalisée à l'aide de la programmation dynamique. L'objectif de cette optimisation est de minimiser le coût de l'énergie que ce soit le coût de l'essence ou de l'électricité ou encore des énergies renouvelables installées localement.

Ensuite deux contrôleurs flous localisés dans le véhicule et dans la maison ont été dimensionnés, testés par simulation (simulation *online*) et validés expérimentalement.

Finalement cette recherche a mis en avant deux cas d'études : un en hivers et l'autre en été. Le cas cas d'hivers présente une réduction budgétaire de 40 % dans la simulation *offline*, 27 % dans la simulation *online* et 29 % en expérimentation. D'autre part, le cas d'été montre une rédution budgétaire de 62 % dans la simulation *offline*, 60 % dans la simulation *online* et 64 % en expérimentation.

CONTENTS

LIST OF FIGURES

LIST OF TABLES

ACRONYMS

AC Alternative Current

AM Ante Meridiem

ADVISOR Advanced Vehicle Simulator

AER All Electric Range

BIPV/T Building-Integrated PhotoVoltaic/Thermal

BMS Battery Management System

CAD Canadian Dollar

CD Charge Depleting

CMHC Canada Mortgage and House Corporation / SCHL: Socété Canadienne d'Hypothèque et de Logement

CO_2 Carbon Dioxide

CS Charge Sustaining

DC Direct Current

DOD Depth of Discharge

DP dynamic programming

EDF Électricité de France

EV Electric Vehicle

FC Fuel Cell

FL Fuzzy logic

FTP-75 Federal Test Procedure

GPIB General Purpose Interface Bus

GPS Global Position System

GUI Graphic User Interface

HP Horse Power

HEV Hybrid Electric Vehicle

ICE Intern Combustion Engine

IEEE Institute of Electrical and Electronics Engineers

INSEE Institut National de la Statistique et des Études Économiques

HEV Hybrid Electric Vehicle

H2G Home-to-Grid

H2V Home-to-Vehicle

LABVIEW Laboratory Virtual Instrument Engineering Workbench

LI-ION Lithium ion

MATLAB Matrix Laboratory
MPPT Maximum power point tracker
NEDC New European Driving Cycle
NREL National Renewable Energy Laboratory
NSERC Natural Sciences and Engineering Research Council of Canada
NZEH Net Zero Energy House
NI-CD Nickel Cadmium
NI-MH Nickel Metal hybrid
OCV Open Circuit Voltage
PHEV Plug-in Hybrid Electric Vehicle
PM Post Meridiem
PV Photovoltaic panel
RES Renewable Energy Source
RPM Rotation per minute
SOC State of Charge
SBRN canadian Solar Building Research Network
SOD State of Discharge
SOH State of Health
UC Ultra-Capacitor
UDDS Urban Dynamometer Driving Schedule
UTBM University of Technology Belfort Montbéliard
US United States
V2G Vehicle-to-Grid
V2H Vehicle-to-Home

ACKNOWLEDGMENT

First and foremost is to offer my sincere gratitude to my supervisors, Dr Abdellatif Miraoui and Dr Sheldon Williamson, who have supported me throughout my thesis with their patience and knowledge while allowing me the independence to pursue my research interest. I also appreciate the confidence of Dr Abdellatif Miraoui to propose me to accomplish this work in cotutelle (joint supervision) with Dr Sheldon Williamson, who gave me an opportunity to work under his supervision.

Then, I would like to thank my French co-supervisors: Dr David Bouquain and the late Dr Benjamin Blunier. Benjamin was and is still a role model to me. Our meetings were always constructive, and he guided me to give always the best of myself. On the other hand, David has always been there when I needed his advice. His practical approach, has been very helpful during this four years.

I would like to thank Dr. Mohamed Benbouzid and Dr Stéphane Ploix for accepting to review this dissertation, despite their very busy schedules, and for their helpful comments. I would like also thank my committee in Montréal for their help during my PhD. Dr Pragasen Pillay and Dr Shahin Hashtrudi Zad for their comments during the proposal and the seminar, and Dr Andreas Athienitis for his confidence to integrate me in his network and to work with him on the ÉcoTerra house. I would also like to thank Dr Mohamed Gabsi and Dr Christian Schaeffer for accepting to participate in my defense.

I appreciate the financial support of UTBM, especially the UTBM Foundation, Sheldon Williamson as well as NSERC, Canada throughout this period.

I am thankfull to my teammates: Dr Mohammed Kabalo, Dr Nicolas Watrin, Dr Robin Roche, Dr Alexandre Ravey, Damien Guilbert and Nanfang Yang. I would like to thank all the persons that I met and worked with at UTBM : Dr. Fei Gao, Dr. Arnaud Gaillard, Mr Hugues Ostermann, Dr Mikael Guarisco, Dr DonDong Zhao, Dr. Daniela Chrenko, Dr Damien Paire, Dr Beatrice Bouriot, Dr Abdoul N'diaye and all the engineers, technicians and co workers: Pierre, Djelalli, Abdelmajid (your cavern helps me a lot) Patrice and Eric. Your enthusiasm made these four years fly.

Then, I would like to thank my DOCEO (Ph.D. organization) team: Emilie, Elise, Gillian, Sebastien and Ahn-Tuan, for the year we have passed together to improve the Ph.D. experience at UTBM, with the help of Danielle Bertrand and Ghislain Iste.

I would like to thank all my colleagues at Concordia University: Jemimah, Rachel, Lesedi, Arbi, Manu, Chirag, Arvind, Ebrahim and others who made me feel at home, far from my family. Special thanks to my lovely colleague John Wanjiku who helped and supported me a lot in the last two years.

In addition, I would like to thank all my friends in France and in Québec, espacially Marie-Josée and her husband, Jean Pierre and their daughter

Justine who welcomed me with open arms and revitalized me. My Alsacian friends: Sophie, Dimitri, Sonia, Pierre, Sandrine, Thomas, Delphine, Nicolas, Ellie and Baptiste for their support during the last four years, my friends in Belfort: Delphine, David and Théo and the other Pierre, Thibault ...

Finally, I am extremely grateful to my family for their love, encouragement and confidence in me. Specifically, I would like to thank my parents, my grandparents and my sister for their continuous trust and support throughout the years.

INTRODUCTION

Climate change is one of the challenges that is currently facing the world. The Carbon Dioxide (CO_2) emission analysis of Québec [1] and France (FIGURE. 1) show that transportation is a major contributor of CO_2 emissions; especially personal vehicles. In the French case, personal vehicles represent 52.9% of the transportation emissions (FIGURE. 2). This analysis can be extended to the global level as well.

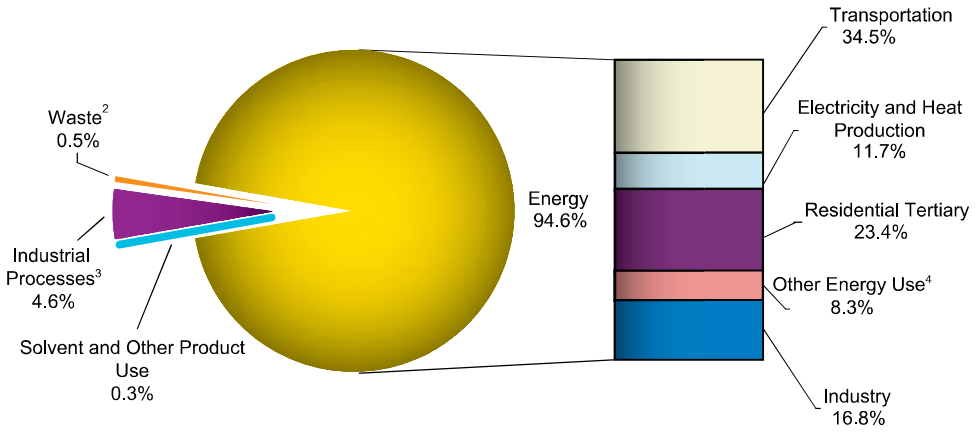

Figure 1. Distribution by sources of CO_2 emissions in France in 2009 [2]

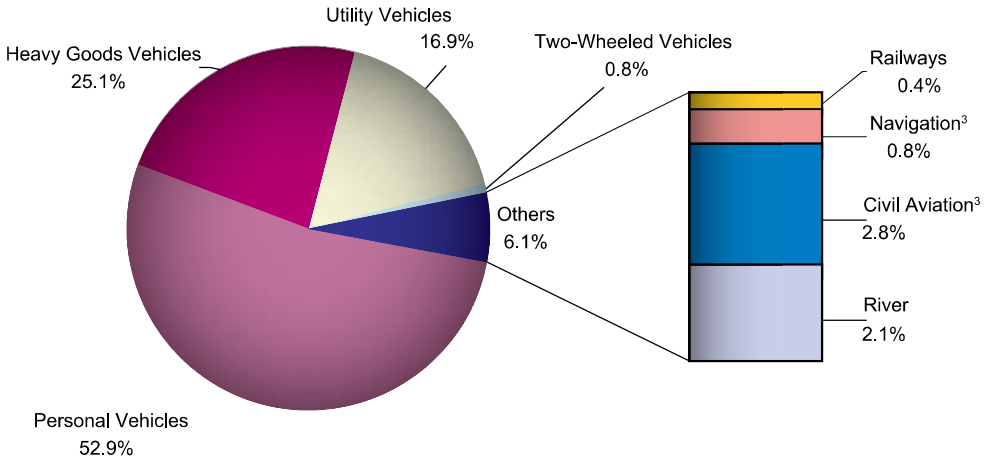

Figure 2. CO_2 emissions by method of transportation in metropolitan France [3]

Emissions from personal vehicles can be reduced by the use of Electric Vehicle (EV) and Plug-in Hybrid Electric Vehicle (PHEV). These vehicles reduce the dependency of fossil fuels, by using the battery to power the vehicles, which requires charging. Considering the number of personal vehicles, this charging will definitely have an impact on the utility grid. This may require the building of new power plants, that include nuclear and coal power plants. This present both an economic and policy challenges, which stifles the switch to EV/PHEV, in addition to other challenges.

To avoid the construction of new polluting power plants, household (local) and distributed renewable energy plants can be built. As most renewable energy sources are intermittent, energy storage systems and advanced controls also need to be developed. This raises the cost of renewable energy sources system at low reliability.

EV and PHEV can have an important role to play in such an infrastructure as a storage system as well as an energy producer, by utilizing their battery systems. This reduce the stress on the grid and the number of required new power plants.

According to [4], most of the vehicles are at home between 8.00 PM and 7.00 AM. Moreover, most people use their vehicle between 8.00 AM and 9.00 AM and from 4.00 PM to 5.00 PM. Therefore, 11 hours are available, where the vehicle can be used as a storage/production system depending on the battery SoC. During this time, the EV/PHEV can be charged or discharged, depending on the user needs. This is enable by charging at night, when the demand on the grid is low and using the control strategy for transport needs and shaving peak during on-peak period.

The other factor that promotes the practicability of the system is the knowledge that an EV/PHEV does not exhaust the battery energy at the end of the day. For example, the Chevy Volt® [5] with an electric range of 35 miles (61 km), retains 11 km battery range at the end of the day, if a one way home to work estimation is about 25 km.

To be able to use EV/PHEV, the interactions of the vehicle with the grid, renewable energy sources and the transportation schedule of the user are important.

Electricity production

Energy production has continuously increased in the last 30-40 years (FIGURE. 3), to supply ever increasing load demand. Oil is still the most significant resource of electricity production worldwide. Few other energy sources, such as nuclear power and natural gas have seen this kind of increase over the past few years.

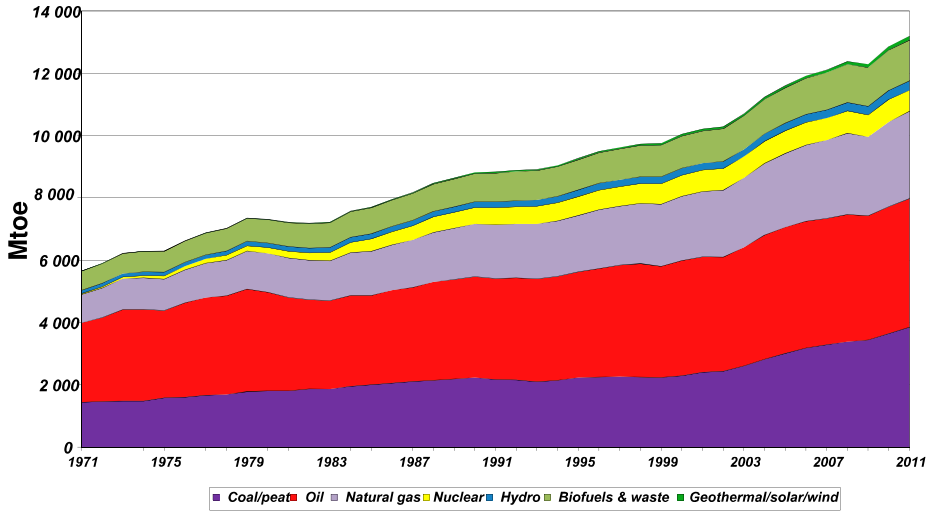

Figure 3. Energy production in the World [6]

However, in France (FIGURE. 4), the nuclear power is the choice source. Some people consider nuclear to be a "green" source of energy because nuclear power plants reject hot water and steam. However these power plants have to be built near a water body source (such as a river or lake), to provide the working and coaling fluids. Rejection of hot water into these water sources, modifies the water ecosystem [7]. Moreover, the disposal of spent radioactive fuel is still a challenge. It is buried underground, which is not a sustainable solution.

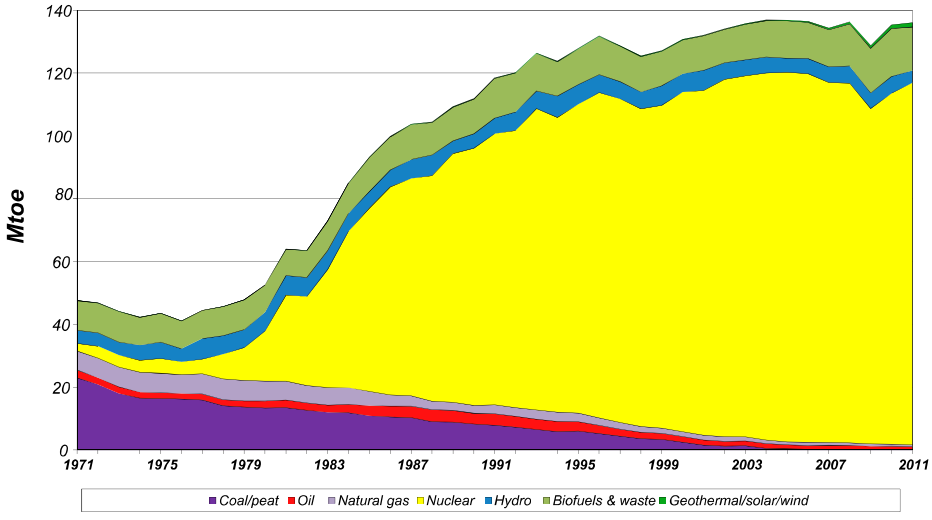

Figure 4. Energy production in France [8]

Oil and natural gas sources are part of Canada energy mix (FIGURE. 5). The renewable energy component is very low compared to fossil fuels.

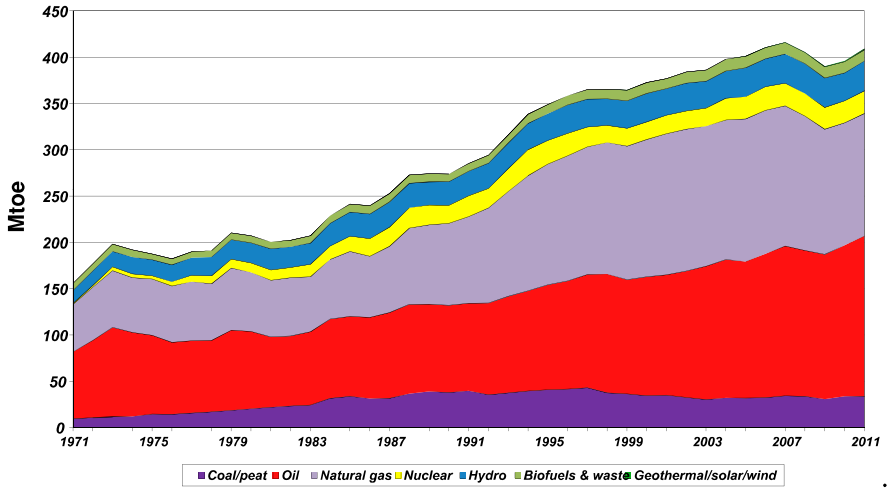

Figure 5. Energy production in Canada [9]

However, the province of Quebec is one of the cleanest and greenest regions in the world (FIGURE. 6): 97% of the energy production comes from renewable energy sources and more especially from hydro-electricity. [10].

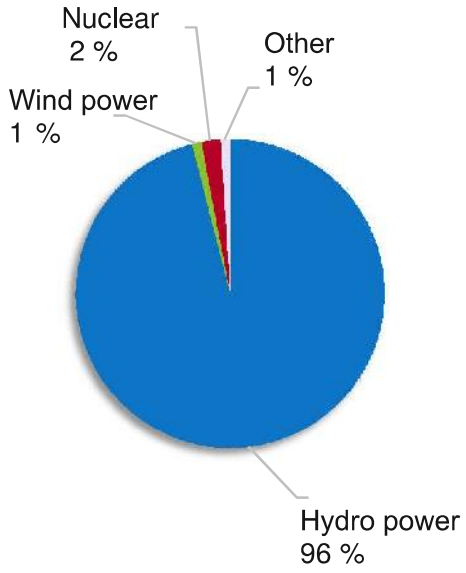

Figure 6. Energy production in Québec [11]

Fuel cost and production

Household, transportation and industrial loads have been dependent on petroleum, being one of the cheaper energy options. The demand for petroleum has dramatically increased over the past decade especially due to the transportation sector. This has made the hard to extract oil, such as in the tar sands, deep sea drilling, flacking etc profitable. This sources of oil are energy intensive and have a huge impact on the environment, that is yet to be understood. The petroleum price fueled by the demand has been steadily increasing over the years as shown in (FIGURE. 7).

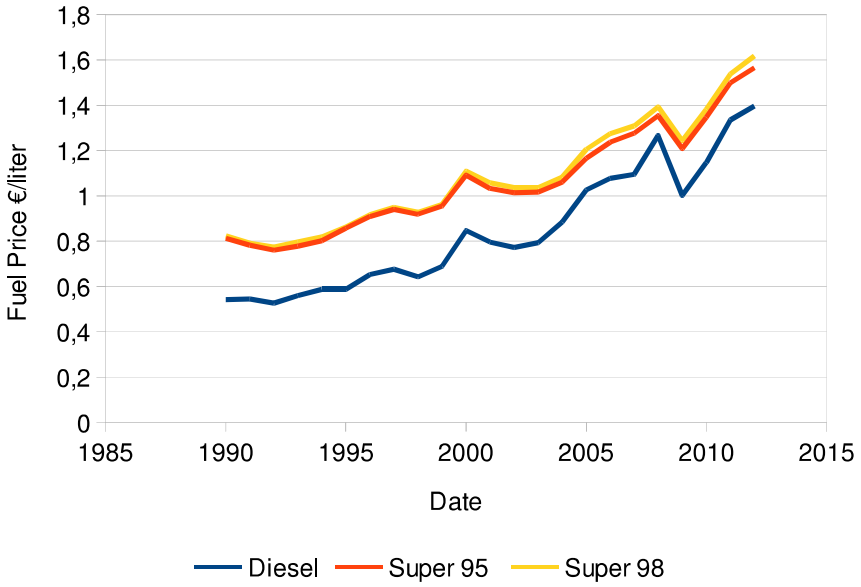

Figure 7. Gas cost [12]

The energy cost is significant for households as well as industries. From the household expenses analysis report of Institut National de la Statistique et des Études Économiques (INSEE) [13], transportation is reported as the third largest expense.

EV and PHEV penetration

The BLUE Map scenario, created by the International Energy Agency, has a target to reduce CO_2 emissions by 50%. This is the target for the year 2050 (compared to 2005 level). To achieve this objective, the International Energy Agency estimates that emissions in the transportation sector has to be reduced by 30% (FIGURE. 8), considering that it is the second main producer of CO_2.

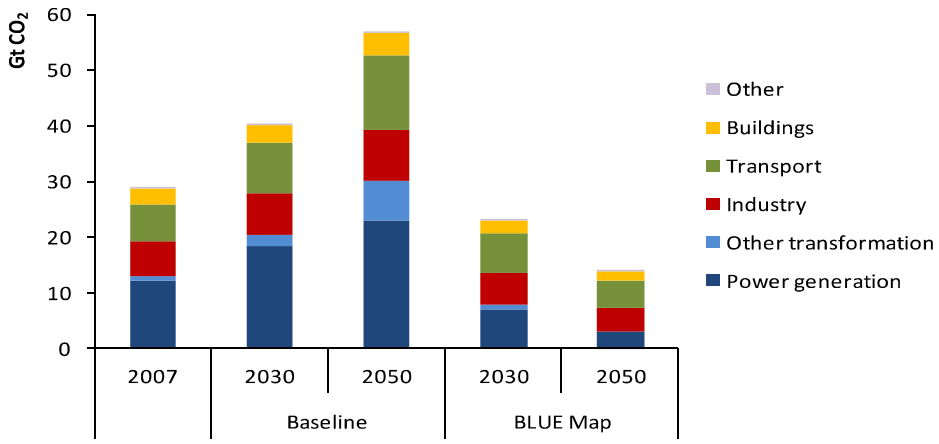

Figure 8. Comparison between Baseline and Blue Map [14]

This target can be achieved by selling 50 million light duty EV and 50 million PHEV per year, by 2050 (FIGURE. 9). This means, a yearly increase of 100 million cars that need to be charged, and interact with the grid.

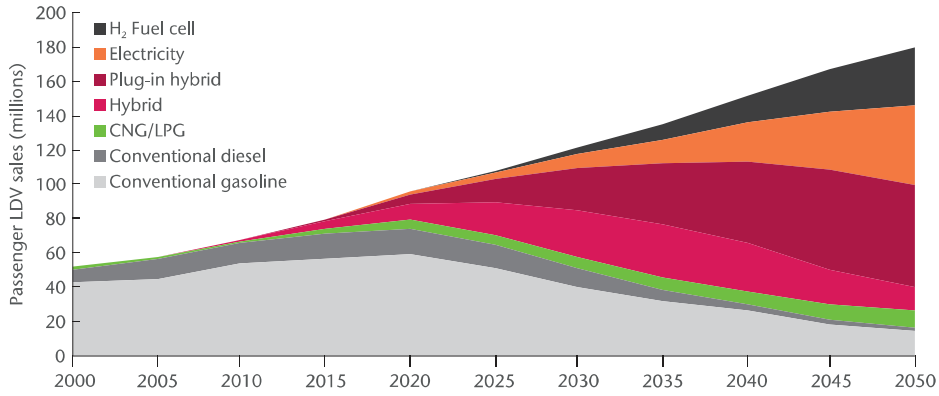

Figure 9. Vehicle distribution base on Blue Map [14]

This is important, because it shows the additional demand that the grid has to handle. Unlike other household loads, the EV/PHEV can be consider as an active load. It is charging/discharging can be optimized on when to connect and disconnect. This should be done to reduce the on-peak loads, and help in peak shaving depending of SoC of the battery.

Research Objective

The research objective is to minimize the energy cost of a real household which interfaces with local renewable energy sources and PHEV. The energy cost includes the fuel price and the grid price.

Motivation

The main challenge in this century is to meet energy demand, as well as limit emissions. The price of fuel continues to increase, due to the rising demand and the scarcity of cheap energy sources. Moreover, the increasing demand of energy will only escalate, according to [15], which suggests that more than half of the auto industry will consist of EV and/or PHEV. This implies an additional energy need in the evenings, when the cars reach home, will worsen the peaking problem [16].

On one hand, reducing CO_2 emission and on the other, building polluting power plants is not a good trade-off with the future. Unless there is CO_2 capture and storage at the power plant. However, by introducing Vehicle-to-Home (V2H) and Home-to-Vehicle (H2V) capabilities, the system energy balance can be altered. The bidirectional EV battery charger not only charges the PHEV battery, but also allows the battery to help the grid to meet the household loads.

According to [17], the average home to work vehicle trip length is 12 miles (19,4 km), which gives a gap to use some of the energy in the battery. The EV can supply the home loads at on-peak period, when the driver reaches home, then the charging of the battery is shifted to the night during off-peak period. At this time, the EV battery works as a buffer or an energy storage system.

In addition, to increase the energy production by renewable energy sources, the home includes local renewable energy sources, such as wind turbines and solar power.

Literature review

The novel and more recent concept of using PHEV as an energy storage system for propelling the vehicle, and at the same time, the EV battery for assisting the grid to supply household loads, is one of the keys to the newer smart electric grid.

Most of the research is tuned to the global impact of the new vehicle fleet charging [18] or of the Vehicle-to-Grid (V2G) capability [19, 20, 21]. They show that using V2G in aggregate, presents benefits in term of cost and in global energy production. Indeed, the V2G capability permits to peak shave the power in the evening.

However, this research is focused on a smaller scale: at household or local scale. Indeed, before extend the benefit of V2G to a larger scale, the user has to be the center of attention and shown the necessity of V2H or V2G capability in terms of cost and environment to commit the user at the new usage of the grid. V2G capability allows to sell the battery energy to the grid whereas the V2H permits only to use the battery in the micro-grid.

This study approaches the problem by building two energy power flow controllers which manages the battery usage in terms of SoC. The first controller is located in the PHEV and the second one in the house.

On the PHEV side, a lot of energy control strategies and optimizations have been proposed according to the standard driving cycles as presented in [22, 23, 24, 25]. In [24, 25] a rule based control strategy is proposed, whereas in [24], the control is based on the battery SoC, to chose when to use the Intern Combustion Engine (ICE). In [22, 25], the secondary source which is a fuel cell is the main control strategy input. The goal is to maintain the fuel cell power constant. This is done in [22] by a fuzzy logic controller which according to [26] is good for modeling uncertainty and complex decisions, as in a PHEV. In addition, fuzzy logic deals with natural language which is easier to work with. This study uses a fuzzy logic presented [22, 27, 28, 29] which it is used to control the battery SoC and drive cycle loads. However, the battery charging aspect is not taken into account which is an important aspect of the energy control strategy. By considerably battery charging, it is possible to reduce CO_2 emissions and save money as much as possible.

On the house side, [30, 31, 32] the controller optimizes the schedule to charge and discharge the PHEV. This study implements a real time energy control strategy to manage the PHEV battery when the vehicle is connected to the house, and is linked with the PHEV control strategy via the battery SoC.

Methodology

A real house, called ÉcoTerra instrumented in 2010, is used to provide solar and household loads profiles. This study is divided into four steps:

1. interface,
2. offline simulation,
3. online simulation,
4. experiment.

The first step, is to develop an interface which can create a 24h scenario including solar and household load profiles, PHEV departure and arrival, and PHEV drive cycle.

The next step is to find the cost reference which is the minimum energy cost over a 24h scenario. To find this reference a dynamic programming algorithm is used where the objective function includes the different power flow prices: the electricity, the fuel and the renewable energy sources. The constraints are the battery capacity, the battery charger size, the ICE size, the maximum battery current and the final SoC.

The third step develops a real time energy control strategy that minimizes the energy bill compared to the reference. To build the energy control strategy, two controllers located in the house and the PHEV control the battery power flow. As mentioned previously, these two controllers use the fuzzy logic technique. The house controller is built according to the battery SoC limitation, the electricity price system, the battery charger, whereas the PHEV

controller is constructed according to the battery SoC limitation, the ICE, the maximum battery power and the SoC objective. This SoC objective is the SoC that the PHEV has to have when it reaches home. This value is calculated according to data for the last 10 days household loads, solar profile and driver schedule.

The last step is to validate the two controllers in a real time environment.

Chapter organization

Chapter 1 describes the different elements of the global project, such as the solar power system, wind turbine, and different vehicle architectures as well as varying levels of charging.

Chapter 2 presents the ÉcoTerra house which is used to collect real data of solar and household loads power. In addiction, an interface scenario program is described. The interface allows the creation of scenario that the energy control strategy will be tested in this thesis. A last section in this chapter concerns the choice of the topology of the system study.

Chapter 3 shows an offline energy control strategy using dynamic programming to be able to optimize the global system. A winter and summer cases are described, showing the gains of the system.

Chapter 4 presents an online control strategy using fuzzy logic controller. The same winter and summer cases are used to demonstrate that the system reduces the energy cost.

The last chapter proposes an experiment set-up to validate the developed controllers as effective.

1 FROM ENERGY PRODUCTION TO USAGE AND STORAGE

To reduce pollution from transportation, there exist three possibilities: EV, Hybrid Electric Vehicle (HEV) and PHEV. HEV and PHEV are the short-term solution. The real solution to eliminate CO_2 emission is all-electric vehicles charged by renewable energy sources. However, the grid has to be adapted to this massive future influx of EV.

The HEV uses at least two sources such as engine, fuel cell, battery, flywheel, or ultra capacitor as energy storage. HEV can have different architectures: series, parallel, or complex (combined series and parallel), which allows development of different control strategies.

PHEV is an electric range extended HEV, with the main difference being the plug-in capability, which allows charging the battery by an electric outlet.

This section describes EV, HEV, and PHEV architectures, with their control strategies. In addition, a description of energy sources such as battery, fuel cell, ICE, and Ultra-Capacitor (UC), which is using in green vehicles, is also provided. Moreover, a description of level charging in Europe as well as in US is given. Finally, a summary of renewable energy sources and more specially solar and wind power is presented. These renewable energy sources can be used in local, to be able to charge EV/PHEV cleaner.

1.1 VEHICLES

1.1.1 *Automobile History*

The automobile history and development characterizes the great inventions that have marked the XIX and XX century. However, the origin of the automobile started in the XVII century. In 1680, Newton invented the trolley reaction, which worked with the principal of action and reaction, by moving the gravity center virtually. It is only in 1769 that François Joseph Cugnot realized the dray, which was the first attempt proven to be free of animal traction using a steam motor.

Seeing the steam machine had no future in automobile, because of its heavy weight and slow starting, researchers turned to the ICE and electric motors. Alessandro Volta discovered the battery in 1800, which could drive an electric motor independently. In 1899, the first ever propulsion vehicle developed, was an EV, which could run at a speed of over 100 km/h. This vehicle is presented in FIGURE. 10.

Nevertheless, the ICE presented more opportunities for the future. In 1860, Étienne Lenoir developed the dual motor. And in 1862, after the development

Figure 10. First vehicle with a speed over 100 km/h [33]

of the electric spark plug, a spark that triggered an explosion is produced. Alphonse Beau de Rochas deposited a patent about the theoretical cycle of a quad ICE, transforming thermal energy into mechanical energy. At the end of the XIX century, the automobile industry started to focus more on the ICE vehicle.

The oil crisis in 1970 slowed the development and marketing of the ICE automobile in the United States, caused by the amount of gasoline consumes in the ICE. Conversely, in Europe, automakers planned a series of small cars, which consumed minimal fuel. Furthermore, diesel engine research took priority, which helped reduce fuel consumption further.

At the same time, the emergence of Japanese auto market changed the vision of automobile production. Engineer Taiichi Ohno, at Toyota, introduced the concept of *just-in-time*, *kaizen* (continuous improvement) and *kanban* (information system indicating the level of stocks of parts along the chain), which allowed the reduction in manufacturing costs considerably. Hence, vehicles became cheaper and the mass production occurs.

In the late 1990s, Toyota sold its first hybrid car: the Prius®. This marked a new era in the automotive sector.[34]

Figure 11. Toyota Prius®: first commercialized PHEV [35] (Picture courtesy Toyota)

In fact, "green" vehicles (EV, HEV and PHEV) will continue to be developed by car manufacturer in Japan, north America and Europe.

The next section will explain the topology of each "green" vehicles associated with its energy control strategy.

1.1.2 *EV Architecture*

The EV architecture presented in FIGURE. 12. The power train is designed either by an AC or a DC traction electric motor. Batteries (Lead acid, Nickel Cadmium (Ni-Cd), Nickel Metal hybrid (Ni-MH), or Lithium ion (Li-ion)), in conjunction with power electronic converters, can provide regulated power to the traction motor.

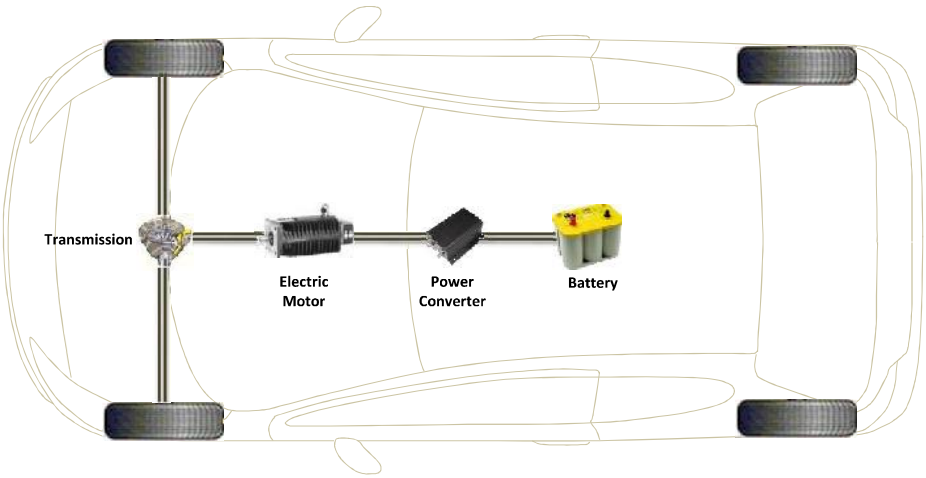

Figure 12. EV architecture

In 2012, Renault commercialized the EV: Twizy®, Kangoo®, and Fluenze® presented in FIGURE. 13 with vehicle characteristics in TABLE. 1.

Obviously, the major drawback of any EV is its battery autonomy. Thus, the user has to have a specific plug at home, to charge the EV battery pack when he/she comes back home. EV is best reserved to an urban driving schedule, because then, the vehicle can charge the battery during frequent starts and stops (using regenerative braking mode of the traction motor). In addition, the cost of an EV is comparatively higher than a conventional vehicle of the same category (due to battery and motor costs). However, the price of battery charging does not exceed more than a few dollars. Another problem with EV is battery recycling. Nevertheless, the EV is easy to drive. There is no clutch and gear box, and there exists no CO_2 emissions, except if electricity production is taking in account.

	Twizy®	Kangoo®	Fluenze®
Battery	Li-ion	Li-ion	Li-ion
Range	80 km (urban cycle)	170 km (NEDC cycle)	185 km (NEDC cycle)
Battery capacity	6.1 kWh	22 kWh	22 kWh 65 Ah
Battery charging time	3h30	8h	11
Electric motor	Induction motor	Synchronous motor	Synchronous motor
Maximum power	13 kW	44 kW	70 kW
Maximum torque	57 Nm	226 Nm	226 Nm
Maximum speed	80 km/h	130 km/h	135 km/h

Table 1. Characteristics of Renault EV [36]

Twizy Kangoo Fluenze

Figure 13. Twizy®, Kangoo® and Fluenze® (Picture courtesy Renault SA)

1.1.3 *HEV Configurations*

The term hybrid in EV means using at least two energy sources. These sources can either be a battery, ultra-capacitor, gasoline, hydrogen, and/or a kinetic energy source, coupled in series, parallel or complex mode.

The common configuration is a battery coupled with the ICE or fuel cell. This configuration is used to explain the different methods of coupling.

Series HEV

The series architecture (FIGURE. 14) consists of using the ICE directly coupled to an electric motor. It is the electric motor, which provides all the propulsion power. Hence, in a way, the series HEV is an all-electric propelled vehicle.

This vehicle architecture is very good for frequent acceleration and braking, like in an urban drive cycle for transit bus applications. The control strategy is simple compared to other systems.

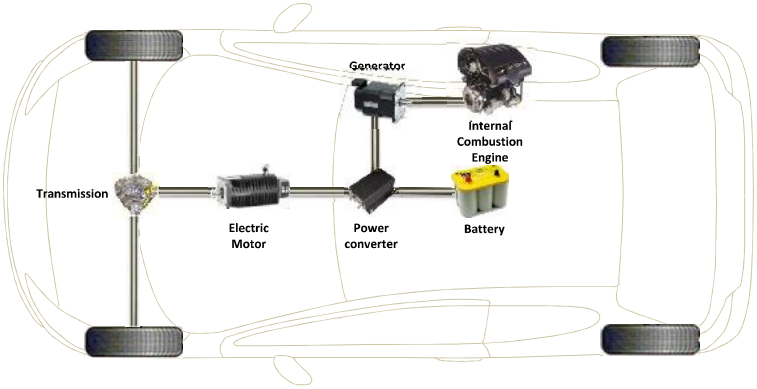

Figure 14. Series HEV architecture

The following are the different operating modes of a series HEV (FIGURE. 16) [37, 38] as in FIGURE. 16:

- at starting and when the vehicle is moving at a low speed (25 - 30 km/h), the battery supplies the motor via the power electronic converter,
- during acceleration, the battery and the ICE operate together, to provide peak power,
- when the vehicle is cruising (constant speed), the ICE is running, and it supplies the electric motor to move the vehicle and recharge the battery at the same time. In this mode, the engine is operating at its maximum efficiency,
- during braking, the kinetic energy is recuperated through regenerative braking of the motor, to recharge the battery.

The popular PHEV Chevy Volt® (FIGURE. 15) and the Opel Ampera® (in Europe) use the series architecture. Both vehicles have motor with a maximum power output of 149 HP and maximum torque of 370 Nm. The battery technology used for both cars is of Li-ion chemistry, with a capacity of 16.5 kWh [5].

Figure 15. Chevy Volt® (Picture courtesy Chevrolet)

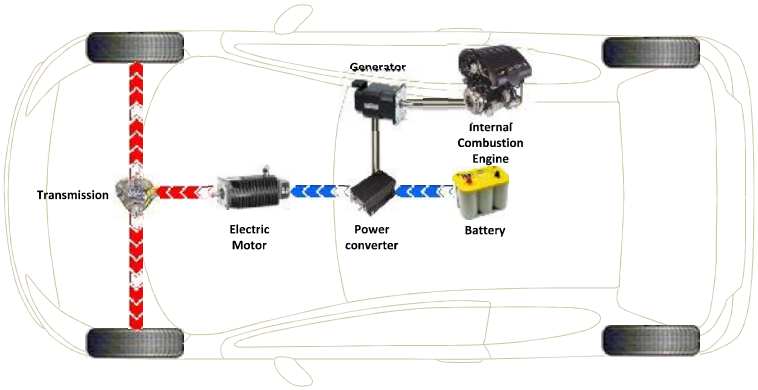

(a) Start mode

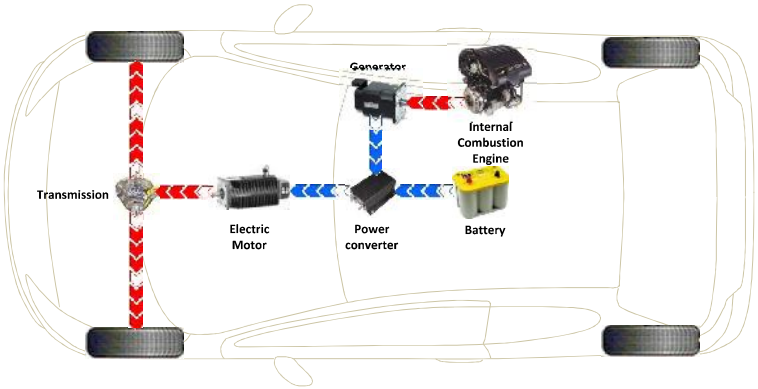

(b) Acceleration mode

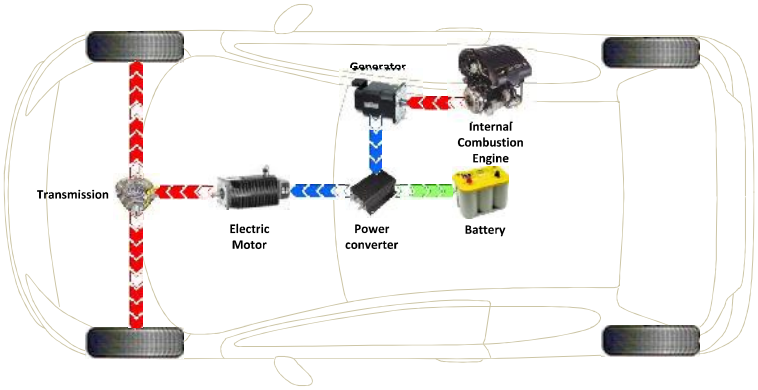

(c) Steady speed mode

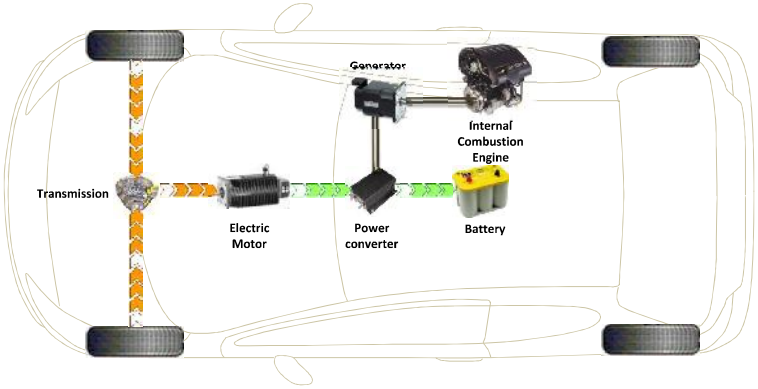

(d) Regenerative braking mode

Figure 16. Series HEV operation mode

Parallel HEV

The parallel architecture (FIGURE. 17) allows usage of the ICE independently. In reality, there exist two power trains; one for electric traction, and one for conventional ICE traction.

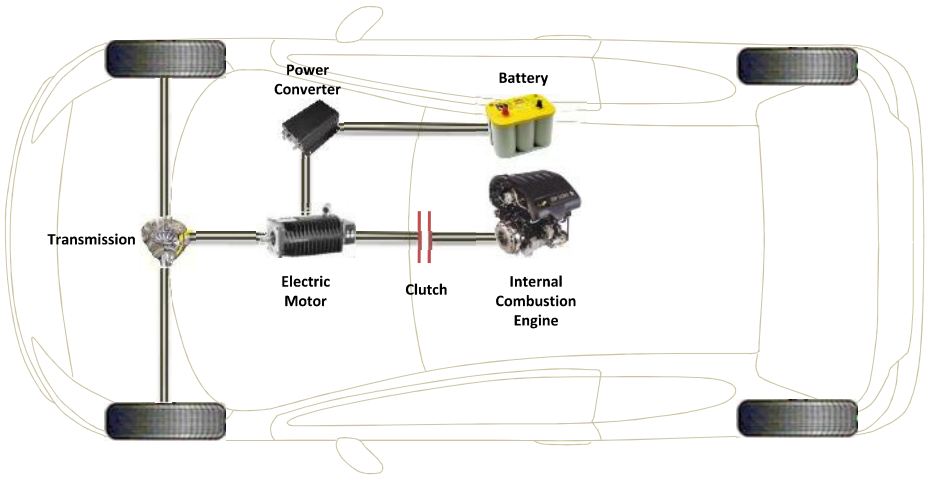

Figure 17. Parallel HEV architecture

The parallel HEV's control strategy is more flexible and complicated to implement. However, the power train is more modular. Thus, each energy source can work independently. The different operating modes of a parallel HEV are as follows [37, 38] as in FIGURE. 18:

- at starting and when the vehicle is moving at a low speed, the battery supplies the traction motor via the power electronic converter,
- during acceleration, the battery and the engine work together,
- during cruising (constant speed), the engine provides the energy to move the vehicle; at the same time, the engine recharges the battery,
- when the brake is applied, the resulting energy is used to recharge the battery.

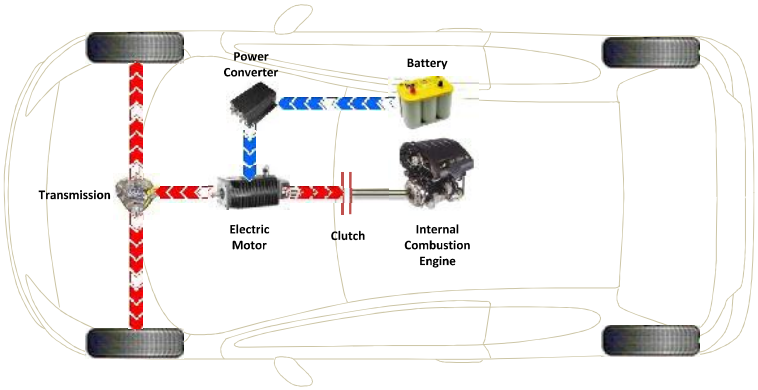

(a) Start mode

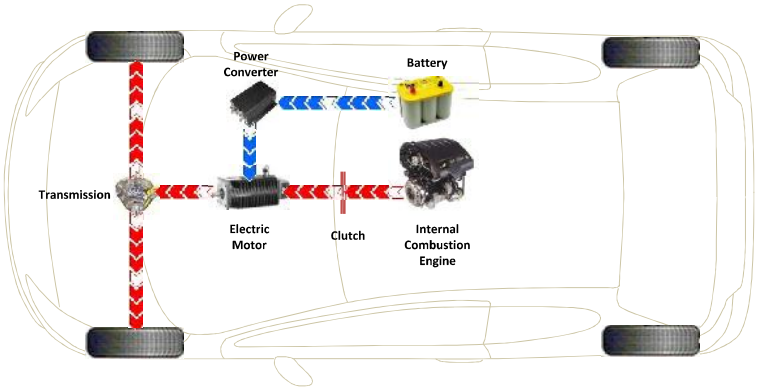

(b) Acceleration mode

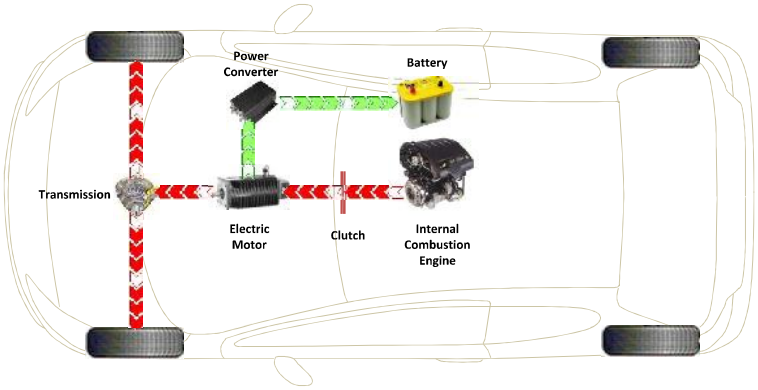

(c) Steady speed mode

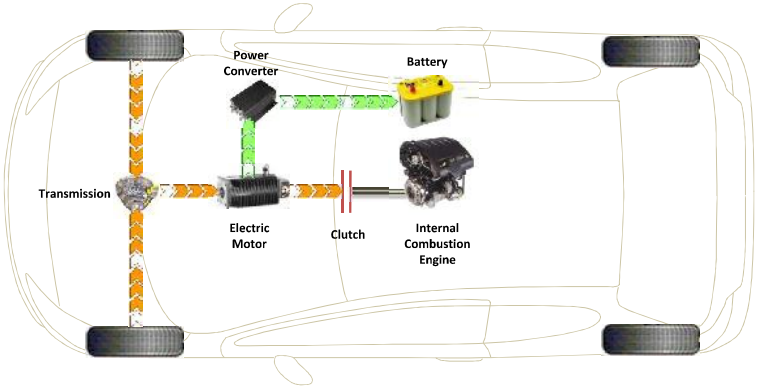

(d) Regenerative braking mode

Figure 18. Parallel HEV operation mode

Peugeot® opted to commercialize a parallel HEV architecture with the 508 HYbrid4® and the 3008 HYbrid4®. The popular Honda Insight also has a parallel HEV architecture as presented in FIGURE. 19.

Figure 19. Honda Insight® (Picture courtesy Honda)

The Honda Honda Insight® develops a 98 HP at 5800 RPM with the electric motor and the ICE [39].

1.1.4 *Complex HEV Configuration*

The complex HEV takes advantage of both the parallel and series architectures. This architecture is flexible and has a high efficiency. However, its complexity lies in the energy control strategy and mechanical coupling. Toyota Prius® uses this hybrid architecture.

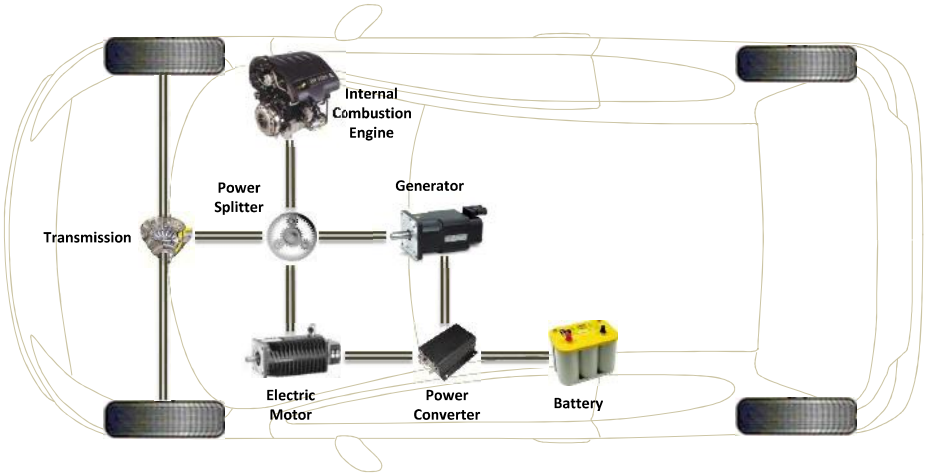

Figure 20. Complex HEV architecture

Other configurations could use traction motors directly connected to the wheels or one motor on each axle. In this way, the designers can reduce the power ratings of the motors and increase overall drive train efficiency.

1.1.5 *PHEV Configuration*

To improve the efficiency of a conventional HEV, a more electric configuration is adopted, known as plug-in HEV (an electric outlet is required to charge the larger battery pack). The idea is to charge the battery at night, when electricity is available and cheaper. During the day, instead of the engine, the battery is used to run the vehicle as much as possible.

There exist three different modes of operation: all-electric, Charge Depleting (CD) mode, and Charge Sustaining (CS) mode. The all-electric mode is when the battery alone is used to propel the vehicle; from the beginning of the drive cycle until when the ICE is turned on. The CD mode is when the SoC falls to its minimum. The CS mode is when the engine is switched on and off. The engine is used at its best efficiency when it produces more energy than the vehicle needs for propulsion. The difference between the energy required to propel the vehicle and the energy produced by the engine, is the energy that is used to charge the battery. Using the engine at its best efficiency, which is a maximum of 30 % allows the reduction of losses. Once the battery is fully charged, the ICE is turned off and the battery is used again[40].

Managing the energy in PHEV depends on the load the vehicle has to satisfy, either in urban drive cycles or highway drive cycles (FIGURE. 21). Indeed in urban drive cycle, it is better to use at first the CD mode as an all electric mode and then if necessary uses the CS mode, due to the number of stop, whereas for a highway drive cycle, the battery has to discharged slowly, then a CD mode following by a CS mode is more appropriated.

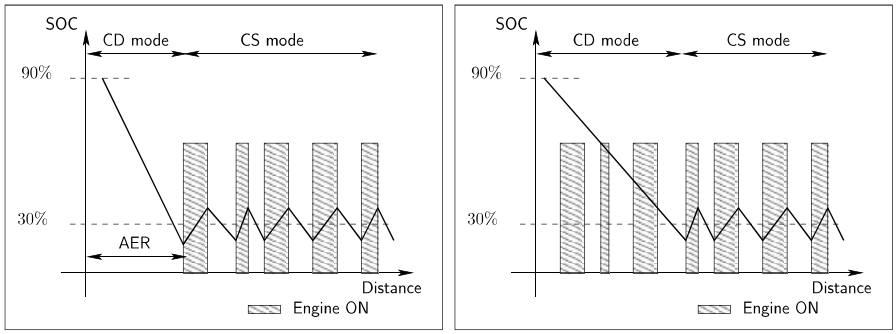

(a) Urban drive cycle (b) Highway drive cycle

Figure 21. PHEV control

1.2 ENERGY SOURCES

As seen in the previous sections, an HEV could have various architectures, with different energy sources. This section describes the 4 main clean and "green" energy sources, which can be used in PHEV/HEV. In FIGURE. 22, the specific energy and specific power of different kinds of batteries, flywheel, fuel cell, capacitor, and ultra capacitor is provided.

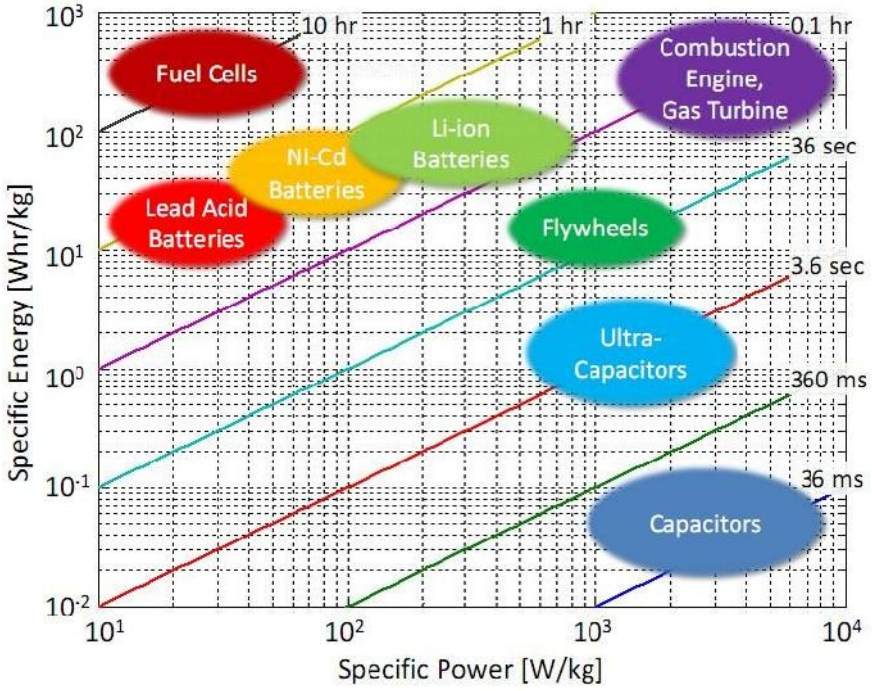

Figure 22. Ragone diagram [41]

According the Ragone diagram, fuel cells is a tank of energy but not power, then it has to be associated with a source of power like Li-ion battery. It is to notice that the combustion engine is the best candidate for transportation in terms of specific power and energy, it do not need a second source. However, the gasoline is pollutant. The transverse lines represent the required time for charging or discharging the storage system.

1.2.1 *Battery*

Batteries are storage systems, which allow conversion of chemical energy into electric energy. There are different kinds of batteries, such as lead acid batteries, nickel-cadmium batteries, and lithium ion batteries. This section presents the basic modeling of the lead acid battery with Peukert equation [42, 43] is presented.

The theoretical capacity (Q_t) of a battery is given in (1.1), where x is the number of moles of limiting reactant associated with complete discharge of the battery, n is the number of electrons produced by the negative electrode discharge reaction and F is Avogadro constant (96412.2C/mol).

$$Q_t = xnF \tag{1.1}$$

The most critical battery parameter is the SoC. SoC indicates the amount of remaining capacity (Ampere-hours) in the battery. This variable is the main contributor to the vehicle control strategy. Usually, battery SoC should be maintained the linear part of the open-circuit voltage, between a SoC of 30 % and 90 % (FIGURE. 23). The equation is given in (1.2).

$$SoC_t(t) = Q_t - \int_0^t i(t)\,dt \tag{1.2}$$

State of Discharge (SoD) is the quantity of current used in the battery (1.3).

$$SoD_t(t) = \int_0^t i(t)\,dt \tag{1.3}$$

The equation of SoC becomes:

$$SoC_t(t) = Q_t - SoD(t) \tag{1.4}$$

However, there is a difference between the theoretical capacity (Q_t) and the practical capacity (Q_p) (FIGURE. 23), due to Depth of Discharge (DoD). DoD is the region where the battery Open Circuit Voltage (OCV) can never reach.

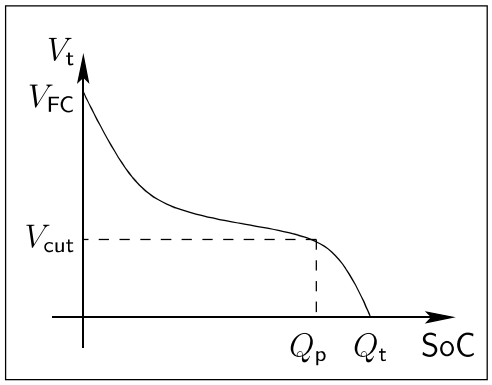

Figure 23. Battery terminal voltage

This value is a function of the battery State of Health (SoH) and temperature. Q_p using by the following equation (1.5).

$$SoC_p(t) = \int_0^{t_{cut}} i(t)\,dt \tag{1.5}$$

There exist two ways to model a lead-acid battery; one is given by [44], which models the battery as an electric circuit, including transient. The second way is to use the Peukert model, which uses the following equations.

$$Q_{peukert}(t) = I^k t \tag{1.6}$$

Where k is the Peukert constant. This constant can be found by experiments, using discharge time function of current (1.7). Usually, the value k for a lead acid battery is around 1.2.

$$k = \frac{\log T_2 - \log T_1}{\log I_1 - \log I_2} \tag{1.7}$$

Although, lead-acid battery technology is widely used and well known, car manufacturers have gradually converted their preferred battery technology from lead-acid to Li-ion. This is because Li-ions batteries have much higher energy density and specific power in addition to better overall charge/discharge efficiency (TABLE. 2 [45]). In addition, Li-ion batteries do not have memory effect compared to the lead-acid battery and does not have temperature regulation compared to the Ni-Cd batteries.

Battery	Specific Energy (Wh/kg)	Peak power (W/kg)	Efficiency (%)	Cycle Life
Lead-acid	35-50	150-400	>80	500-1000
Ni-MH	70-95	200-300	70	750-1200
Ni-Cd	50-60	80-150	75	800
Li-ion	80-130	200-300	>95	>1000

Table 2. Battery comparison

Ni-MH batteries have several advantages compared to Ni-Cd batteries. First, the energy density and power density of Ni-MH batteries is higher. Secondly, the Ni-MH batteries is easy to use, there is no temperature regulation. Finally, the Ni-MH battery is less toxic than the Ni-Cd battery. However, in Ni-MH batteries, the end of the charging is hard to detect due to the small OCV and the overcharged is not allowed.

1.2.2 *SoC estimation*

Many SoC estimation methods exist including: direct, indirect and adaptive. The two main methods used are the Kalman filter and the Coulomb counter method.

The Coulomb counter is an open loop system which can give important error, due to the incertitude of the initial SoC and the real battery capacity. However, it is often used because of it ease of usage. The Coulomb counter equation is given in (1.8), where SoC_{init} is the initial SoC, I is the battery current (A) and C the battery capacity (Ah) [46].

$$SoC(t) = SoC_{init} - \frac{I}{C} \tag{1.8}$$

The Kalman filter is a powerful mathematical tool which estimates the system state as function of its previous state, specific command and noise measurement. The Kalman filter is composed of 5 equations: 2 prediction equations and 3 correction equations [47].

The prediction equations are:

$$x_{\bar{k}} = A \cdot \hat{x}_{k-1} + B \cdot u_{k-1} + w_{k-1} \tag{1.9}$$

$$P_{\bar{k}} = A \cdot P_{k-1} \cdot A^T + Q \tag{1.10}$$

The correction equations are:

$$K_k = P_{\bar{k}} \cdot H^T (H \cdot P_{\bar{k}} \cdot H^T + R)^{-1} \tag{1.11}$$

$$\hat{x}_k = \hat{x}_{\bar{k}} + K_k \cdot (z_k - H \cdot \hat{x}_{\bar{k}}) \tag{1.12}$$

$$P_k = (I - K_k \cdot H) \cdot P_{\bar{k}}) \tag{1.13}$$

Where :

- x : SoC vector $\rightarrow$ System's state variable
- u : Control input $\rightarrow$ Change state system (Current)
- z : Measurement vector $\rightarrow$ Vector used for comparison
- A : Covariance matrix $\rightarrow$ Link z_{k-1} to z_k
- B : Covariance matrix $\rightarrow$ Link u_{k-1} to u_k
- C : Covariance matrix $\rightarrow$ Link z_k to x_k
- D : Covariance matrix $\rightarrow$ Link u_k to z_k
- w : Process noise $\rightarrow$ Model's derivations
- v : Measurement noise $\rightarrow$ Measurement imperfections

- P : Covariance matrix → Projects the error covariance ahead
- Q : Variance of the process → Corrects covariance matrix
- H : Measurement matrix covariance → Corrects measurement parameters
- R : Covariance matrix of the measurement noise → Given by battery data
- K : Kalman filter gain → Minimizes the posteriori error covariance

1.2.3 *Fuel Cell*

A fuel cell converts hydrogen and oxygen into electricity, heat and water by electrochemical reaction (FIGURE. 24)[48].

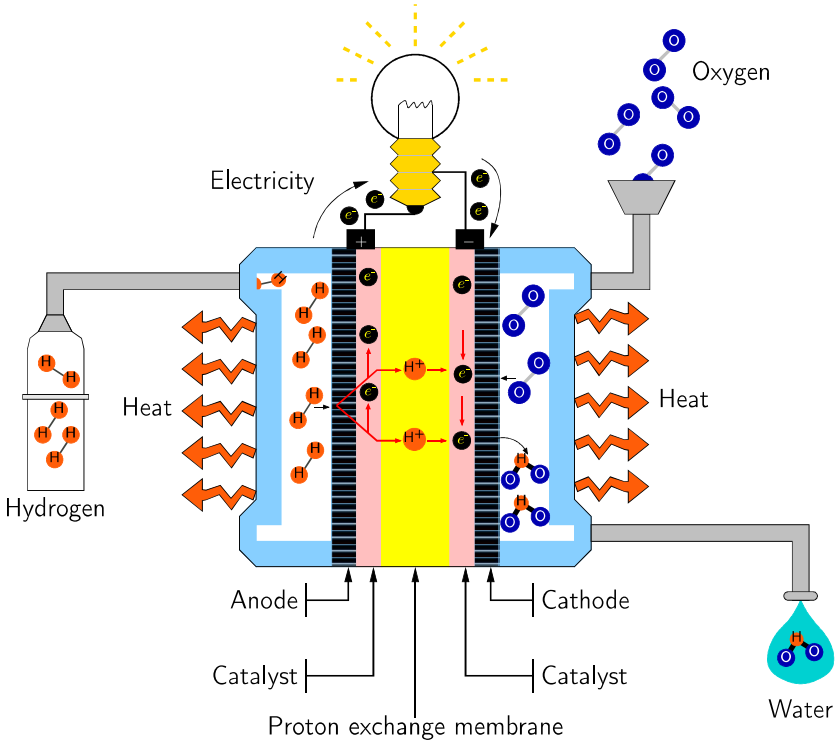

Figure 24. Fuel cell principle

The fuel cell is composed of three main elements: anode, cathode, and the proton exchange membrane. Anode is supplied by a fuel, which is usually hydrogen and the cathode fed with oxygen. The proton exchange membrane that separates the two electrodes, allows the diffusion of ions produced by the oxidation reaction of the fuel. The membrane has to avoid electron passage, which go through the electric circuit. The global reaction is in (1.14).

$$2H_2 + O_2 \rightarrow 2H_2O \tag{1.14}$$

The invention of the fuel cell for automobile was a good idea but in reality, the system of fuel cell needs the implementation of many auxiliary systems, such as air compressor, humidifier, and cooling. This makes the system difficult and inefficient for an automobile.

Although, the discovery of the fuel cell makes the vehicle more green, the production of hydrogen might be more pollutant than gasoline, if the complete production system is taken into account.

Using fuel cell as the second source instead of ICE, can be less polluting, if the hydrogen is provided by the renewable energy sources. Indeed, most of the time, when the local solar energy is produced, PHEV/EV batteries are not available to be charged by the green energy. During this time, solar energy can be converted into hydrogen from a green source to be used as a buffer storage. This hydrogen can then be charged into the car during evenings. This concept is under development in Mobypost project [49].

1.2.4 *Ultra-capacitor*

Conventional capacitors store energy by the separation of equal positive and negative electrostatic charges. The basic structure of a capacitor consists of two conductors (plates), separated by a dielectric, which is an insulator. UC are a derivative of conventional capacitors (FIGURE. 25), where the power density is increased [50].

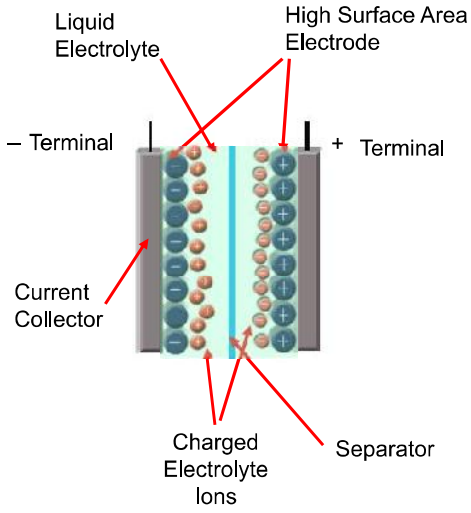

Figure 25. Ultracapacitor diagram [51]

The energy which is stored in a capacitor is given in (1.15) where C is the capacity in Coulomb and v the voltage across the UC. The UC is used in the vehicle to store the energy from regenerative braking rapidly. Alternatively,

power for speedy accelerations can also be provided by UC, which a normal battery pack cannot provide but a high voltage drop.

$$E_c = \frac{1}{2} C \cdot v^2 \tag{1.15}$$

Thus, a UC can lengthen the life of a battery pack, by providing transient power, while the battery can provide constant energy during a typical drive cycle. In addition, due to the higher faradaic efficiency compared to the battery, UC regenerates more energy in regenerative braking mode than batteries.

1.2.5 *Internal Combustion Engine*

ICE convert chemical energy into mechanical energy. The chemical energy is stored in fuel as diesel or gasoline.

The flammable air-fuel mixture is introduced into a cylinder, compressed by the piston. It then ignites the mixture which burns very quickly. Gases subjected to high temperatures and very high pressures violently push the piston down. When the combustion is finished, the exhaust gas is discharged to the outside and then, this cycle begins again. The ICE using a 4 stoke engine cycle, and works in the following steps (FIGURE. 26) :

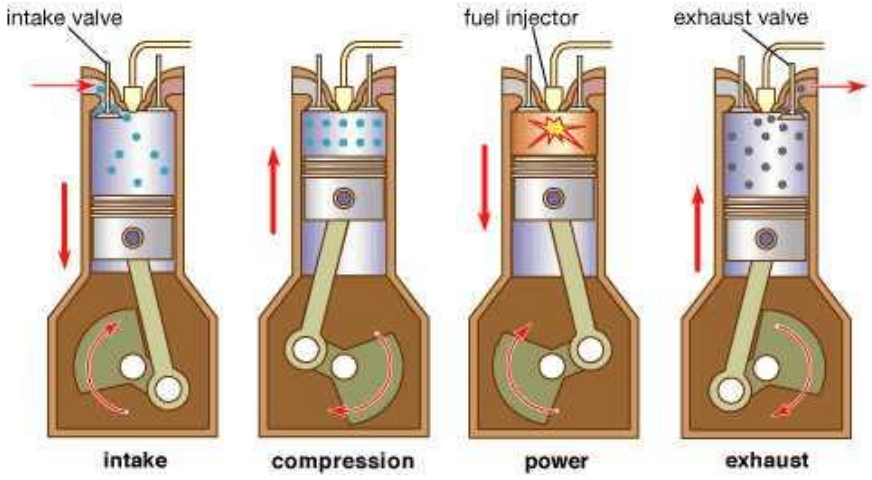

Figure 26. 4-stroke engine cycle with Gasoline direct injection [52]

- Step 1: The intake valve opens and the piston moves down, drawing the air-fuel mixture
- Step 2: The intake and exhaust valves are closed. The piston rises, compressing the air-fuel mixture
- Step 3: Both valves, spark plug emits a spark causing the explosion of the fuel-air mixture. The pressure supplied to allow the piston down

– Step 4: The exhaust valve opens and the piston back to the evacuation of burnt gases which is found at the exit of exhaust

The most famous example of a vehicle which is using a ICE is the Bugatti Veyron ®,(FIGURE. 27). This car is a 1001 HP (736 kW), and can accelerate from 0 to 100 km/h in 2.5 seconds. However, its consumption is 24 liters per 100 km in a regular mode and 80 liters per 100 km in a sportive mode. The Bugatti Veyron ® is the most expensive car in the world, its price is about 2.2 million $ US, only 450 vehicles were built.

Figure 27. Bugatti Veyron ® vehicle, (Picture courtesy Bugatti)

In our study, the main ICE characteristic is the iso-consumption map which is shown in FIGURE. 28. This figure shows the map consumption according the ICE speed and torque. The dash line shows the optimal ICE operation; where the ICE should always operate to use less fuel as possible.

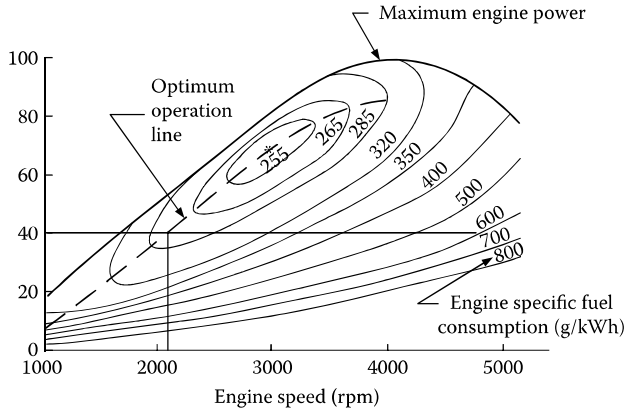

Figure 28. ICE iso-consumption map[45]

The goal in a PHEV or HEV is to be able to work always at its best efficiency or at the lower specific fuel consumption, even if the drive cycle power is lower than the engine power. The difference between the required power and the power at best efficiency is given to the battery. The relation between the efficiency and the specific fuel consumption is given in (1.16), where the energy density is 42.7 MJ/kg for fuel and 41.9 MJ/kg for diesel.

$$\eta_{ICE} = \frac{1\text{kg} * 3.6\,\text{MJ}(1\text{kW}h)}{\text{energy density} \cdot \text{specific fuel consumption}} \tag{1.16}$$

1.2.6 *Conclusion*

This study considers only a PHEV which uses two sources: battery and ICE. However the system is adaptable and can be used with all sources which were described before. The SoC estimation used in this dissertation is the Coulomb counter method for its ease of usage.

1.3 LEVEL CHARGING

According to [17], North America has developed three levels of EV battery charging. Level-1 charging is for residential and commercial buildings. Maximum power for level-1 charging is 1.44 kW, with a 120 VAC and 20 A. In other cases, this current value could be only up to 15 A. Level-2 charging is specified for public and private facilities. The maximum power is 8 kW with single phase of 240 VAC and 32 A. Normally, building outlets are designed for 15 A, which is enough to charge small EV battery packs. Finally, level-3 charging, called *Fast charging*, is the only comparative charging level that can match gasoline time of re-fuelling. The power in level-3 charging is between 50 kW and 100 kW, with 480 VAC (three phase supply).

However, in France and Europe in general, level-1 is called *Standard*, level-2 is called *Accéléré*, and level-3 is *Rapide*, with power levels of: 3 kVA (230 VAC, 16 A), 22 kVA and 43 kW in AC mode (400 VAC, 63 A), and 50 kW in DC mode (500 V, 100 A), respectively. Renault has also developed the *Quick drop*, which is a battery station. It is a robot that replace the discharged battery with a fully charge battery

Time for charging is provided in the following TABLE. 3.

Level-1	Level-2	Level-3	Quick-drop
6h - 8h	3h - 4h	10 min for 50 km	3 min

Table 3. EV battery time charging

In this dissertation, only levels 1 and 2 are considered, and it is assumed that the EV does not use another source of charging (EV is only charged at home - either from grid or Photovoltaic panel (PV)/wind/grid combination).

1.4 RENEWABLE ENERGY SOURCES

Renewable energy is an energy source renewing fast enough to be considered inexhaustible on a human time scale. Renewable energy is derived from regular or constant natural phenomena, mainly the sun (radiation), but also the moon (tides) and the earth (geothermal energy). It exists also hydro-energy which comes from water, wind-energy which is generated by wind-turbines and biomass. Biomass refers to the set of animal or fungal plant origin (including algae), organic matter (fungi) can become a source of energy by combustion (eg : wood energy) after anaerobic digestion (biogas) or after further chemical transformations (biofuel).

In this study only wind and solar energy are considered. These two energies are described in this section.

1.4.1 *Wind power*

A wind turbine captures wind kinetic energy and converts it into a torque, which turns the rotor blades. Three factors give the relation between the wind energy and the mechanical energy recovered by the rotor: the air density, the blade diameter, and the wind speed.

If we consider a "pack"of air, with a mass m that runs at speed v, its kinetic energy E_c is given by

$$E_c = \frac{1}{2} m v^2 \tag{1.17}$$

By definition, the power is the energy per unit time. The power derived P_a from an air mass m running at a speed v through a section A is:

$$P_a = \frac{Energy}{Time} = \frac{1}{2} \frac{Mass}{Time} v^2 \tag{1.18}$$

The mass flow $\dot{m}$ through a section A is the product of the air density ρ, the speed v, and the section A :

$$\frac{Mass\ of\ air\ passing\ through\ A}{Time} = \dot{m} = \rho A v \tag{1.19}$$

In combining (1.18) and (1.19), the important relation is given by:

$$P_W = \frac{1}{2} \rho A v^3 \tag{1.20}$$

where:

P_W : Wind power (W)
ρ : Air density (kg/m^3) at 15°C and 1atm, ρ = 1.225 kg/m^3
A : Section which the mass of air through (m^2)
v : Wind speed (m/s)

1.4.2 *Wind Turbine*

A wind turbine is composed of different parts (FIGURE. 29):

- Tower: is more or less high depending of the height of the wind turbine. More the tower is height, better is the efficiency because the blades are not hindered by obstacle. Some tower can reach up to 100 meter in hight.

- Nacelle: is the heart of the wind turbine. It is here that the energy is produced by the movement of the propeller in electricity and the rest of the equipment which directs the blades depending in the strength wind (brake, controller...) The nacelle supervise the wind turbine which can be stopped as soon as the wind is not enough or too strong.

- Rotor: consists of the nose of the wind turbine and the propeller. The propeller is usually composed of three blades. The blades are placed in font of the nacelle. The blades produce mechanical energy which is converted into electricity by the nacelle.

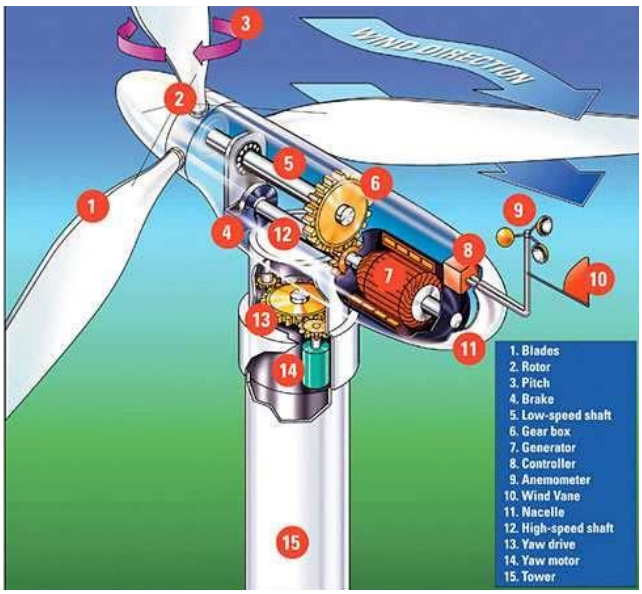

Figure 29. Wind turbine description [53]

1.4.3 *Solar Energy*

Solar energy is the energy from sunlight. Solar energy is the source of all energy on earth, with the exception of nuclear energy, geothermal, and tidal power. This energy is harnessed using different solar technology mainly solar PV, solar thermal.

Equivalent Circuit of PV

The simplest equivalent circuit, describing the behavior of a PV cell is given by FIGURE. 30. It consists of a diode in parallel with an ideal current source. This current source provides a current, which depends directly on the solar irradiation on the cell.

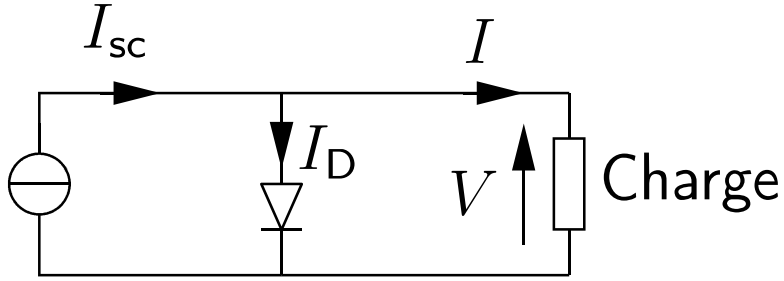

Figure 30. Simplify PV diagram

The voltage-current (VI) characteristic for the p-n junction diode is described by the Shockley diode equation:

$$I_d = I_o(e^{\frac{qV_d}{KT}} - 1) \tag{1.21}$$

where:

Id	:	Current of the diode
V_d	:	Voltage of the diode
I_o	:	Saturate current
q	:	Electron charge 1.602 x 10^{19} C
k	:	Boltzmann constant 1.381 x 10^{-23} J/K
T	:	Temperature in Kelvin

The equation resulting from the FIGURE. 30 is:

$$I = I_{sc} - I_d \tag{1.22}$$

Combining equations (1.21) and (1.24), the final equation is:

$$I = I_{sc} - I_o(e^{\frac{qVd}{KT}} - 1) \tag{1.23}$$

A more detailed (complex) equivalent circuit model of a PV cell is given in FIGURE. 31. The circuit comprises of a leakage resistance R_p in parallel with a current source and a series resistance R_s, which corresponds to the contact resistance.

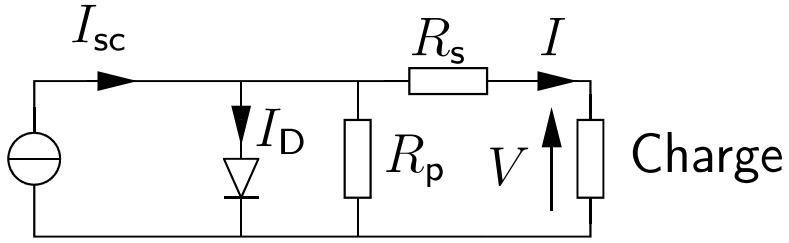

Figure 31. PV diagram

The cell equation becomes :

$$I = I_{sc} - I_d = I_{sc} - I_o(e^{\frac{qVRs}{KT}} - 1) - (\frac{V + IR_s}{R_p}) \tag{1.24}$$

The power, which is produced by the PV module, is given by the basic equation $P = U \cdot I$, where U and I are the voltage and the current of the PV respectively.

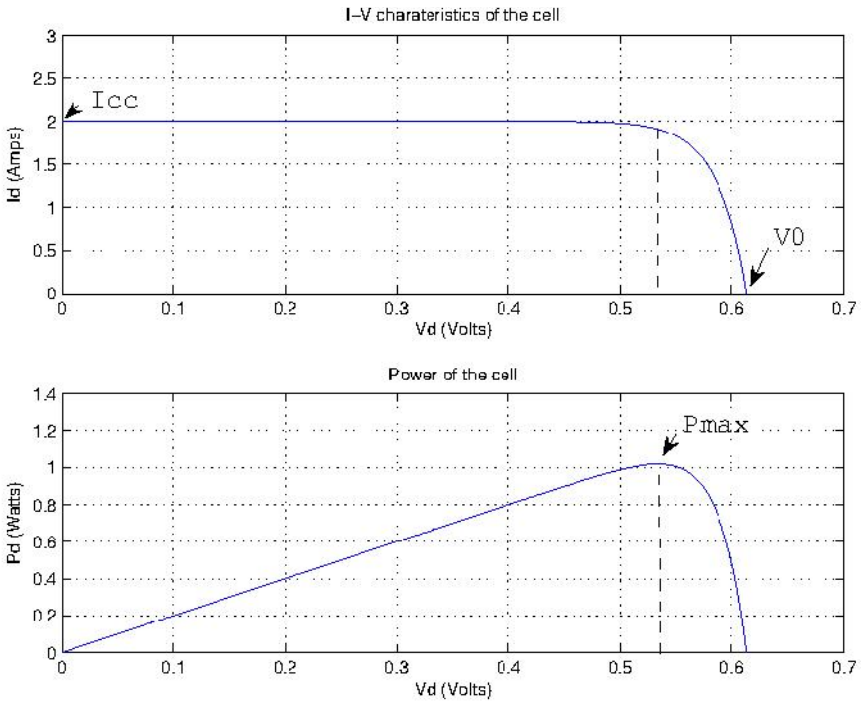

Figure 32. I-V and power diode characteristics

1.5 CONCLUSION

This chapter covered different EV/HEV architectures including PHEV which is a derivation of HEV architecture.

The main objective is to eventually move to all-electric vehicle propulsion, and charging from green, renewable energy sources, like wind and PV. However, before shifting all conventional vehicles to EV/PHEV, the mentality and lifestyles of the common public has to change. In addition, charging infrastructure has to be ready and up-to-date. As more EV/PHEV are sold in the market, the price of these vehicles will come down. A new and smart grid has to be implemented to support the quantity of EV/PHEV battery charging.

The next chapter presents the ÉcoTerra house which is Net Zero Energy House (NZEH) located in Eastman (Québec, Canada) where the consumption and production energy were collected. In addition, a scenario interface is presented. This interface allows to create a one day cycle. Moreover, different system topologies are also described.

2 PROBLEM DESCRIPTION

This project is part of a larger Natural Sciences and Engineering Research Council of Canada (NSERC) project titled "Smart Net-Zero Energy Buildings Strategic Research Network". The main objective of this NSERC project is to develop ways to integrate the control of all building subsystems so as to optimize the net renewable energy fed into the grid and the electricity demand profiles [54]. This study is aligned with the main project under two sections: section 1 title "Smart building operating strategies for net zero energy homes and small buildings", and subsection *c* title "EV/PHEV utilization for electrical storage for a solar house".

In this research, section 1 is taken into account by using data from NZEH to generate the household loads and local production production profiles. This loads are part of the micro-grid that includes a PHEV as shown in FIGURE. 33.

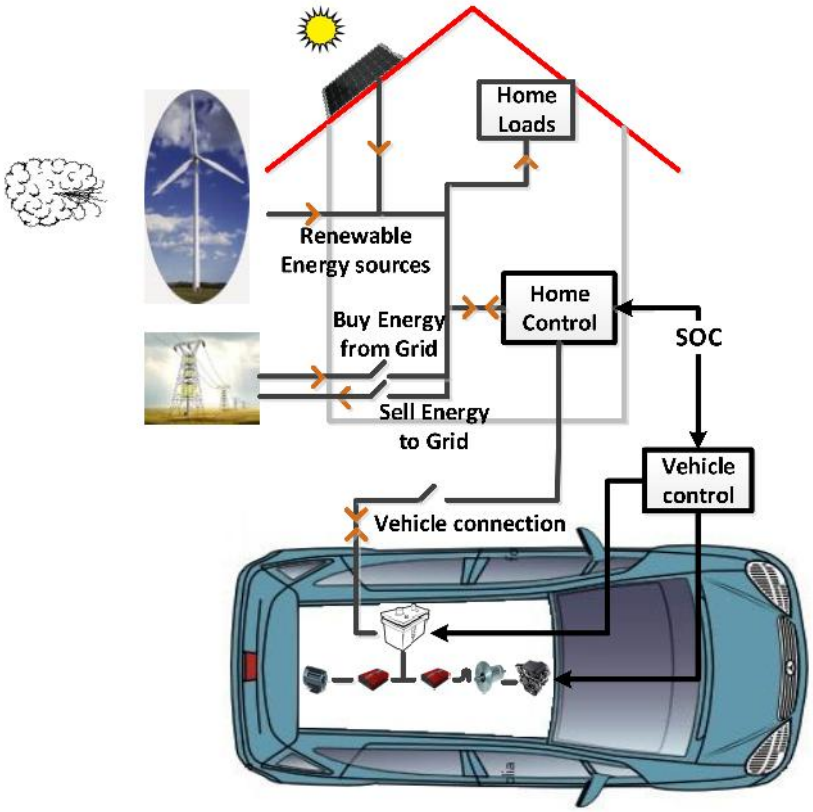

Figure 33. Micro-grid diagram

The PHEV battery used to store energy that is later used for the peak shaving. Therefore this work proposes two controllers that manage the power flows in the micro-grid and the PHEV which main goal is to minimize the overall energy cost. This accounts for subsection *c* of the main project, by using renewable energy sources and PHEV battery for energy storage.

According to [55] the micro-grid system is defined as: a micro-grid is an electrical system that includes multiple loads and distributed energy resources that can be operated in parallel with the broader utility grid or as an electrical island.

In this system, the home is connected to the grid and to N-number of renewable energy sources. In FIGURE. 33, renewable energy sources are represented by the solar and wind energy. However, more renewable energy sources can be added.

When the PHEV is connected to home, the battery can be charged either from renewable energy sources, or the grid, or both. This energy flow is called Home-to-Vehicle (H2V). The battery can also supply home loads, which in turn, helps back-up the grid. This energy flow is called Vehicle-to-Home (V2H). When the PHEV is disconnected from the home, the vehicle is propelled either by the battery, or the engine, or both. The battery is used as a buffer, and can be charged from the renewable energy source(s), whenever available.

In addition, two controllers are implemented to manage the energy flows in both cases. Indeed, the home controller is turned on when the vehicle is connected to home and the PHEV controller is switched on when the vehicle is used.

In this chapter, the drive cycle, the battery and the ICE models will be presented. The drive cycle model is based on the Newton second law, the battery and ICE models are based on real data collected from Advisor software developed by National Renewable Energy Laboratory (NREL).

Afterwards, this chapter will present an interface scenario where the consumption and production data from the ÉcoTerra house is stored. Moreover, the interface scenario is used to fill the vehicle and the battery parameters, and the prices which are involved in the system. Finally, the last part, will describe three different topologies whereby the system can be used.

2.1 ÉCOTERRA HOUSE DESCRIPTION

ÉcoTerra house is one of the 12 houses which won the CMHC's EQuilibrium™ [1] competition.

ÉcoTerra was constructed by Alouette Homes with research support from the SBRN [2] and funded from NRCan [3], CMHC, HydroQuébec, Régulvar and others.

The main goal of building the ÉcoTerra house, presented in FIGURE. 34,

1. Canada Mortgage and House Corporation /SCHL: Socété Canadienne d'Hypothèque et de Logement
2. Canadian Solar Buildings Research Network
3. Natural Resources Canada

was to achieve a near NZEH, which means the energy consumption meets the solar energy production over a year, while maintaining the indoor comfort. This 141 m^2 house is built in a 1.1 ha field and is located in Eastman (Québec, Canada). In addition, the house is inhabited by a couple. The house has downstairs, consist of a living room, a dinning room, a kitchen and toilettes (includes the washer and the dryer). Upstairs, there are two bedrooms, an office and a bathroom.

Figure 34. EcoTerra house [56]

FIGURE. 35 shows the comparison between national, R-2000 house[4] and ÉcoTerra house consumption. This figure shows that the house has reduced consumption due to its construction and the addition of solar energy. The net energy consumed by the house is almost zero.

4. The R-2000 Standard includes requirements related to energy efficiency, indoor air quality and the use of environmentally responsible products and materials. However, it does not specify exactly how a house must be built [57]

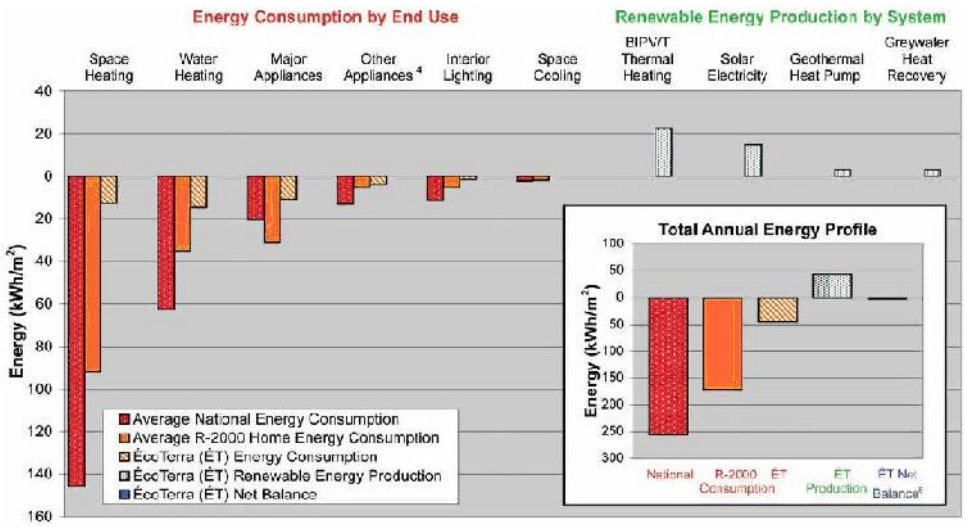

Figure 35. Comparison between National consumption, R-2000 house and ÉcoTerra house [58]

The ÉcoTerra house is not only a near NZEH, but its construction is also environmental friendly. It was made of prefabricated modules to maximize the quality of construction and to reduce the impact on the immediate environment. The house consists of both renewable energy technologies and construction techniques focused on energy efficiency.

This house is equipped by Building-Integrated PhotoVoltaic/Thermal (BIPV/T) located on the south roof. These BIPV/T produce electricity and thermal energy. The thermal energy is used to heat the house, domestic hot water and to supply the dryer via a geothermal pump (FIGURE. 36). A 3 kW BIPV/T was installed to provide 3 420 kWh per year, to help the grid supply household loads.

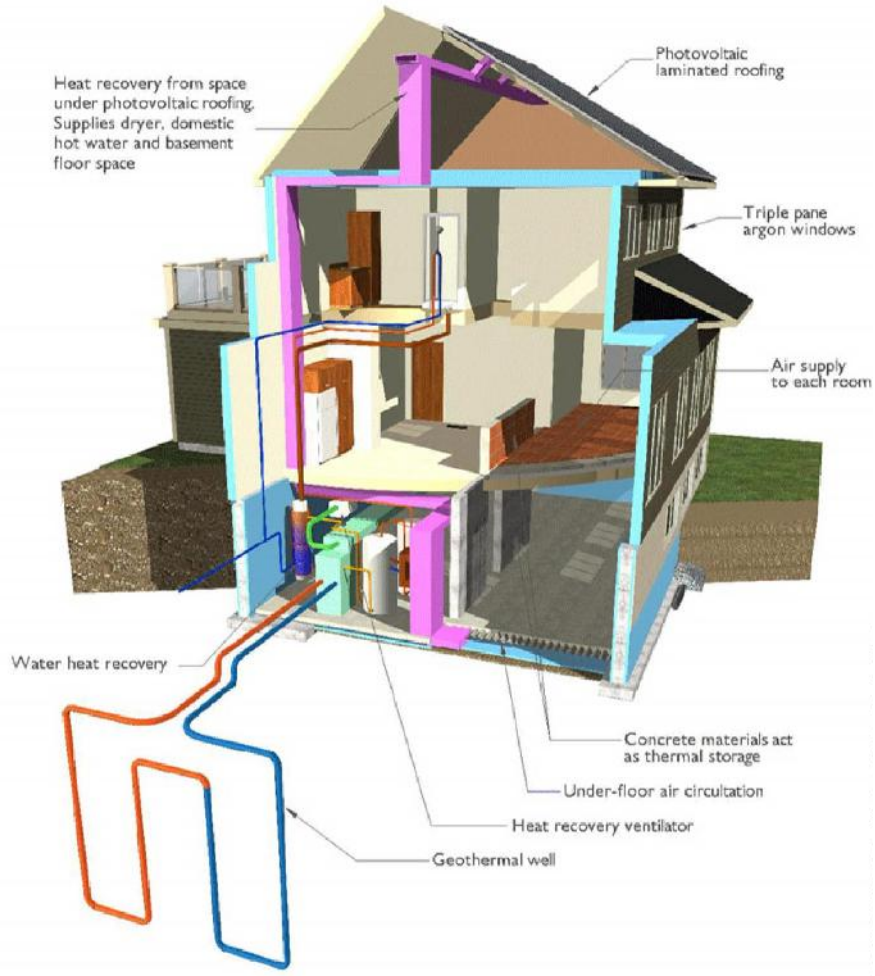

Figure 36. Renewable energy technology diagram [56]

The house was instrumented in 2010 to be able to collect thermal and electrical data. The electrical data is used in this dissertation.

2.2 VEHICLE MOVEMENT DESCRIPTION

This section presents vehicle propulsion power modeling. The main forces acting on the vehicle are aerodynamic drag (F_{air}), rolling resistance (F_r), and grade resistance (F_t). These forces are illustrated in FIGURE. 37 and are a function of vehicle characteristics, acceleration, and vehicle speed.

To calculate the power required to propel the vehicle, the following dynamic equations are applied, (2.1) and (2.2) [38, 45].

$$M_v \frac{d\vec{v}}{dt} = \sum F_{outside} \tag{2.1}$$

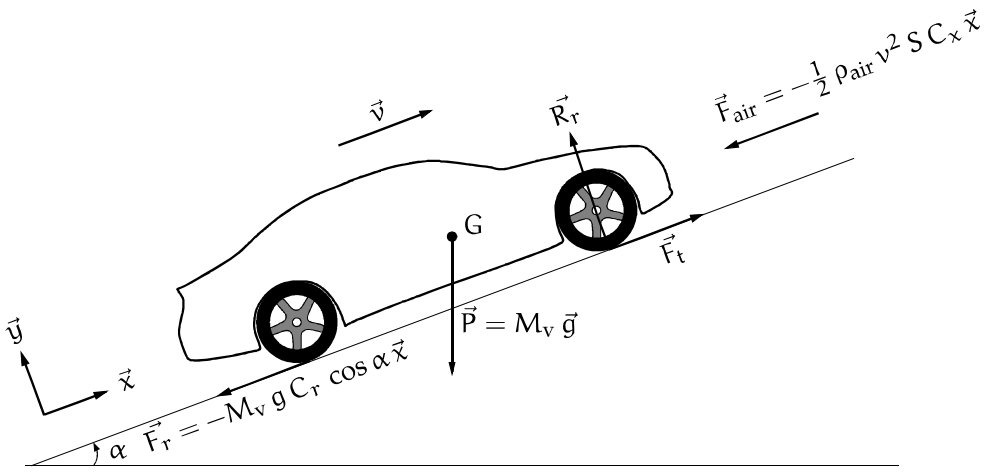

Figure 37. Force acting on a vehicle in motion

$$M_v \frac{d\vec{v}}{dt} = \vec{F}_{air} + \vec{P} + \vec{F}_r + \vec{F}_t + \vec{R}_r \tag{2.2}$$

The gravitational force depends on the road gradient; when the vehicle climbs a hill, the gravitational force is positive. Alternatively, when the vehicle drives down a slope, the gravitational force becomes negative. The gravitational force is provided in equation (2.3)

$$\vec{P} = -M_v g \sin\alpha \vec{x} \tag{2.3}$$

where:

$\vec{P}$	:	Gravitational force (N)
M_v	:	Vehicle weight (kg)
g	:	Gravitational constant (9.81 m/s^2)
α	:	Elevation angle of the road from the horizontal plane

Aerodynamic drag is the air resistance against the car propulsion, the crosswind effects, the lift, and the down-force effects. The vehicle which is represented by the aerodynamic drag coefficient (C_x), plays an important role in the aerodynamic drag calculation.

This coefficient is directly related to the fuel consumption. Aerodynamic drag (F_{air}) also depends on vehicle speed (v) and vehicle frontal area (S) in (2.4).

$$\vec{F}_{air} = -\frac{1}{2}\rho_{air} v^2 S C_x \vec{x} \tag{2.4}$$

where:

$\vec{F}_{air}$: Aerodynamic drag (N)
ρ_{air} : Air density (kg/m^3), ρ = 1.225 kg/m^3
S : Vehicle frontal area (m^2)
v : Vehicle speed (m/s)
C_x : Aerodynamic drag coefficient

Rolling resistance is due to tire friction. The higher the coefficient of drag (Cr), higher is the vehicle resistance, which leads to higher fuel consumption. TABLE. 2.5 gives some rolling resistance for different road conditions.

Condition	Rolling Resistance Coefficient
Car tires on a concrete or asphalt road	0.013
Car tires on a rolled gravel road	0.02
Tar macadam road	0.025
Unpaved road	0.05
Field	0.01-0.35
Truck tire on a concrete or asphalt road	0.006-0.01
Wheel on iron rail	0.001-0.002

Table 4. Rolling resistance coefficient [45]

To reduce the power needed to propel the vehicle, the rolling resistance has to be as low as possible. This can be achieved by using high-quality tires. The rolling resistance is given in (2.5)

$$\vec{F}_r = -M_v g C_r \cos\alpha \, \vec{x} \tag{2.5}$$

where:

$\vec{F}_r$: Rolling resistance (N)
C_r : Rolling coefficient as given in TABLE. 2.5

Then equation (2.2) becomes

$$M_v \frac{dv}{dt} = (-\frac{1}{2}\rho_{air} v^2 S C_x - M_v g \sin\alpha - M_v g C_r \cos\alpha + \vec{F}_t)\, \vec{x} \tag{2.6}$$

Then, the total traction power (P_t) is the traction force on $\vec{x}$ multiplied by the vehicle speed as in (2.7).

$$P_t = v(M_v \frac{dv}{dt} + \frac{1}{2}\rho_{air} v^2 S C_x + M_v g \sin\alpha + M_v g C_r \cos\alpha) \tag{2.7}$$

Equation (2.7) is implemented in the scenario interface program to be able to calculate the required drive cycle power.

2.3 BATTERY MODEL

Different battery models are available in literature [44, 59, 60]. However, these models are too complex to be implemented. Higher the accuracy requires, longer computation time simulation. Therefore, a basic model from Advisor software which is based on real data is implemented. To calculate the battery SoC at each time step, the algorithm calculates the battery's:

- efficiency
- voltage
- current and
- the new SoC

Efficiency calculation: The first step includes efficiency calculation based on the charge ($\eta_{charged}$) or discharge ($\eta_{discharged}$) efficiencies. These efficiencies can be different. The equation is given in (2.8).

$$e = \frac{P_{bat} > 0}{\eta_{discharged}} + (P_{bat} < 0) \cdot \eta_{charged} \tag{2.8}$$

Voltage calculation: The second step is the voltage calculation as described in equation (2.9), where SoC_{list} is a list of SoC given according to V_{OC}, $R_{charged}$ and $R_{discharged}$. The interpolation uses real data from Advisor software.

$$v = interpolation(\overrightarrow{SoC}, \overrightarrow{V_{OC}}; SoC(t-1)) \tag{2.9}$$

Current calculation: The third step calculates the current through the battery. First, the internal resistance has to be calculated as in equation (2.10), this resistance depends on the battery SoC and the battery mode: charge or discharge.

$$\begin{aligned} R = P_{bat} > 0 \cdot interpolation(\overrightarrow{SoC}, \overrightarrow{R_{discharged}}; SoC(t-1)) + \\ P_{bat} < 0 \cdot interpolation(\overrightarrow{SoC}, \overrightarrow{R_{charged}}; SoC(t-1)) \end{aligned} \tag{2.10}$$

Then the current is calculated as given in equation (2.11) where e is the battery efficiency, v is the battery voltage, R is the internal resistance and P_{bat} is the battery power which is an input for the algorithm.

$$I_b = e \cdot \frac{(v - \sqrt{v^2 - 4 \cdot R \cdot P_{bat}})}{2 \cdot R} \tag{2.11}$$

New SoC calculation: Once, the current across the battery is known, the new SoC can be calculated as in equation (2.12) where $Capa$ is the battery

capacity in Ah and T the number of samples for one hour (e.g. 3600 if the sample is in second).

$$SoC(t) = \frac{-I_b}{Capa \cdot T} + SoC(t-1) \tag{2.12}$$

2.4 ICE MODEL

Power $[P_{engine}]$, speed $[\Omega_{engine}]$, torque $[T_{engine}]$ and efficiency η_{engine} are matrix calculated based on the Advisor data: speed vector, torque matrix, torque map and fuel consumption map. Output vectors are taken from the best ICE efficiency which is the red curve on the FIGURE. 38.

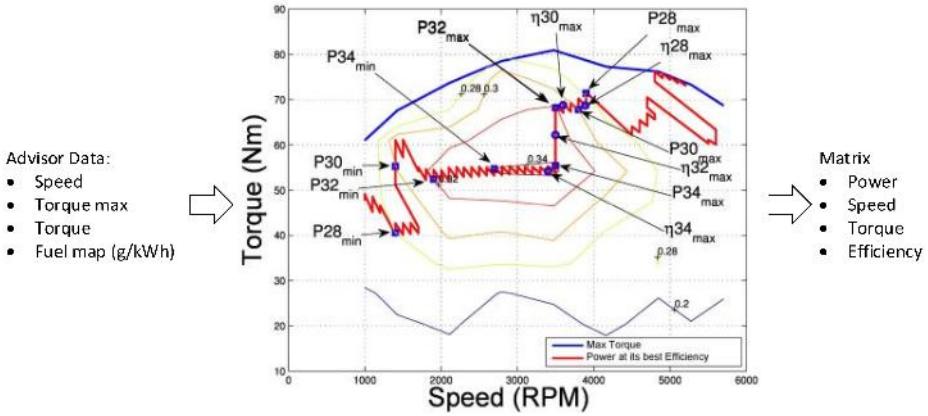

Figure 38. ICE model

To be able to calculate the fuel cost according to a ICE power reference, the algorithm has to calculate the following:

- Real engine power;
- Engine efficiency;
- Fuel cost

Real engine power: The real engine power is calculated as in equation (2.15) where Ω_{engine} and T_{engine} are respectively the interpolation of the speed (2.13) and the torque (2.14) at the engine power P_{ice} reference.

$$\Omega_{engine} = interpolation([P_{engine}], [\Omega_{engine}]; P_{ice}) \tag{2.13}$$

$$T_{engine} = interpolation([P_{engine}], [T_{engine}]; P_{ice}) \tag{2.14}$$

$$P_{engine} = T_{engine} \cdot \Omega_{engine} \frac{2 \cdot \pi}{60} \tag{2.15}$$

Engine efficiency: The engine efficiency is interpolated as in equation (2.16), where P_{engine} is the real engine power and $\overrightarrow{\eta_{engine}}$ the engine efficiency vector.

$$\eta_{engine} = interpolation([P_{engine}], [\eta_{engine}]; P_{engine}) \tag{2.16}$$

Fuel cost: The fuel cost is defined as in equation (2.17) where $Price_{fuel}$ is the fuel price. A figure of 1.351 is used in the conversion of kilograms to liters for gasoline (for diesel is 1.192), m_{fuel} is the fuel mass in kilogram (2.18). Where LCV is the low calorific value (42.7 MJ/kg for gasoline and 42.6 MJ/kg for diesel), η_{engine} is the ICE efficiency and P_{engine} is the real ICE power.

$$Cost_{fuel} = m_{fuel} \cdot 1.351 \cdot Price_{fuel} \tag{2.17}$$

$$m_{fuel} = \frac{P_{engine}}{\eta_{engine} \cdot LCV} \tag{2.18}$$

2.5 SCENARIO INTERFACE

An interface presented in FIGURE. 39, using Graphic User Interface (GUI) from Matlab® software is used to create cycles. A cycle is 24 hours long that consider: solar production, household consumption, drive cycle and drive cycle schedule, parameters of the battery and the PHEV. The price is also defined as on/off peak price. Local solar production and the household consumption data is from the ÉcoTerra house.

In FIGURE. 39, four categories of parameter are detailed to create the scenario. These parameters are explained further under the following: vehicle parameters, energy price, schedule and battery parameters.

Vehicle parameters: Vehicle parameters are set according to the type of vehicle used. TABLE. 5 presents the parameter for the Nissan Leaf® Chevrolet Volt® and the Renault Zoé®. These parameters are related in 2.2. The interface assumes that the road elevation is equal to zero.

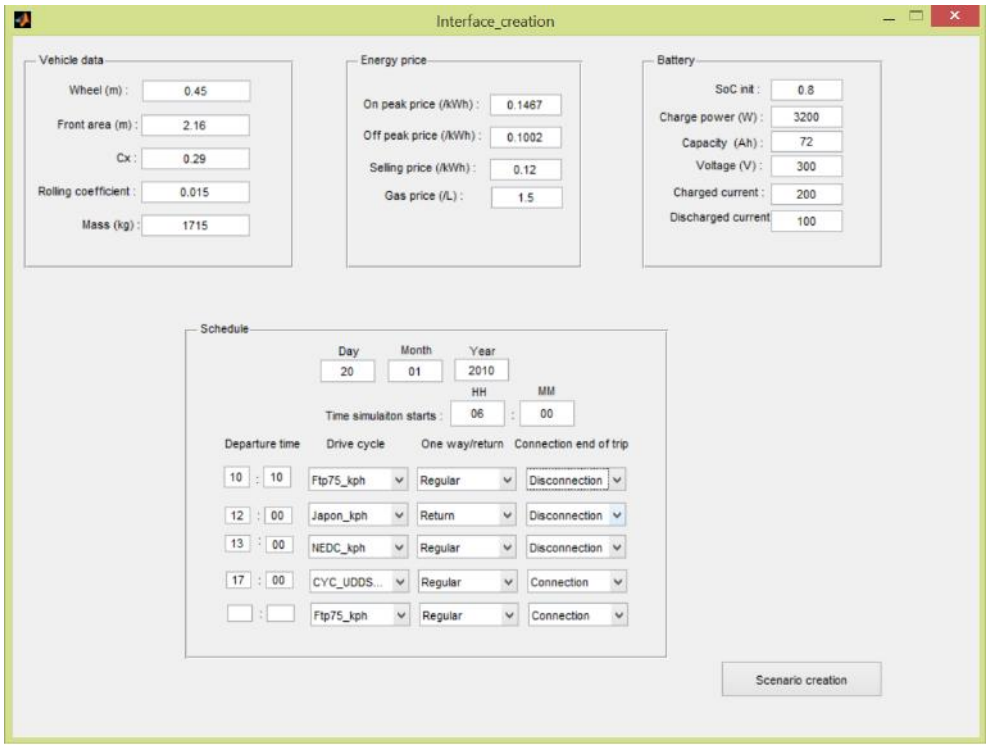

Figure 39. Scenario interface

	Nissan Leaf®	Chevrolet Volt®	Renault Zoé®
Mass	1493 kg	1715 kg	1468 kg
Front area	2.3 m^2	2.16 m^2	2.7 m^2
Drag coefficient (C_x)	0.28	0.28	0.29

Table 5. Vehicle parameters

Energy price: Energy prices in the system are the: fuel, selling and on/off peak power cost. The on and off peak time are defined as in France by Électricité de France, where on peak starts at 6 AM and ends at 10 PM, whereas the off-peak time starts at 10 PM to 6 AM. These periods are correlated to their respect prices; However, it is possible to implement dynamic prices as in [61].

The Québec price can also be used in the system but there is no on and off peak prices. The daily price for the first 30 kWh is 0.056 $ CAD/kWh, after which it becomes 0.083 $ CAD/kW (D tariff). Therefore, the Québec electricity price system is not a function of peak time. The French electricity price system is used in this study to take advantage of the low off-peak prices.

Schedule: The schedule displays the cycle which will be tested. First, the date of the simulation has to be entered according to the data based on the ÉcoTerra house. Then, the start time is chosen for a 24 hour cycle. Afterwards, the departure time(s) of the drive cycle(s) have to be determined. The drive cycles that can be entered in the interface are: Urban Dynamometer Driving Schedule (UDDS), New European Driving Cycle (NEDC), Federal Test Procedure (FTP-75) and Japan 10-15. The drive cycle can be one way or a return (reverse drive cycle). The last column determines if at the end of the drive cycle, the car is connected to home or not.

Battery parameters: These parameters allows to define the determination of the initial battery SoC, the maximum charging power depending on the used charging level, the maximum allowable current in charge mode and discharge mode, the capacity and the voltage of the battery. These last two parameters are used to calculate the number of cells in parallel and in series.

The next section presents two case studies which are used to compare the offline and online simulations, and the experiments.

2.6 CASE STUDIES

This section describes two case studies which will be used in the offline simulation, the online simulation and in the experiments. The first case is a summer day (June 22^{nd} 2010) and the second is a winter day (January 17^{th} 2010). Both cases are 24 hours and comes with the same schedule as:

- 6 AM: simulation starts;
- 8 AM: driver goes to work using the UDDS driving cycle;
- 12 PM: driver goes to lunch place using the NEDC driving cycle;
- 1 PM: driver goes back to work using the reverse NEDC driving cycle;
- 5 PM: driver goes back home using the reverse UDDS driving cycle and connects the PHEV;
- 6 AM the day after: simulation ends.

The ICE map is depicted in FIGURE. 40 and its characteristics are [5]:

- Maximum power: 41 kW at 5700 RPM
- Peak torque: 81 Nm at 3477 RPM

5. This data comes from transient testing on the FTP-75 drive cycle

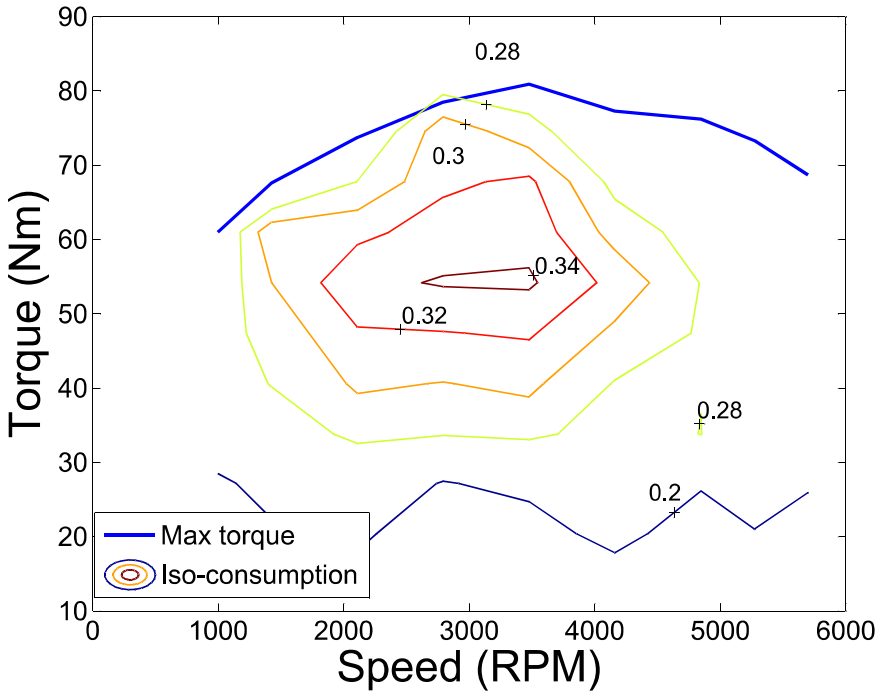

Figure 40. ICE map

The following battery pack characteristics are:
- Capacity : 72 Ah
- Battery voltage: 300 V
- Maximum power in the bidirectional charger: 3200 W
- Maximum current in charging mode: 200 A
- Maximum current in discharging mode: 100 A
- Initial SoC: 0.8

This study assumes that the battery can only be charged at home, and the PHEV used is a series topology. In addition only 60 % of the regenerative braking is taken into account.

The vehicle characteristics are as follows:
- Wheel diameter: 0.45 m
- Front area: 2.16 m^2
- C_x: 0.29
- C_r: 0.015
- Mass: 1716 kg

All these characteristics are used to calculated the power required for the different drive cycles. The results are shown in FIGURE. 41

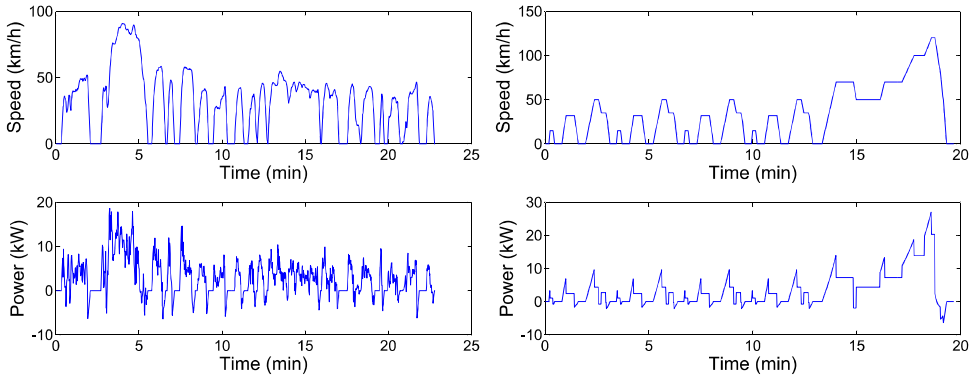

(a) Home to work: UDDS drive cycle

(b) Work to lunch: NEDC drive cycle

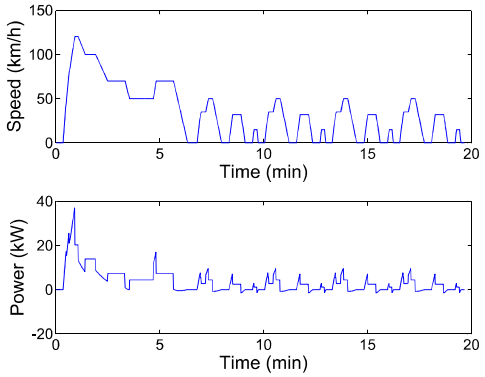

(c) Lunch to work: reverse NEDC drive cycle

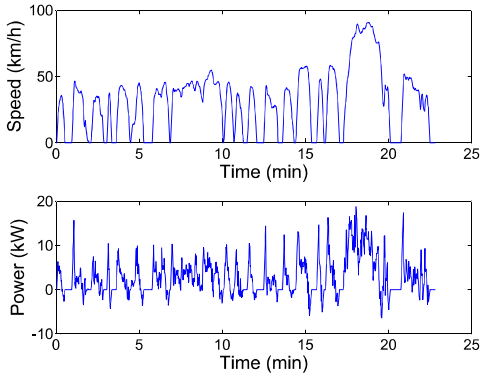

(d) Work to home: reverse UDDS drive cycle

Figure 41. Speed and power of drive cycles

This study uses the electricity price as defined in France by Électricité de France as presented in FIGURE. 42.

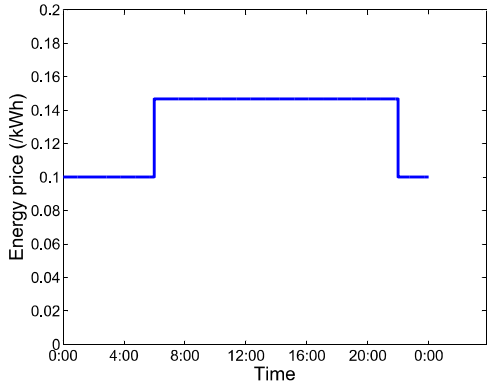

Figure 42. Electricity price during a day

Off-peak starts at 10 PM and ends at 6 AM, at a cost of 0.1002 €/kWh. The rest of the day is on-peak at a cost of 0.1467 €/kWh. The selling price to the grid is set at 0.12 €/kWh which occurs only when the production is higher than the consumption and if the PHEV is connected, the battery is fully charged.

The gasoline price is set at 1.5 €/liter.

Summer case The summer solar production and household consumption are presented in FIGURE. 43.

The solar production is at its highest point at around midday. There are two peak periods: one in the morning at 10 AM and the other one in the evening around 8 PM. The peak in the morning will be absorbed by the solar production, whereas evening one has to be reduced by the PHEV battery to smoothen the electric grid production.

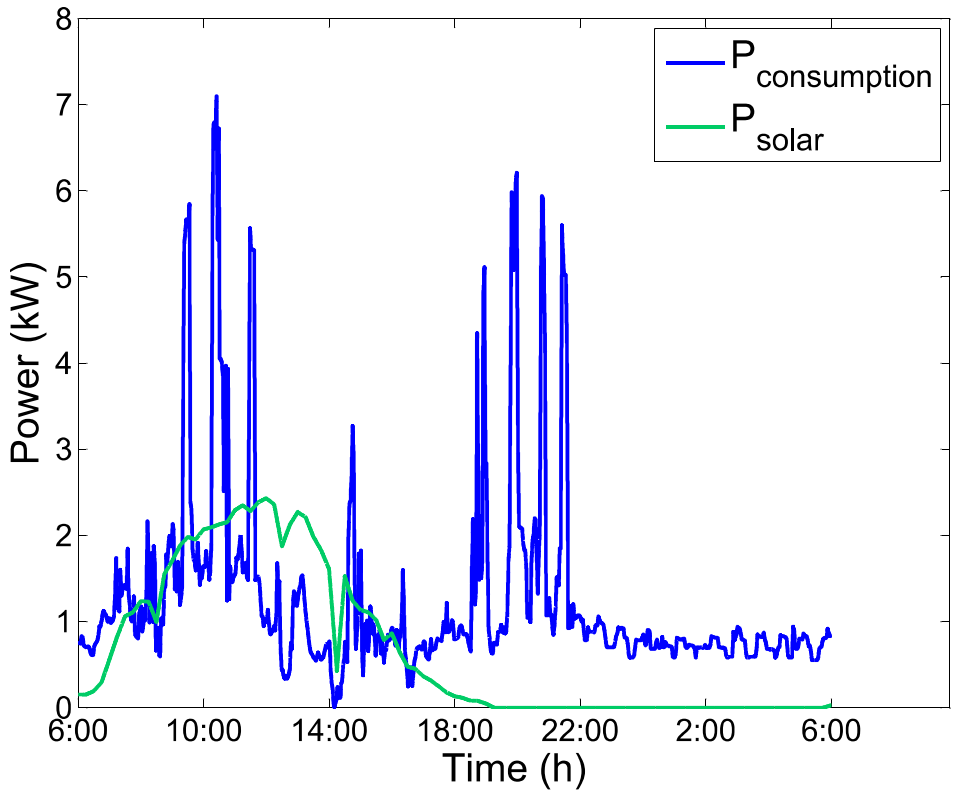

Figure 43. Solar production and household loads for a summer day: June 22nd

Winter case The winter case shown in FIGURE. 44 shows the important peaks in the morning before driving to work, and in the evening when people get home.

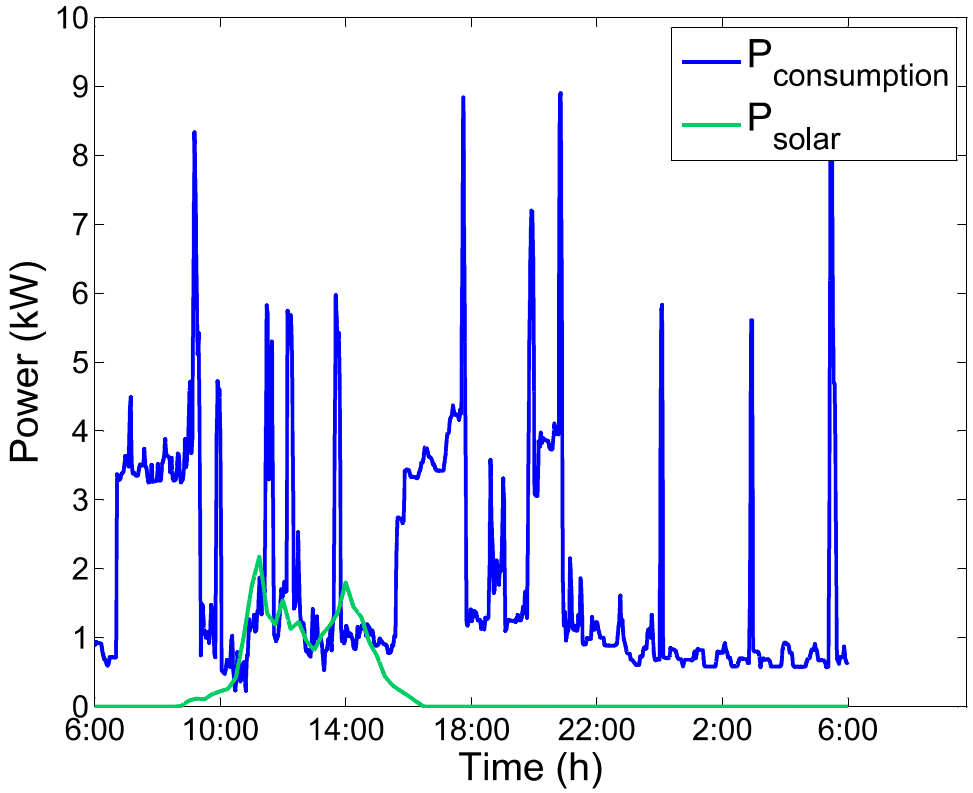

Figure 44. Solar production and household load during a winter day: January 17^{th}

Other peaks are due to heating. The solar production is low. The energy control strategy has to reduce these peaks to smoothen the electric grid production.

To be able to simulate the system, three topologies can be implemented. The next section discusses about these possible topologies: DC bus, AC bus, complex bus.

2.7 SYSTEM TOPOLOGY

To implement the system, three different topologies exist which are the DC bus, the AC bus or the complex bus (combination of AC and DC buses). The system includes the power production from wind turbine, PV, the household loads, the EV/ PHEV battery and the grid.

2.7.1 *Topology 1: DC Bus*

The DC bus topology, shown in FIGURE. 45 includes five energy conversions, where one is inside the PHEV:

- from PV to the DC bus including an Maximum power point tracker (MPPT);
- from wind turbine energy production to the DC bus;
- from the grid to the DC bus and from the DC bus to the grid;
- from the DC bus to the household loads;
- from the DC bus to the PHEV battery and from the PHEV battery to the DC bus.

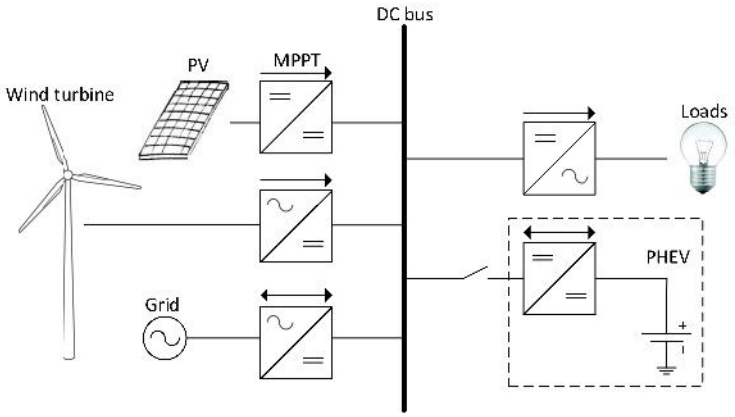

Figure 45. Topology 1: DC bus

This topology has higher losses due to the number of energy converters. However, every module is controllable with its associated converter.

2.7.2 *Topology 2: AC Bus*

The AC bus topology, presented in FIGURE. 46 uses only three converters. An AC/DC bidirectional is implemented in the EV/ PHEV to be able to charge the battery and to supply the AC bus. The MPPT DC/AC converter is a combination of a DC/DC converter and a DC/AC converter.

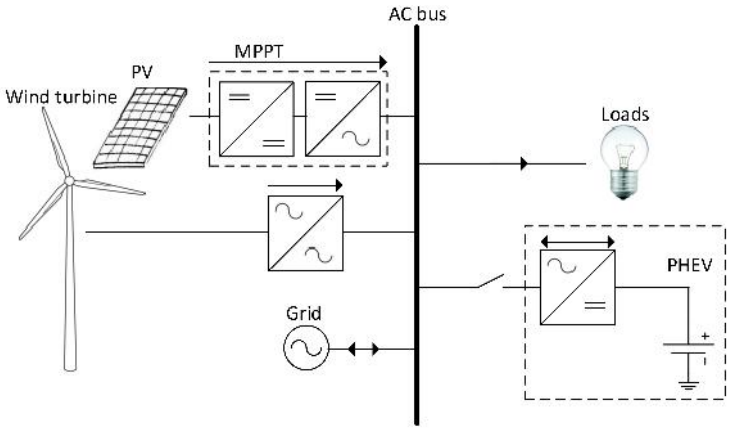

Figure 46. Topology 2: AC bus

This topology uses less number of converters than the previous topology using a DC bus. Nevertheless, to control an AC bus is not easy, because it has to comply with the grid standard to be able to inject energy into the grid.

According to the Commission de Régulation de l'énergie, in France [6], the frequency has to be between 49.5 Hz and 50.5 Hz and the voltage has to be at 230 V (± 10 %). In addition the power factor has to be higher than 93 %. Whereas, according to the Canadian Standards Association, the voltage has to be between 106 V and 127 V for a nominal voltage of 110 V. The power factor cannot be below 95 % and the frequency is around 60 Hz.

2.7.3 *Topology 3: complex bus*

The last topology depicted in FIGURE. 47, is a more complex architecture which is composed of a DC and AC bus. Both buses are connected by a bidirectional DC/AC converter. The other two converters are associated with their renewable energy sources. The on-board EV/ PHEV charger is included in the bidirectional DC/AC converter.

This topology uses only three converters, that requires more complex control strategy but it reduces the energy conversion losses [62]. This topology has also meet the grid interconnection standards, defined in section 2.7.2. Removing the on-board charger, reduces the weight of the EV/PHEV, in addition to reducing the energy consumption. However, the battery has to have an access on the DC bus to be able to charged the battery somewhere else that at home.

This topology is chosen to be implemented in the simulations and experiment because of the less number of converters, and according to the availability in the laboratory.

6. Regulatory Commission Energy

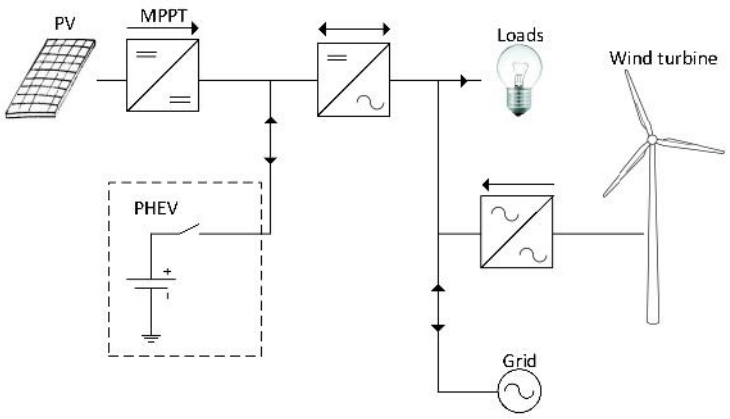

Figure 47. Topology 3: complex topology

2.8 CONCLUSION

This section has presented project: "Smart Net-Zero Energy Buildings Strategic Research Network". The project uses a near NZEH named ÉcoTerra which was instrumented in 2010 to collect temperature, solar production and household loads.

Moreover, the second Newton law was used, to present the drive cycle power which is used to model the vehicle consumption.

Afterward, a scenario interface that is able to create any 24h scenario using the ÉcoTerra data is presented. This scenario interface includes all prices, battery and vehicle parameters which are involved in the system. Finally, three different topologies are presented to model the system, where the third topology (complex topology) that uses the combination of AC and DC buses, is selected for this study.

The next chapter, presents offline simulations using a dynamic programming algorithm. The algorithm is used to find the minimum cost of a day for known values. The findings of this algorithm are used as a reference for the online simulation and the experiment.

3

OFFLINE SIMULATION : DYNAMIC PROGRAMMING ALGORITHM

The offline simulation is the first step in optimizing the energy flows of the micro-grid system (home and PHEV). The simulation goal is to minimize the cost over a 24 hours simulation run, which also generates a reference for online simulation and the experimental studies. There are two optimization families: the global optimization and the real time optimization [63, 64, 65]. Optimization is first used to minimize the energy cost for know input data, that allows the use of global optimization such as linear programming, dynamic programming (DP) or genetic algorithm.

To find the reference cost, a generic dynamic programming Matlab function, developed by O. Sundstrom and L. Guzzella [66] is implemented. The advantage of dynamic programming over the other techniques is that it can be used to find the global minimum cost, whereas genetic algorithm can give minimum local cost. However, the drawback of dynamic programming algorithm is the longer computation time compared to genetic algorithm.

Dynamic programming solves complex problems by breaking them into simple subproblems. The key is to use simple models to reduce computation time.

This chapter presents the optimization objective function and its constraints. Summer and winter results, as well as the monthly cases are also discussed.

3.1 SYSTEM MODEL: MICRO-GRID SYSTEM

The micro-grid system is divided into two parts: when the vehicle is connected to home (FIGURE. 48) and when the vehicle is disconnected (FIGURE. 49, FIGURE. 50).

In the first case, the vehicle is connected to home (FIGURE. 48). Renewable energy sources ($P_{production}$) supply the household load directly (P_{load}). The energy difference (P_{net}) supplies either the grid (P_{grid}) or the vehicle battery ($P_{battery}$). However, when renewable energy sources are not enough, the grid, or vehicle battery, or both, meet the household loads.

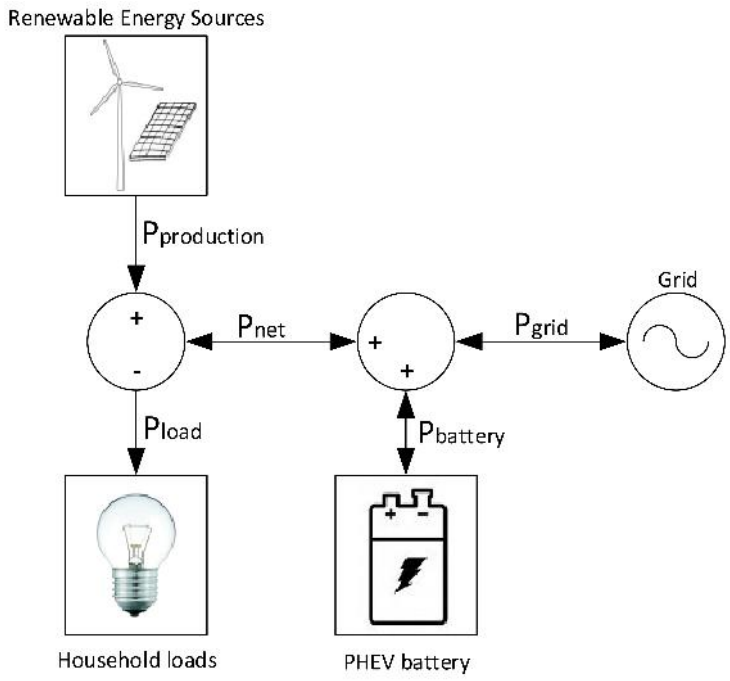

Figure 48. DP function when PHEV is connected to home

In the second case, the vehicle is disconnected from home. This case is divided into two sub cases: home and PHEV.

In the sub case depicted in FIGURE. 49, the drive cycle power can be either positive or negative. When the drive cycle power (P_{drive}) is positive, either the battery or the ICE or both propel the vehicle. P_{drive} is calculated from the second law of Newton in section 2.2. Alternatively, when it is negative, the battery is charged using the regenerative braking mode through the traction motor.

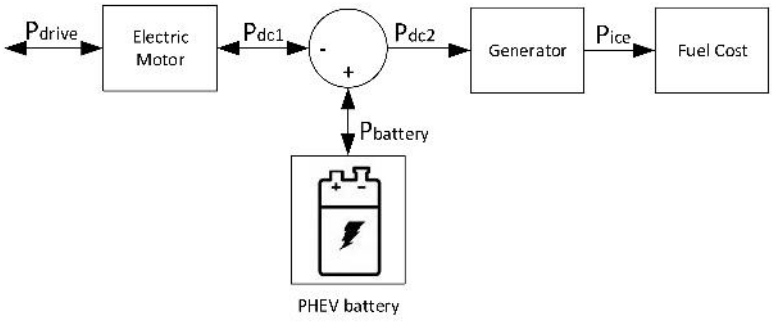

Figure 49. DP function when PHEV is disconnected to home: Series PHEV model

On the house side (FIGURE. 50), the household loads are supplied by the renewable energy sources or/and the grid. In this case there is no control.

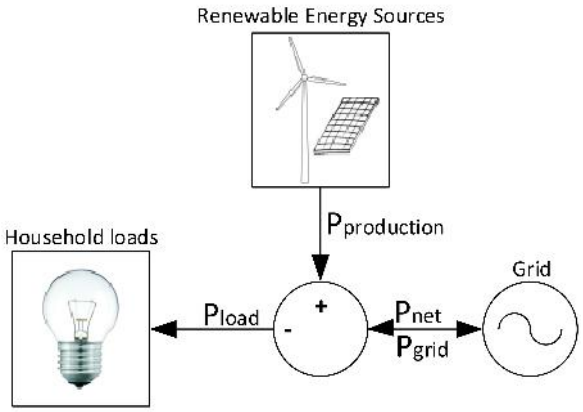

Figure 50. DP function when PHEV is disconnected to home: Home model

The battery is common to both cases; in FIGURE. 48 when the vehicle is connected to home, and in FIGURE. 49 when the vehicle is disconnected. The next section describes the dynamic programming algorithm using the micro-grid model.

3.2 DYNAMIC PROGRAMMING ALGORITHM

Dynamic programming is a mathematical tool for studying the sequential decision making process that calculates the optimal strategy under a given set of constraints. At each time step, the algorithm takes a decision according to the objective function.

The dynamic programming principal is to solve a complex problem by combining the solutions of the subproblems. Dynamic programming is usually used when the subproblems are dependent on each other. The algorithm developed by O. Sundstrom and L. Guzzella [66] is divided into two parts: the backward dynamic programming and forward dynamic programming algorithm.

The backward algorithm shown in FIGURE. 51, calculates all the possible cases and stores the values in a table, which prevents the recalculation of the same case.

In addition, the algorithm variable is the ICE power (P_{ice}) when the vehicle is disconnected from the house (FIGURE. 48) and the grid power (P_{grid}) when the vehicle is connected to the house (FIGURE. 49) .

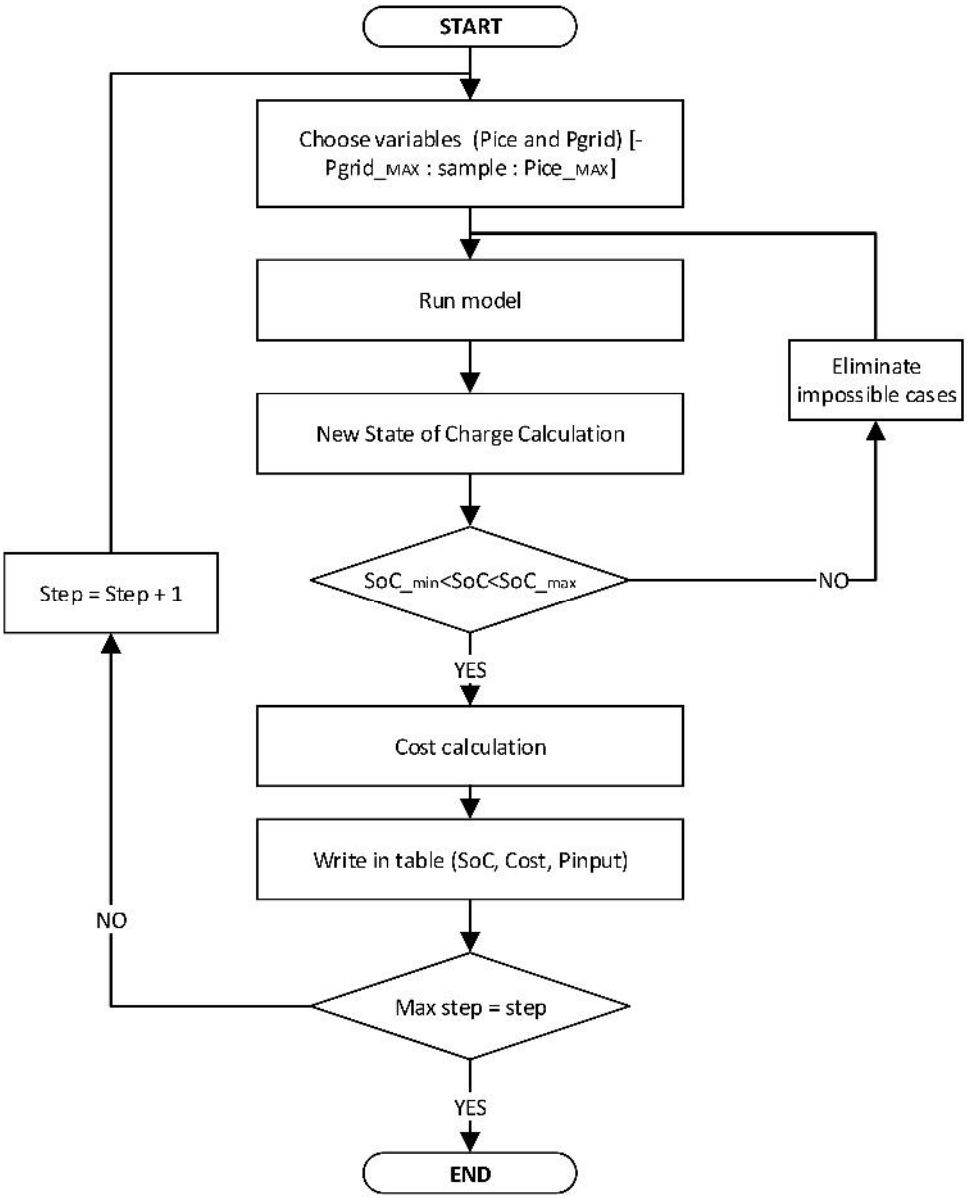

Figure 51. Dynamic programming backward flowchart

The forward algorithm presented in FIGURE. 52, is used to find the minimum or maximum cost taking into account all the possibilities calculated in the backward algorithm within the optimization constraints.

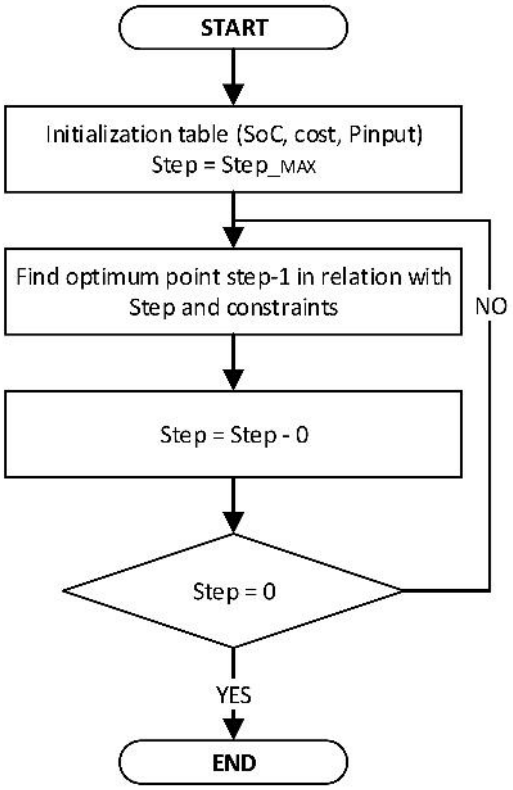

Figure 52. Dynamic programming forward flowchart

The dynamic programming control strategy gives only the minimum or maximum value of the optimization cost function with known value. However, another algorithm has to be used for an online control strategy where the values are not known before the start of the simulation. The algorithm which is used is the fuzzy logic algorithm which is introduced in the next chapter.

3.3 OPTIMIZATION OBJECTIVE FUNCTION

The optimization objective is to minimize the energy cost, including fuel and grid cost based on the equation (3.1).

$$Cost = min \sum_{N=1}^{+\infty} [P_{grid} \cdot Cost_{grid} + P_{N\_renewable} \cdot Cost_{N\_renewable} + P_{fuel} \cdot Cost_{fuel}] \cdot T_s \tag{3.1}$$

Where T_s is the sample time of the simulation. In this case, the sample time is 1 second. $P_{N\_renewable}$ and $Cost_{N\_renewable}$ are the power produced by the

renewable energy sources and its associated price. In this study, it is assumed that renewable sources have been fully paid back or fully subsidized that is there is no associated cost with the use of renewable energy sources. P_{grid} and $Cost_{grid}$ are the grid power and its associated cost, when, P_{grid} is positive, the system sells energy to the grid whereas when it is negative, the system buys from the grid. As described in section 2.5 the grid price is divided into two: on and off peak prices. Finally, P_{fuel} and $Cost_{fuel}$ are the fuel power and the fuel cost respectively.

3.4 OPTIMIZATION PROBLEM

This problem uses the battery has its dynamic system which is defined in (3.2). Where I_b is the battery current, T_s the sample time, C_{bat} the battery capacity (Ah). The battery is limited by its minimum and maximum SoC, as presented in (3.3). Referring to section 1.2.1, the main battery constraint is the SoC, which is set between 30 % (SoC_{min}) and 90 % (SoC_{max}). The discretization of the SoC is 1 %. This value is a good trade-off for the accuracy and the time simulation.

x_0 in (3.4) represents the initial SoC which will depend on the case study.

To make the simulation realistic, a constraint is added; the final SoC equated to the initial SoC. Then, if the simulation starts with a fully charge battery, the simulation has to end with the same SoC that makes the simulation repeatable.

The simulation duration is 24 hours being 86 400 seconds as shown in (3.6) where N is the number of state and T the simulation duration.

$$x_{k+1} = \frac{-I_b \cdot T_s}{C_{bat} \cdot 3600} + x_k \tag{3.2}$$

$$x_k = SoC \in [30\,\%, 90\,\%] \tag{3.3}$$

$$x_o = SoC_{init} \tag{3.4}$$

$$x_n \Rightarrow SoC_{final} = SoC_{init} \tag{3.5}$$

$$N = \frac{T}{T_s} = 86\,400s \tag{3.6}$$

According to the model presented in section3.1, the two variables are P_{grid} when the vehicle is connected to the house, and P_{ICE} when the vehicle is in driving mode. The discretization of the two variables are 200 W. This figure is a compromised between the simulation time and the precision of the system.

3.5 SYSTEM CONSTRAINTS

The proposed problem has three system constraints: the ICE size, the battery current, and the battery charger size.

ICE size is characterized by the maximum power that the ICE can produce where the relation between P_{fuel} and P_{ice} is given in (3.8). Where P_{ice} is the

ICE power and η_{ice} is the ICE efficiency, a function of the ICE power.

$$0 \leqslant P_{fuel} \leqslant P_{fuel\_max} \tag{3.7}$$

$$P_{fuel} = \frac{P_{ice}}{\eta_{ice}} \tag{3.8}$$

The battery current is limited in terms of charge and discharged currents (equation (3.9)). Where $I_{charged}$ is negative and $I_{discharged}$ is positive.

$$I_{charged} \leqslant I_{battery} \leqslant I_{discharged} \tag{3.9}$$

Battery charger size is characterized by the bidirectional converter. The converter is sized according to the level charging described in section 1.3.

$$0 \leqslant P_{charger} \leqslant P_{charger\_max} \tag{3.10}$$

The next sections presents optimization results according to the two scenario described in the previous chapter.

3.6 OPTIMIZATION RESULTS

Based on the scenario describe in section 2.5, two case studies are presented in this section: one in summer and one in winter. Each case is divided into 3 sub cases; where the simulation starts with a fully charged battery, a fully discharged battery and where renewable energy sources are not installed. Each case which is a micro-grid system is compared with the conventional system in terms of cost.

ÉcoTerra data is used to generate the monthly average cost which then gives an annual overview.

3.6.1 *Summer case*

The summer case is divided in three sub cases: where the simulation starts with a fully charged battery (initial SoC = 80 %) , where the simulation starts with a fully discharged battery (initial SoC = 35 %) and the last where renewable energy sources do not exist, and the battery is fully charged (initial SoC = 80 %) .

Battery fully charged: SoC = 80 %

FIGURE. 53, FIGURE. 54 and FIGURE. 55 show the battery SoC, the powers involved in the micro-grid system and the four PHEV drive cycles respectively. This case starts with a battery SoC of 80 %.

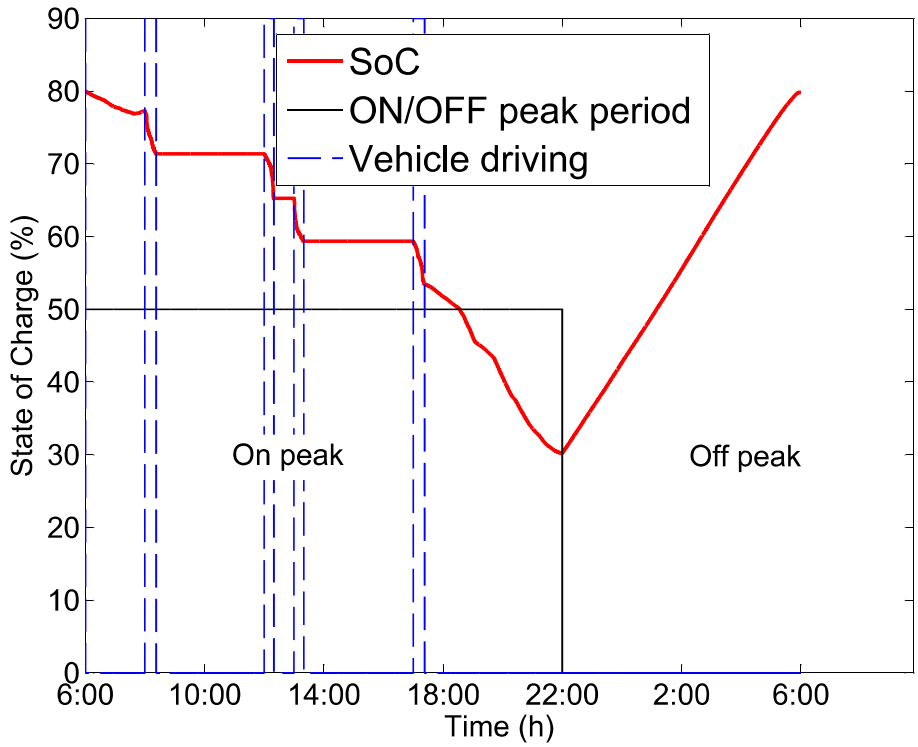

Figure 53. DP: SoC profile for the summer case with an initial SoC of 80 %

The battery is discharged during the on-peak period and is charged during the off-peak period. That is shown in FIGURE. 53 where the discharge occurs between 6 AM and 10 PM, it is then charged in the off-peak period from 10 PM to 6 AM, when the next cycle begins. Moreover, the battery is used at all times during the drive cycle. Only 24 % of the battery SoC is used for driving, while the rest of the energy helps the grid to supply household loads, once the PHEV is connected as shown in FIGURE. 54.

The battery and the grid meet the load demand in the morning before driving to work. It is then used to slightly in the evening before 8 PM, after which it is used for peak shaving up to 10 PM. Once the off-peak period starts, the battery is charged by the grid.

As shown in FIGURE. 55, almost all the way, the battery is used to supply the drive cycle power. However, the ICE is used when the peak drive cycle power is too high to be supplied by the battery (battery size constraint).

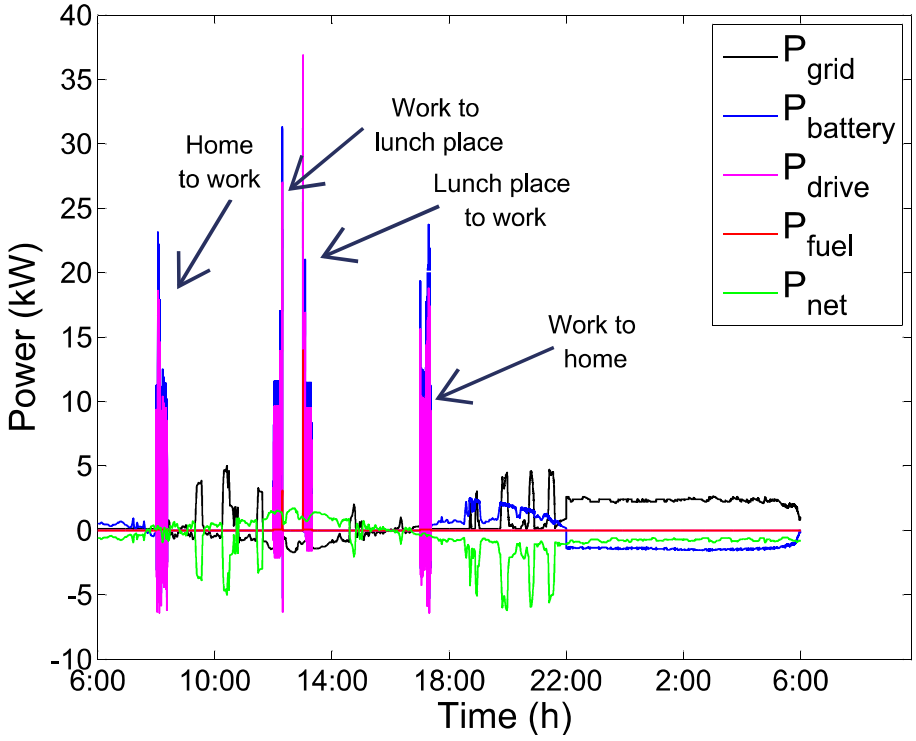

Figure 54. DP: Power profiles for the summer case with an initial SoC of 80 %

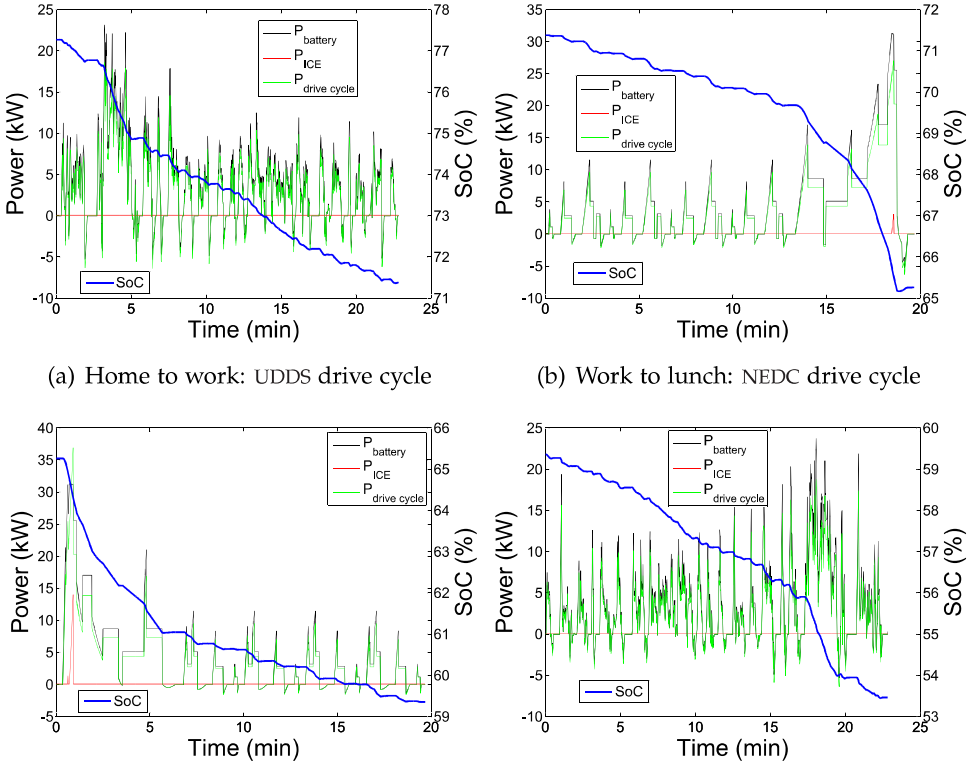

(a) Home to work: UDDS drive cycle

(b) Work to lunch: NEDC drive cycle

(c) Lunch to work: reverse NEDC drive cycle

(d) Work to home: reverse UDDS drive cycle

Figure 55. DP: travel drive cycle for the summer case with an initial SoC of 80 %

TABLE. 6 summarizes energy costs (grid and fuel).

	Conventional system	Micro-grid system
Grid cost	1.92 €	2.41 €
Fuel cost	4.68 €	0.11 €
Total cost	6.60 €	2.52 €

Table 6. DP summer result with a fully charged battery

In this case, about 60 % saving are made by using the micro-grid when compare to the conventional system. The conventional system is a traditional house, where the household loads are connected to the renewable energy sources and the grid. In this system, the vehicle uses ony the ICE for the propulsion. In the micro-grid case, the cost from the grid is higher than the conventional system. However, the fuel cost is almost zero. The conventional system is where the grid supply the household loads and a conventional vehicle is used. These results are shown in TABLE. 6.

Battery discharged: SoC = 35 %

FIGURE. 56, FIGURE. 57 and FIGURE. 58 show the battery SoC, the powers involved in the system and the four PHEV drive cycles respectively. This case starts with a 35 % battery SoC.

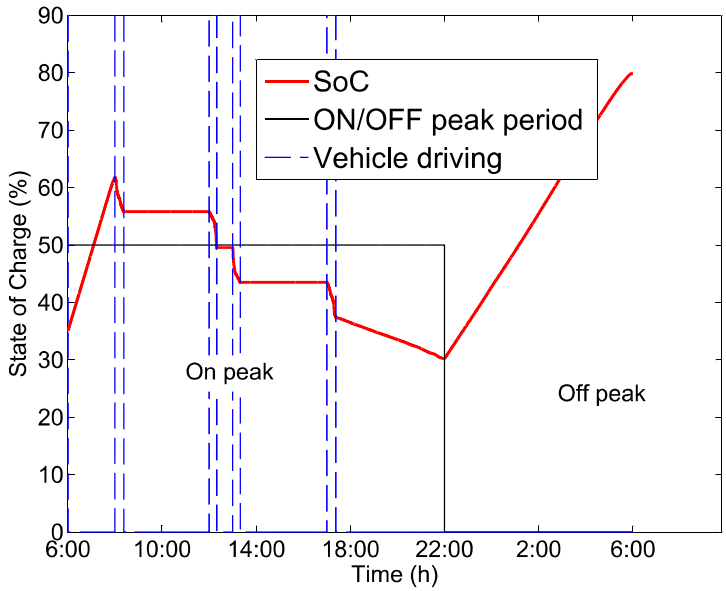

Figure 56. DP: SoC profile for the summer case with an initial SoC of 35 %

For the first two hours, the battery is charged, then the PHEV uses the battery in an all electric range mode. Once the PHEV is connected to home, during the on-peak period, the battery is used to help supply the household loads. It is then charged at the off-peak period to prepare the vehicle for the next day.

FIGURE. 57 shows that in the first two hours of simulation, the net power is negative and low, the grid supplies the loads and also charges the battery. Before the trip to work, the battery is charged to 60 % which is enough for the PHEV's electric range drive mode. This capacity will help the grid during on-peak period. Compared to the previous case, the battery supplies the load with a constant power, which does not take into account the peak power. This is attributed to the level of SoC. Then, during off-peak power the battery is fully charged.

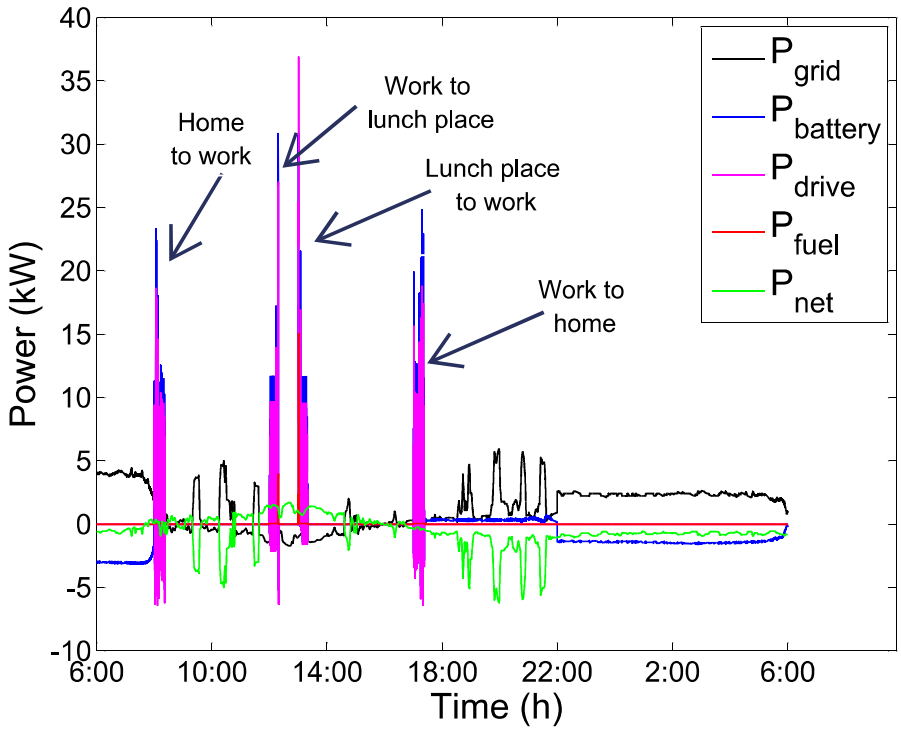

Figure 57. DP: power profiles for the summer case with an initial SoC of 35 %

FIGURE. 58 shows that the battery supply drive cycle power. The ICE is only used when the maximum battery power cannot meet the drive cycle load. During this time, both the battery and the ICE propel the vehicle.

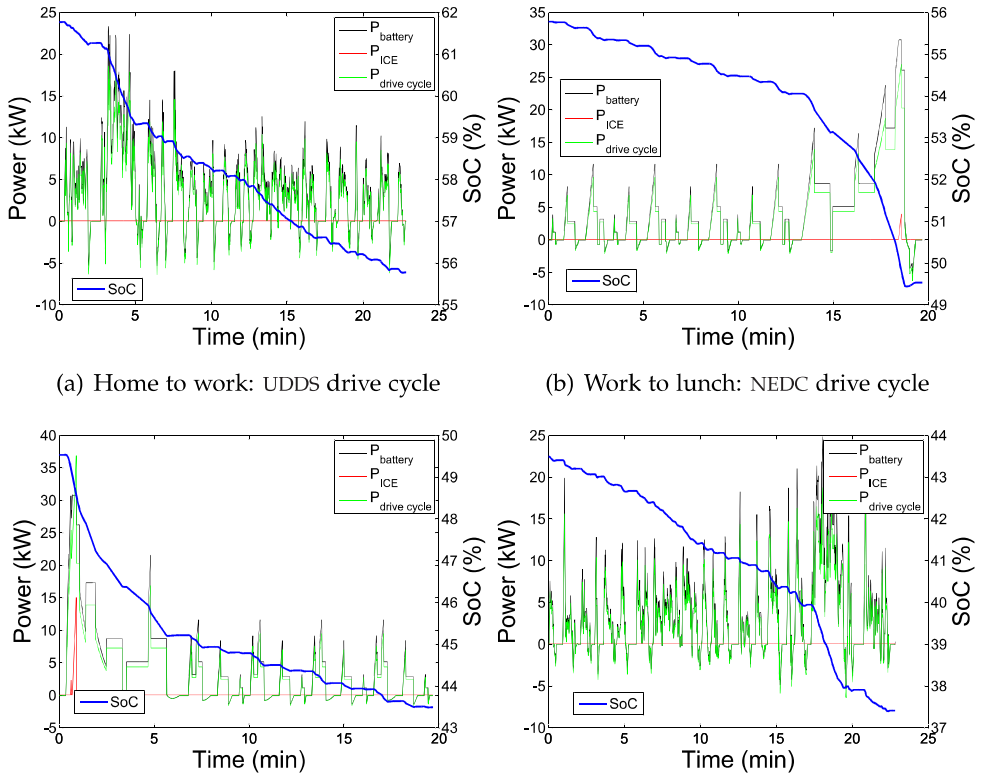

(a) Home to work: UDDS drive cycle

(b) Work to lunch: NEDC drive cycle

(c) Lunch to work: reverse NEDC drive cycle

(d) Work to home: reverse UDDS drive cycle

Figure 58. DP: travel drive cycle for the summer case with an initial SoC of 35 %

Even if the battery was discharged at the beginning of the simulation, a gain of almost 40 % is realized (TABLE. 7).

	Conventional system	Micro-grid system
Grid cost	1.92 €	3.95 €
Fuel cost	4.68 €	0.12 €
Total cost	6.60 €	4.07 €

Table 7. DP summer result with a fully discharged battery

The gain is less than the previous sub case. Nevertheless, the gain justifies the use of the micro-grid system.

Without renewable energy sources

FIGURE. 59, FIGURE. 60 and FIGURE. 61 show the battery SoC, the powers involved in the system and the four PHEV drive cycles respectively. This case presents the summer scenario, but solar energy has been removed.

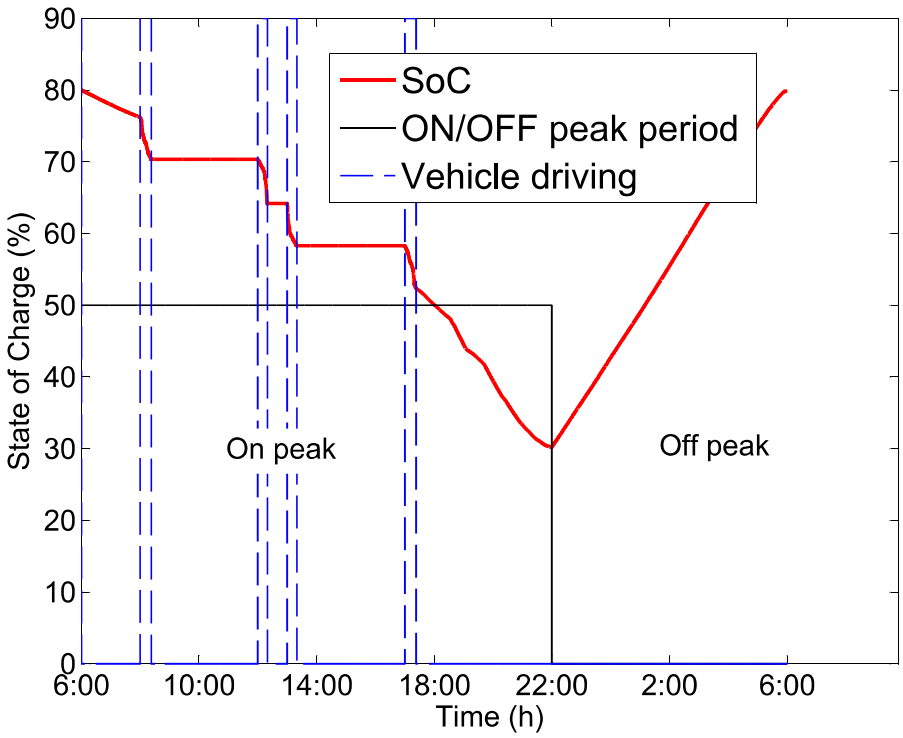

Figure 59. DP: SoC profile for the summer case with an initial SoC of 80 % and without solar energy

The battery behavior in FIGURE. 59 is similar to the first sub case where renewable energy sources are available. This is because solar energy (with no storage) is only available during the day when the vehicle is not connected. The PHEV uses the battery to propel the vehicle as shown in FIGURE. 61.

FIGURE. 60 presents the powers which are used in the micro-grid system. The battery is similarly used in the evening to help the grid to supply the household loads.

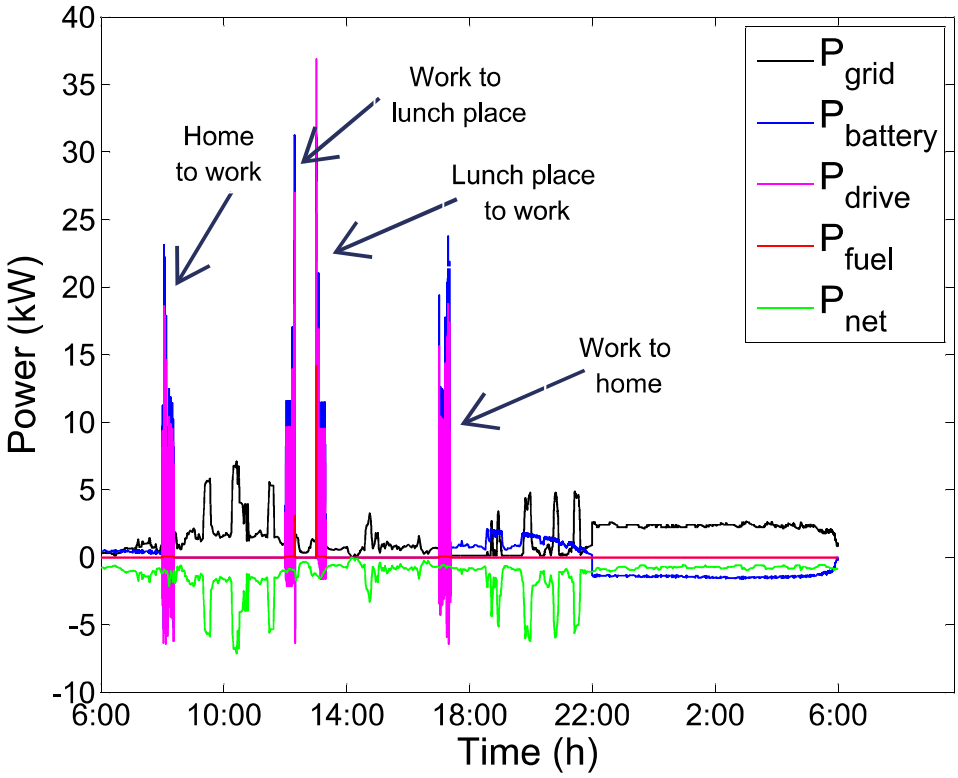

Figure 60. DP: power profiles for the summer case with an initial SoC of 80 % and without solar energy

TABLE. 8 shows that the micro-grid system without renewable energy sources is more expensive than using renewable energy sources. Overall, the micro-grid system is more cost effective than the conventional system, with and without the renewable energy sources. In this case, the micro-grid system gives about a 45 % when compared to the conventional system.

	Conventional system	Micro-grid system without RES	Micro-grid system with RES
Grid cost	4.16 €	4.65 €	2.41 €
Fuel cost	4.68 €	0.11 €	0.11 €
Total cost	8.84 €	4.77 €	2.52 €

Table 8. DP summer result without solar energy and a fully charged battery

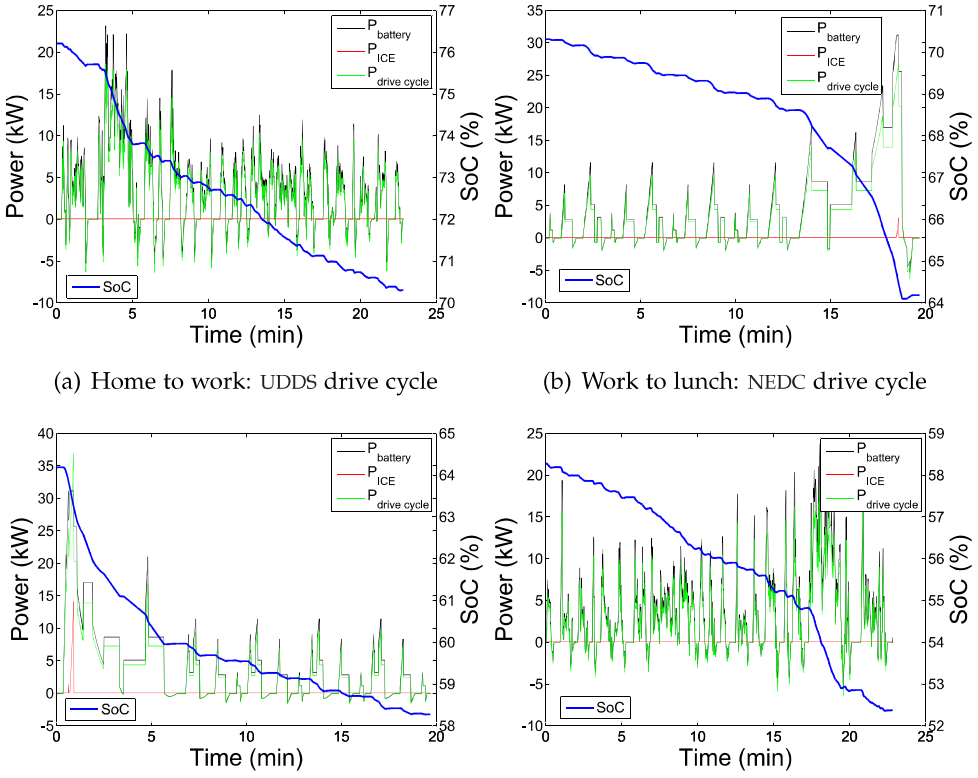

(a) Home to work: UDDS drive cycle

(b) Work to lunch: NEDC drive cycle

(c) Lunch to work: reverse NEDC drive cycle

(d) Work to home: reverse UDDS drive cycle

Figure 61. DP: travel drive cycle for the summer case with an initial SoC of 80 % and without solar energy

Simulation case studies, have shown that the micro-grid system is more cost effective in the summer. In all the cases, the vehicle is propelled by the battery except when the peak power is too high, then the ICE helps the battery to supply the drive cycle power. In addition, the battery is charged during off-peak period for the next day, and at low grid costs.

The winter case with the same sub cases is described next.

3.6.2 *Winter case*

The winter case is similarly divided into three sub cases: where the first case starts with a fully charged battery (SoC=80 %), where the second case starts with a fully discharged battery (SoC=35 %), and where in the last case, renewable energy sources are not considered and the battery is fully charged (SoC=80 %).

Battery charged: SoC = 80 %

The first sub case starts with a fully charged battery. FIGURE. 62 shows the battery behavior, whereas, the battery discharges to meet the drive cycles and

on-peak load shaving. Once the off-peak price appears, the grid charges the battery and supplies the household loads.

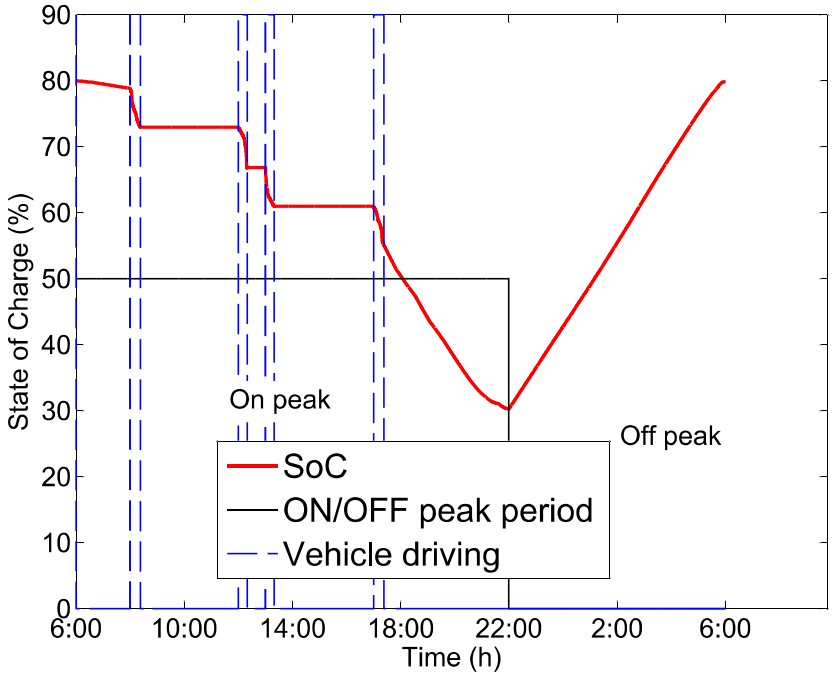

Figure 62. DP: SoC profile for the winter case with an initial SoC 80 %

FIGURE. 63 shows the power profiles which are involved in the micro-grid system. The battery reduces the peak powers. Moreover, the battery is used to propel the vehicle (FIGURE. 64) .

TABLE. 9 shows the cost comparison between the micro-grid and the conventional systems, where the cost reduction is about 40 %.

	Conventional system	Micro-grid system
Grid cost	5.41 €	5.90 €
Fuel cost	4.68 €	0.11 €
Total cost	10.09 €	6.01 €

Table 9. DP winter result with a fully charged battery

The grid cost is higher in the micro-grid than the conventional system. Indeed, the reduction comes from the lower fuel usage.

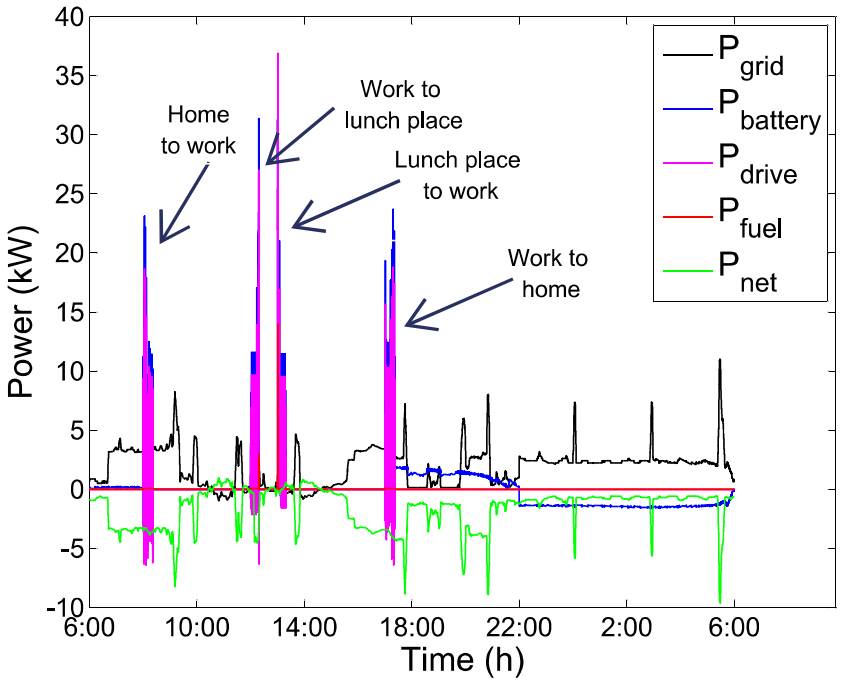

Figure 63. DP: power profiles for the winter case with an initial SoC of 80 %

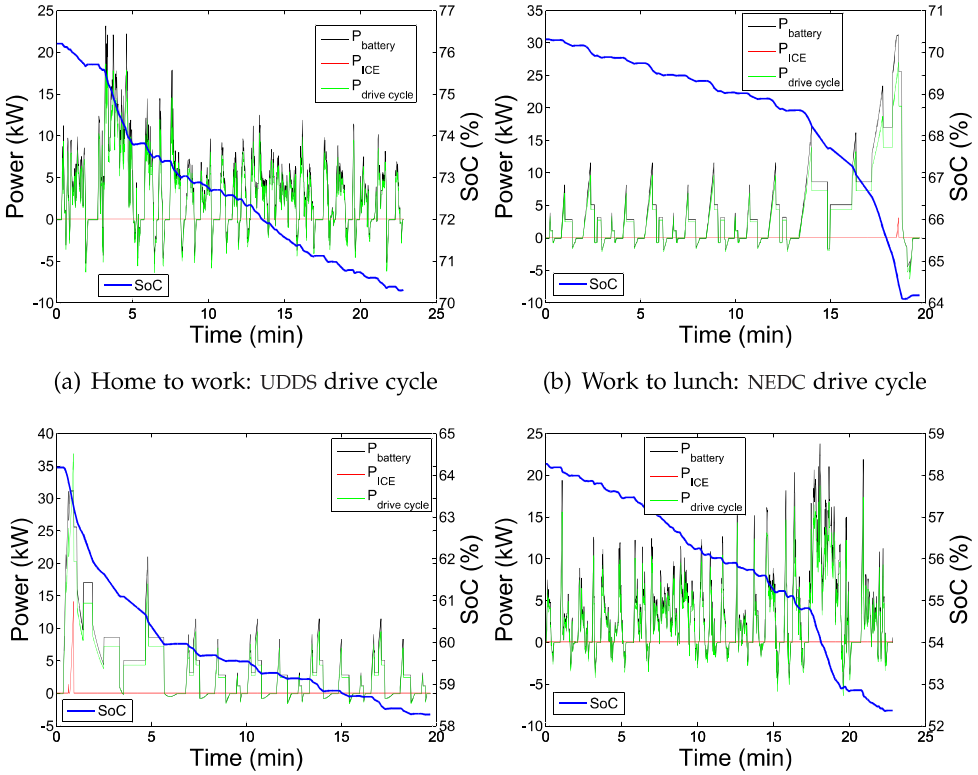

(a) Home to work: UDDS drive cycle

(b) Work to lunch: NEDC drive cycle

(c) Lunch to work: reverse NEDC drive cycle

(d) Work to home: reverse UDDS drive cycle

Figure 64. DP: travel drive cycle for the winter case with an initial SoC of 80 %

Battery discharged: SoC = 35 %

The battery behavior (FIGURE. 65) is the same as in the previous case, the battery is charged in the first two hours. It is then, used during the four trips (FIGURE. 67) to propel the vehicle.

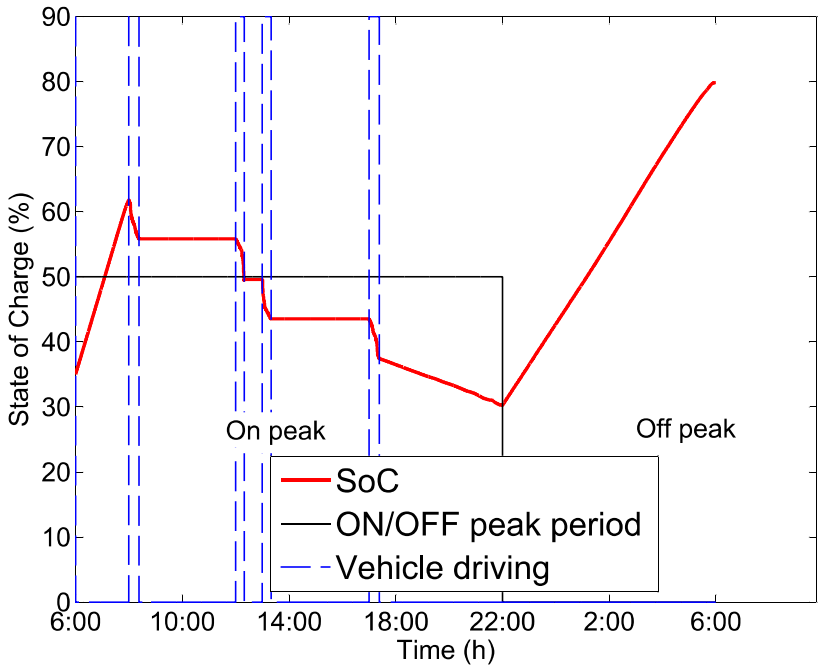

Figure 65. DP: SoC profile for the winter case with an initial SoC of 35 %

The battery is almost discharged when the vehicle is connected to the house (FIGURE. 66). Then the micro-grid system use the last 5 % of the battery SoC to help the grid to supply household loads.

TABLE. 10 gives a summary of the fuel and grid costs for conventional and micro-grid systems. In this case, a gain of 25 % is realized.

	Conventional system	Micro-grid system
Grid cost	5.41 €	7.45 €
Fuel cost	4.68 €	0.12 €
Total cost	10.09 €	7.57 €

Table 10. DP winter result with a fully discharged battery

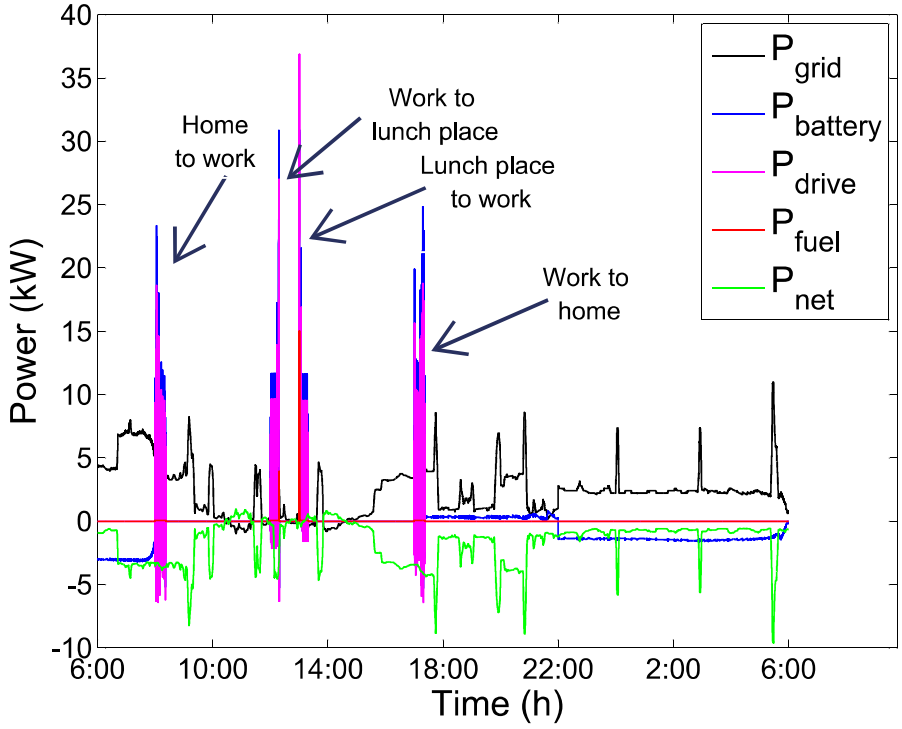

Figure 66. DP: power profiles for the winter case with an initial SoC of 35 %

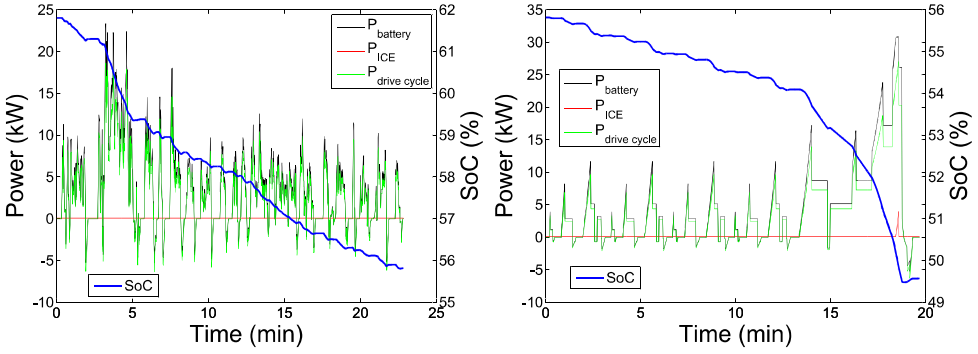

(a) Home to work: UDDS drive cycle

(b) Work to lunch: NEDC drive cycle

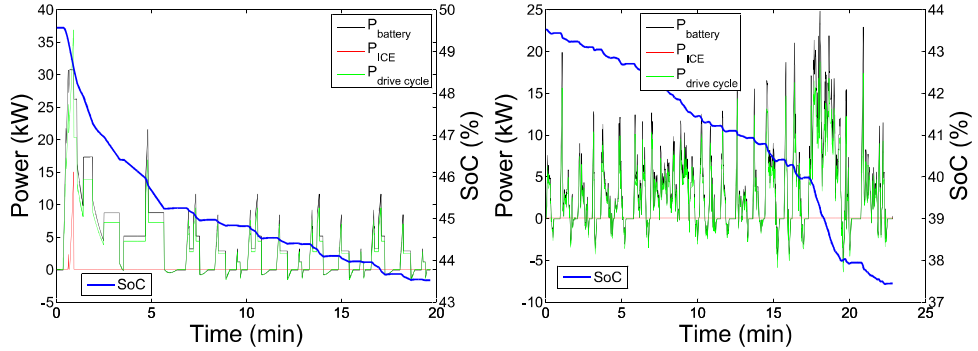

(c) Lunch to work: reverse NEDC drive cycle

(d) Work to home: reverse UDDS drive cycle

Figure 67. DP: travel drive cycle for the winter case with an initial SoC of 35 %

Without renewable energy sources

The last sub case is when the renewable energy sources are not included. FIGURE. 68, FIGURE. 69 and FIGURE. 70 present the battery SoC behavior, the powers involved in the simulation and the four PHEV trips respectively.

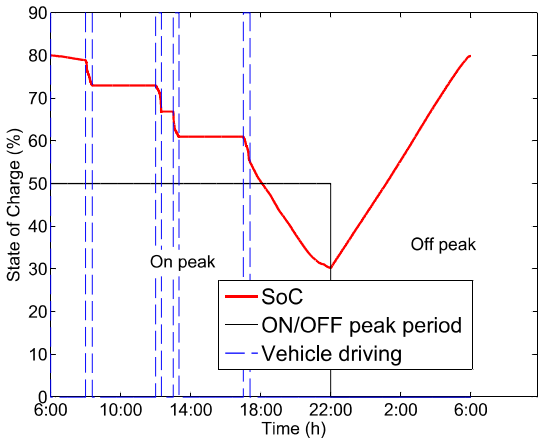

Figure 68. DP: SoC profile for the winter case with an initial SoC of 80 % and without solar energy

The battery behavior is the same as the previous cases when the initial battery is fully charged. During, the on-peak period, the battery and the grid supply the household loads (FIGURE. 69) in the morning before the disconnection of the vehicle, and after its connection in the evening. The battery is charged during the off-peak period.

FIGURE. 70 shows the four trips of day's drive cycle. The battery is used mostly to propel the vehicle. The ICE is only used when the drive cycle power requires more power than the battery can give.

TABLE. 11 summarizes the cost involved in the micro-grid system. The table compares the conventional system with the micro-grid system with and without solar energy. The reduction cost is about 40 % with the micro-grid system due to the no usage of the ICE.

	Conventional system	Micro-grid system without RES	Micro-grid system with RES
Grid cost	6.32 €	6.81 €	5.90 €
Fuel cost	4.68 €	0.11 €	6.11 €
Total cost	11.00 €	6.93 €	6.01 €

Table 11. DP winter results without solar energy and with a fully charged battery

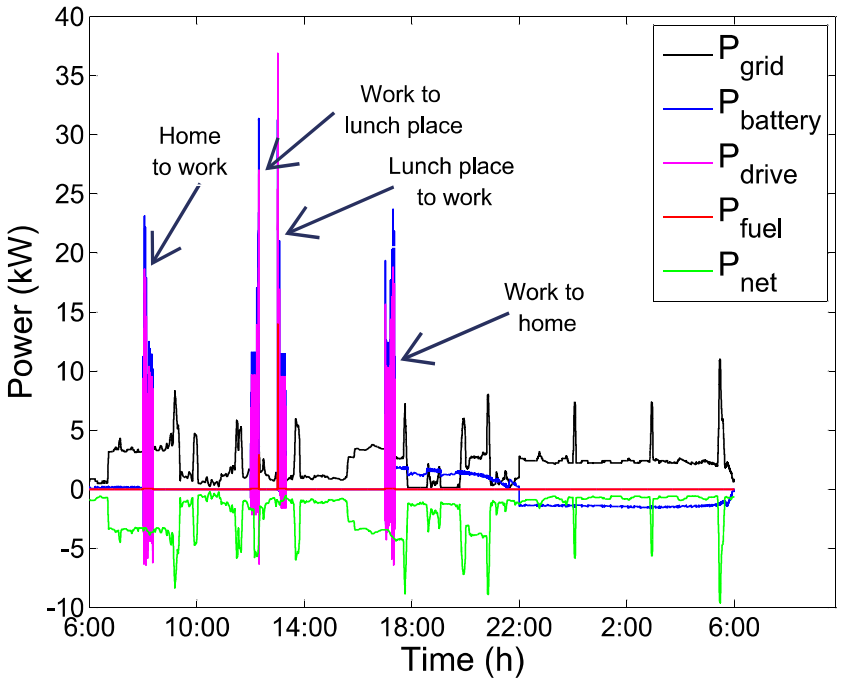

Figure 69. DP: power profiles for the winter case with an initial SoC of 80 % and without solar energy

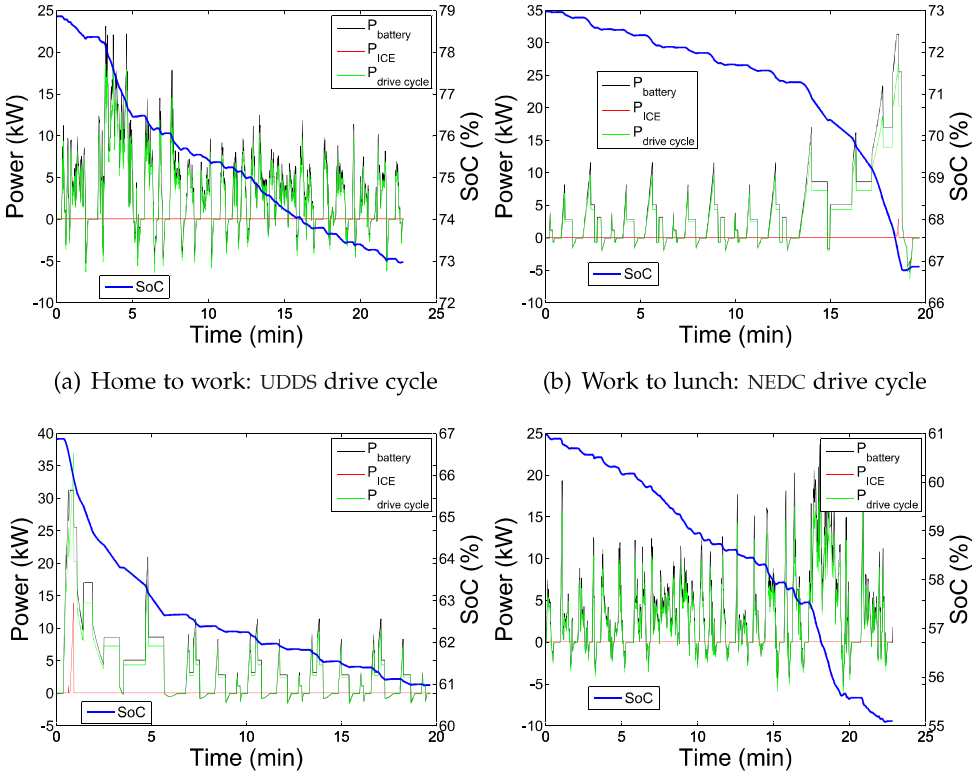

(a) Home to work: UDDS drive cycle

(b) Work to lunch: NEDC drive cycle

(c) Lunch to work: reverse NEDC drive cycle

(d) Work to home: reverse UDDS drive cycle

Figure 70. DP: travel drive cycle for the winter case with an initial SoC of 80 % and without renewable energy sources

This section has presented the results of a winter case which includes three sub cases. The micro-grid system presents a cost reduction in all cases: where the simulation starts with a fully charged battery, a fully discharged battery or when renewable energy sources are not available.

3.6.3 *Conclusion*

As summarized in FIGURE. 71, the higher reduction in energy cost is when the battery is fully charged, and the renewable energy sources are available.

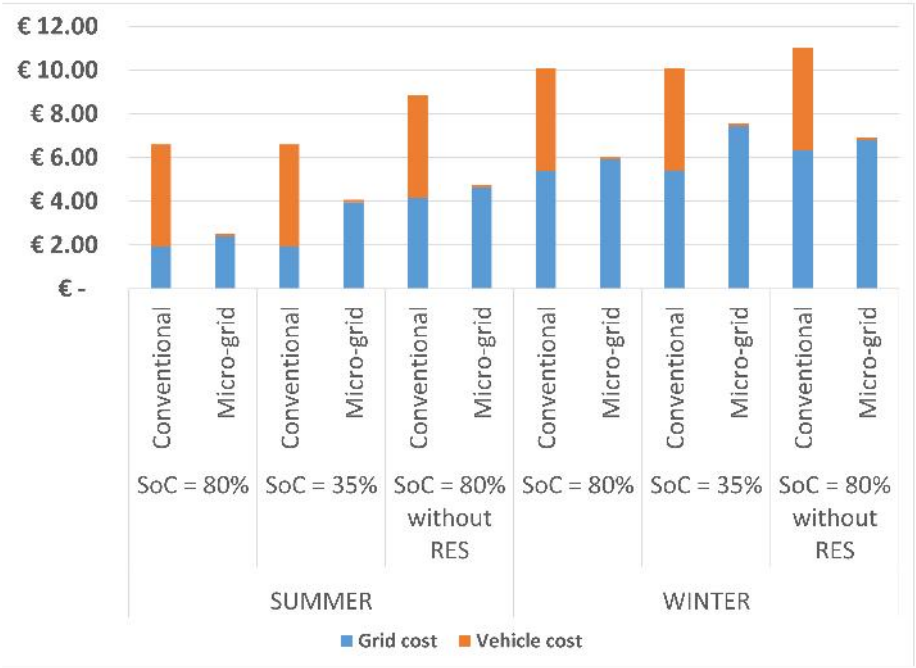

Figure 71. DP: 6 cases comparison

However, when the renewable energy sources are not available or when the battery is discharged at the beginning of the simulation, there is significant cost savings. The next sub section presents the average monthly savings.

3.6.4 *Monthly results*

ÉcoTerra house data was collected for one year in 2010. In each month, a trimmed mean production and consumption curve has been calculated as defined in (3.11).

$$\frac{\sum_{1}^{Nbr(x)}(x) - Max(x) - Min(x))}{Nbr(x) - 2} \tag{3.11}$$

Where x is the production or consumption value for one time step for all days in a month, and $Nbr(x)$ is the number of days in a month. This equation is evaluated for each time step. The time step used for the data collected is 60 seconds.

FIGURE. 72 shows monthly cost of the micro-grid and conventional systems generated using dynamic programming algorithm. To obtain this histogram, the trimmed mean production and consumption are used to calculate the mean price for a day in a given month. The total cost in a given month, is then the product of the mean price of a day and the number of days in the month.

The micro-grid system gives a global cost reduction of about 46 % compared to the conventional system. There is a higher reduction in summer then winter in term of percentage, due to the proportion cost between the fuel and the electricity.

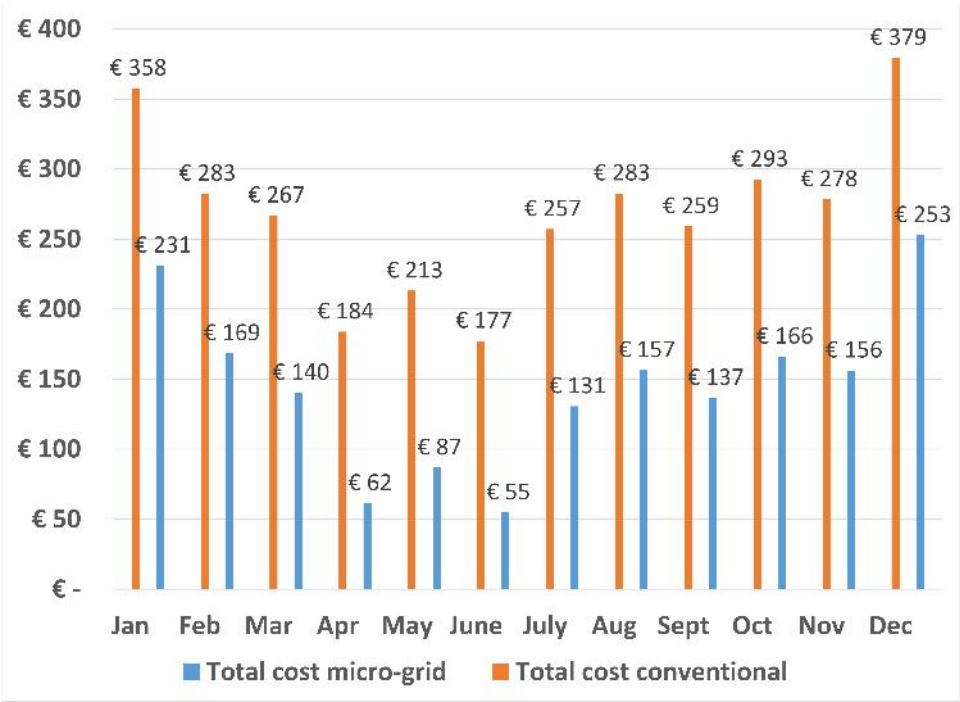

Figure 72. DP: monthly cost comparison

Indeed, FIGURE. 73 shows that in June, 80 % of the energy bill is due to the fuel consumption, whereas in January the fuel consumption is only 40 %. Moreover, to fully charge a battery during off-peak and on-peak periods is 1.30€ and 1.90€ respectively. Therefore all the fuel consumption should be shifted to electricity, which will reduce the energy bill considerably.

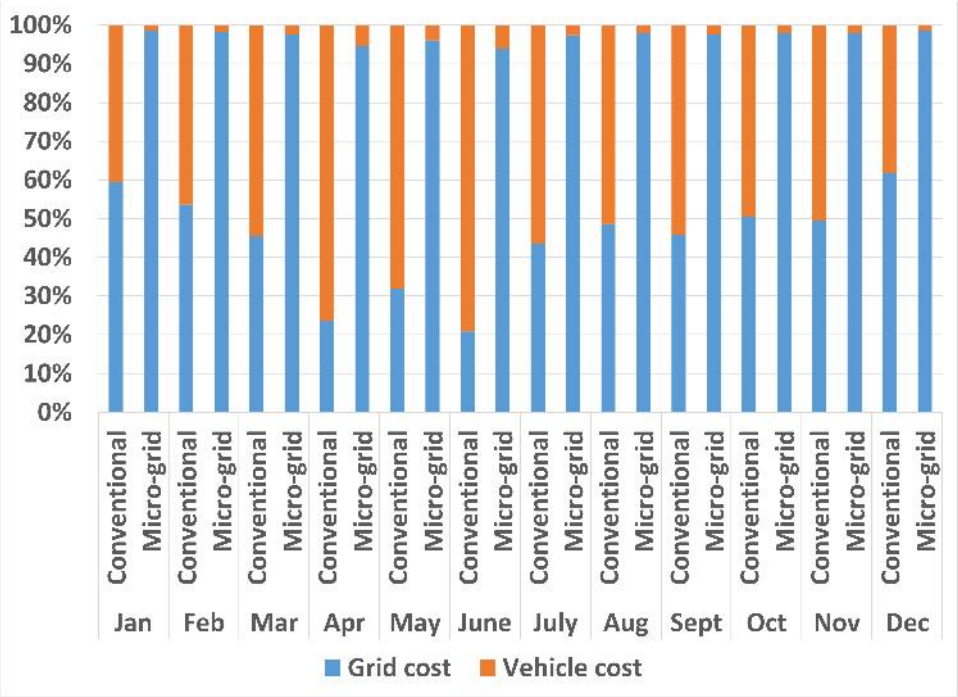

Figure 73. DP: energy cost proportion

However, the installation of the system is not taking into account like the installation of the bidirectional charger and the PHEV itself.

3.7 CONCLUSION

This chapter has presented an optimization technique to find the minimum energy cost of the micro-grid system. The dynamic programming algorithm has been used. The objective function took into account the energy costs such fuel, renewable energy sources and electricity. The constraints of the micro-grid system were defined: size of the battery charger, discharge and charge battery currents, ICE size and the battery SoC.

The results were divided into two sections. The first one considered two cases (summer and winter) where each case was divided into three sub cases. The sub cases are: the simulation starts with a fully charged battery, with a fully discharged battery and where renewable energy sources are not available. In addition, the micro-grid system has shown its flexibility in taking or not into account the solar energy and by extension the number of renewable energy sources.

The second section shows the overall gain in a month. In general, the micro-grid system reduces the energy bill for each situation. However, the cost of the PHEV, the installation of the controller and the installation of renewable energy sources has not been taken into account. In addition, there

was no energy storage for solar energy. Therefore, an energy storage can be added to be able to use this energy in the evening.

Finally, the optimization uses the electricity price difference to control the charging of the battery. Indeed, in every scenario the battery was charged during the off-peak period.

4

ONLINE SIMULATION : FUZZY LOGIC CONTROL

The previous chapter showed how to generated the reference cost. In this chapter, an online control strategy is proposed to control the micro-grid system in real time. According to the classification in [63, 64, 65], two methods based on rules: fuzzy and deterministic, are possible. A deterministic rule based algorithm includes thermostat (ON-OFF) control and state-flow control. However, the fuzzy rule based method is more adequate for PHEV energy control strategy as shown in [26, 27, 29]. Indeed, one of the main advantages using fuzzy logic is to formalize human reasoning into natural language.

This chapter presents the Fuzzy logic (FL) algorithm and its application to the micro-grid system. Two fuzzy logic controllers are implemented: one in the vehicle and one in the house as presented in FIGURE. 33. The vehicle fuzzy logic controller is based on the ICE map and the SoC objective. The SoC objective is the SoC that the vehicle has to have when it reaches home, to be able to help the grid during on-peak period. The house controller is based on the available battery energy and the electricity price.

Finally, winter, summer and monthly results are presented and compared with offline simulation.

4.1 FUZZY LOGIC DESCRIPTION

Fuzzy logic is an extension of the Boolean logic. In 1965, Lotfi Zadeh created this logic, based on the fuzzy set mathematical theory, which is a generalization of the classical set theory. The Boolean logic allows only two states: true or false. Fuzzy logic provides flexibility, allowing inaccuracies and uncertainties measures between the two boolean states.

The fuzzy logic algorithm is divided in three steps as depicted in FIGURE. 74: fuzzification, inference rules, defuzzification.

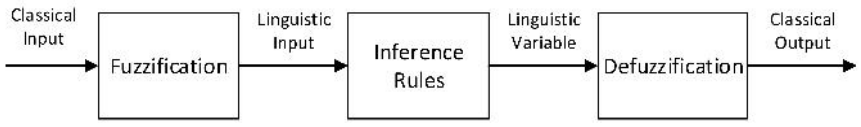

Figure 74. Fuzzy logic algorithm

These three steps are described below.

Fuzzification: The fuzzification converts classical inputs into linguistic variables. To be able to convert them, membership functions has to be designed.

A membership function defines the degree of membership of a digital data into a linguistic variable.

Inference rules: Inference rules describe the system rule in natural language. The inference rules are written as follows: IF *condition* OPERATOR *condition* THEN *action*. The operator can be AND or OR.

The AND operator corresponds at the intersection of two fuzzy sets. This operator can be a minimum or a product operation. Considering *a* and b are two fuzzy sets:

- minimum: a AND b = min(a,b)
- product: a AND b = a . b

The OR operator corresponds to the union of two fuzzy sets. This operator can be a maximum or a product operation:

- maximum: a OR b = max(a,b)
- product: a OR b = -(1-a)(1-b)

Defuzzification: This last step converts the linguistic variables, after applying the rules, into numerical output values. The two main methods are

- centroid method: abscissa corresponding to the gravity center of the membership function
- mean of maximal method: abscissa corresponding to the mean abscissa where ordinate are the maximal value of membership functions.

The next section presents the overall control strategy where two fuzzy logic controllers are implemented.

4.2 OVERALL CONTROL STRATEGY

The global system has two controllers located in the house and in the PHEV (FIGURE. 33). As presented in FIGURE. 75, the house controller is used to manage the battery in its two modes: V2H and H2V. This control is only active, when the vehicle is connected to the house. When the vehicle is disconnected, the house controller is turned off and the PHEV controller is switch on, when the vehicle starts. This controller manages the PHEV fuel, and indirectly the battery power.

The algorithm is flexible and it can be adapted to include the battery charging at the workplace or the marketplace. However, in this study this aspect is not considered.

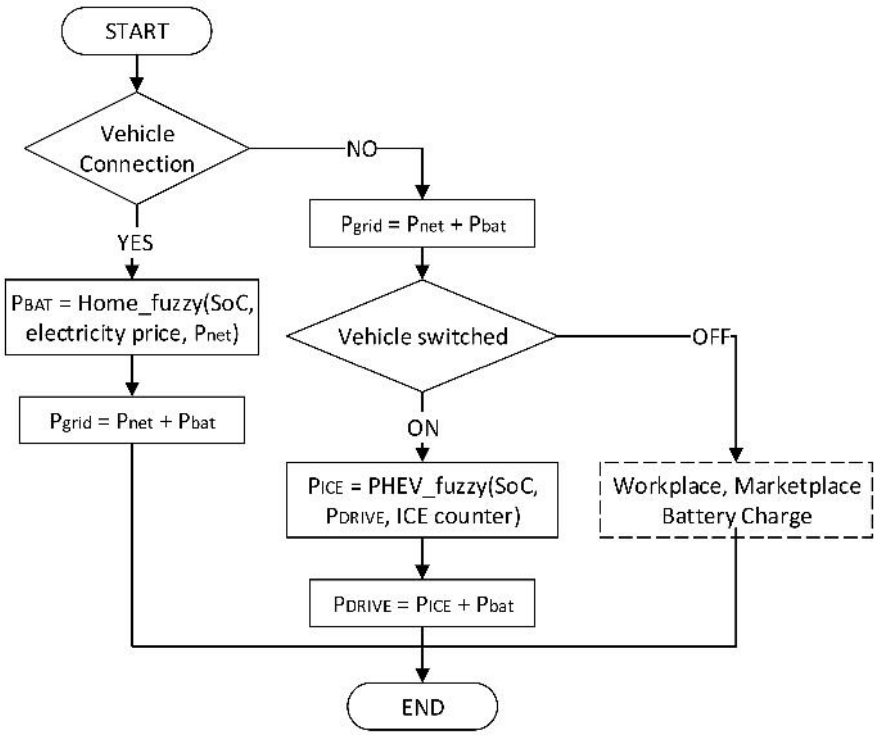

Figure 75. Global algorithm for online simulation

Next sections explain the construction of the two controllers which are located in the house and the PHEV.

4.3 HOUSE FUZZY LOGIC CONTROLLER

The goal of the house controller is to manage the battery energy. The battery power is the output of the fuzzy logic controller as shown the FIGURE. 76. This output depends on the battery SoC, the electricity price and the net power.

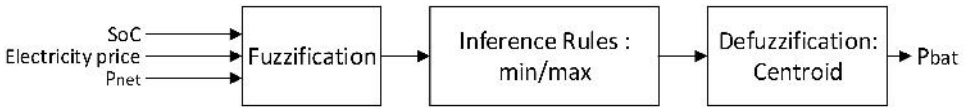

Figure 76. Fuzzy logic house controller

The fuzzy logic controller uses the popular min/max method for the inference rules. Defuzzification is done by use of the centroid method. It is also popular because all output values are taken into account according to their weights.

The net power calculation is as given in (4.1) where P_{solar} and P_{load} are solar and household load power respectively .

$$P_{net}(t) = P_{solar}(t) - P_{load}(t) \tag{4.1}$$

The battery SoC is calculated in (4.2) where $I_{battery}$ is the battery current, $C_{battery}$ is the battery capacity and t is the time step in seconds.

$$SoC(t+1) = \frac{I_{battery}}{C_{battery} \cdot 3600} + SoC(t) \tag{4.2}$$

The house controller is composed of three input membership functions which are the battery SoC, the electricity price and the net power of the household loads. The battery power is the output of the controller. This two sub sections are followed by the fuzzy logic rules.

4.3.1 *Input membership functions*

Input membership functions are defined according to: the SoC constraints, the electricity price and the battery charger size. The construction of these membership functions is described below. It means that, for each micro-grid system, the membership functions are different.

Battery SoC membership functions

The five battery SoC membership functions are a function of the SoC constraints. The SoC constraints are assumed from the previous chapter as: SoC_{min} = 30 % and SoC_{max} = 90 %. To build the SoC membership functions the SoC range is divided by the number of membership functions as given in equation (4.3).

$$SoC_{mf} = \frac{SoC_{max} - SoC_{min}}{\text{Number of membership function}} \tag{4.3}$$

These membership functions are depicted in FIGURE. 77.

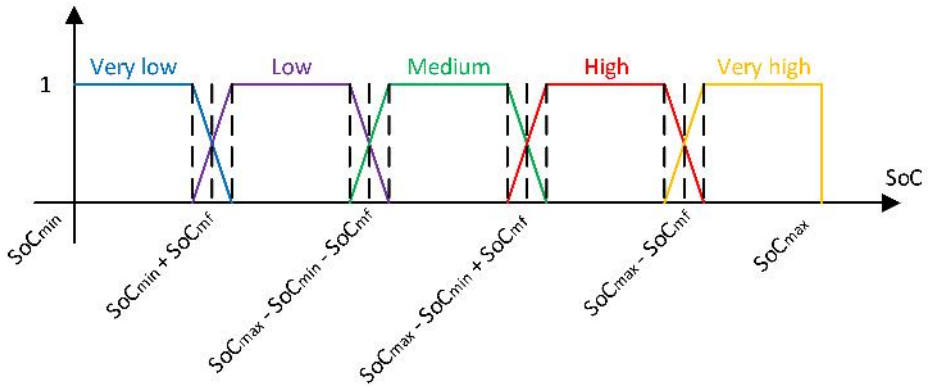

Figure 77. Membership functions : Battery SoC

The five modes are described bellow:
- *Very low*: the battery is charged before use;
- *Low*: in on-peak period, the battery will slow down the usage of V2H capability and charge the battery if extra renewable energy is available, whereas in off-peak period, the battery charges with the renewable energy sources and grid;
- *Medium*: V2H capability is used and the battery is charged if there is extra renewable energy;
- *High*: in on-peak period the battery is used in V2H functionality whereas in off-peak the battery continue to be charged;
- *Very high*: the battery is used to help the grid to meet the household loads.

Electricity price membership functions

The electricity price membership function shown in FIGURE. 78 is derived from two functions: on and off peak electricity price.

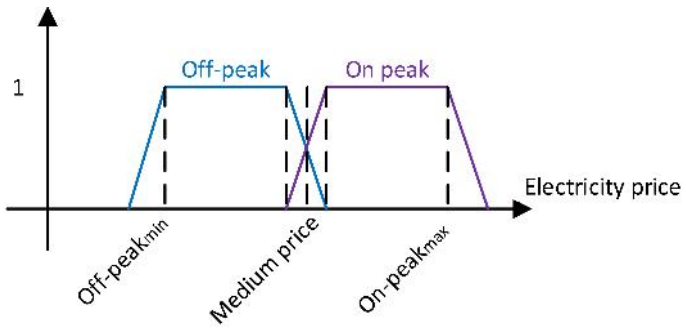

Figure 78. Membership functions : Electricity price

These membership functions can be built in two ways. Either, the electricity price is an on/off peak price as presented in FIGURE. 78, where the price of each period is the middle of the function. Or the price system is dynamic as presented in [61, 67]. Then off and on peak price range has to be predetermined. In addition, with dynamic price, the electricity price membership functions can have more than two functions.

Net power membership functions

The net power (difference between solar and load power) membership functions are built according to the battery charger size. The membership functions are divided into five functions. The net power is positive when the solar power is greater than the load power, and negative when the solar power is less than the load power. These membership functions are depicted in FIGURE. 79, where P_{conv_max} is the maximum converter power.

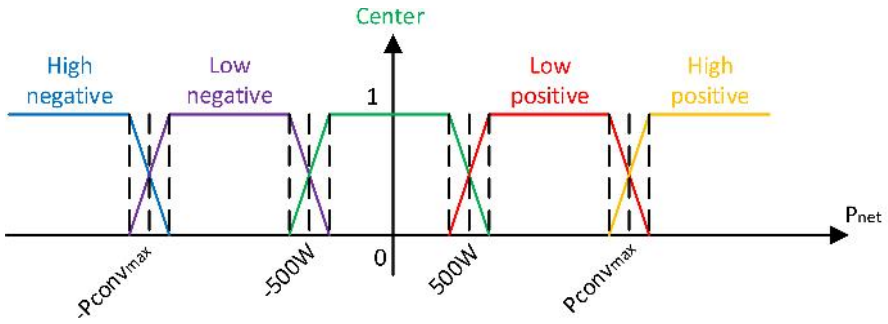

Figure 79. Membership functions : Net Power

These membership functions are defined as follow:
- *High Negative*: P_{net} is over the maximum battery charger power ($-P_{conv\_max}$);
- *Low Negative*: P_{net} is in the range of the battery charger power;
- *Center*: P_{net} is in the range of $\pm$ 500 W;
- *Low Positive*: P_{net} is in the range of the battery charger power;
- *High Positive*: P_{net} is over the maximum batterycharger power (P_{conv_max}).

4.3.2 *Output membership functions:* $P_{battery}$

The house controller output FIGURE. 80 is the battery power which either helps the grid to meet the household loads, or charge the battery. When the battery power is positive the battery supplies household loads, whereas when the battery power is negative, the battery is charged.

The battery power is bounded by the battery charger ($\pm$ P_{conv_max}). The five membership functions are shown in FIGURE. 80.

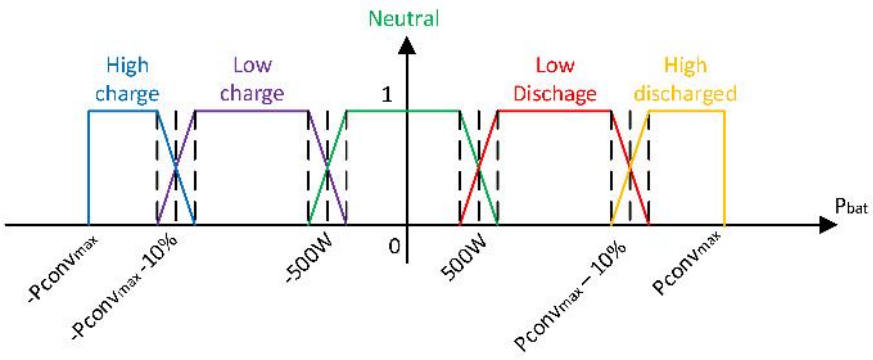

Figure 80. Output membership functions: $P_{battery}$

These membership functions are built as the P_{net} membership functions:
- *High Charge*: the battery charges at its maximum power;
- *Low Charge*: the battery charges according the load demand;
- *Neutral*: the battery charges/discharges at its lower range ($\pm$500 W);
- *Low Discharge*: the battery helps the grid to meet the household loads according to the loads;
- *High Discharge*: the battery helps the grid to meet the household loads at its maximum power.

The next sub section describes the rules used in the house fuzzy logic controller.

4.3.3 *Rules*

Fuzzy logic rules are shown in FIGURE. 81 when the system is in off-peak period and in FIGURE. 82 when is in on-peak period.

FIGURE. 81 shows, when the battery SoC is low and the load is positive, the battery charges due to the availability of renewable energy sources. Moreover, when battery SoC is high, and the load demand is high, the battery helps the grid to meet the household loads at is maximum power. Afterwards, when the battery is not fully charged the battery charges due to the lower electricity price.

During the on-peak period and the battery is charged, it helps the grid to meet the loads. In addition, when the battery is discharged and renewable energy sources are available, the battery charges.

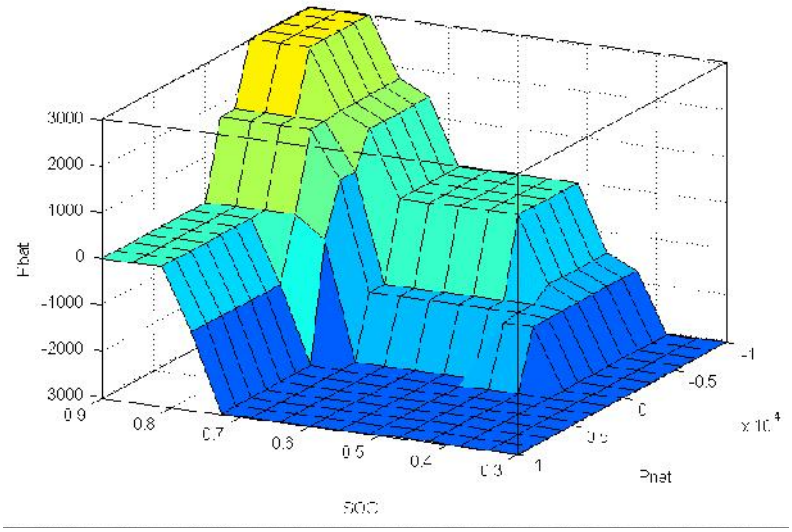

Figure 81. Rules when electricity price is in off-peak period

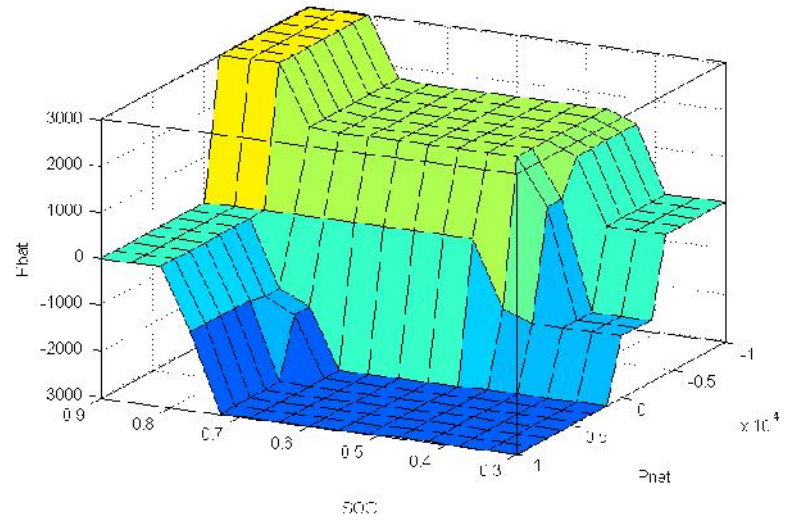

Figure 82. Rules when electricity price is in on-peak period

When, the off-peak period appears, the priority is to charge the battery, whereas when on-peak period occurs, the priority is to help the grid to supply household loads.

The next section describes the PHEV fuzzy logic controller.

4.4 PHEV FUZZY LOGIC CONTROLLER

The fuzzy logic controller located in the PHEV, has three inputs (FIGURE. 83): the battery SoC, the drive cycle power and the ICE timer. The last input presents the unintentional turning on an off of the ICE. The fuzzy logic output is the ICE power and indirectly the battery power.

Figure 83. Fuzzy logic PHEV controller

The min/max method is used for the inference rules. And the mean of maximum method is used for the defuzzification because it takes into account the average value of the most recommended outputs.

Inputs and output construction, and rules of the PHEV controller are described in this section.

4.4.1 *Input membership functions*

The input membership functions for the battery SoC ($30\,\% \leqslant \text{SoC} \leqslant 90\,\%$), the ICE timer and the drive cycle power are as shown in FIGURE. 84, FIGURE. 85 and FIGURE. 86 respectively.

These membership functions are defined according to the ICE, the maximum battery power, whereas, the SoC functions are updated with the new SoC objective value everyday.

Battery SoC membership functions

The battery SoC membership function is based on the SoC objective calculated in the next section (section 4.5), in a $\pm\ 5\,\%$ window range. The battery SoC objective gives the SoC that the battery has to have when it reaches home. FIGURE. 84 shows the SoC membership functions.

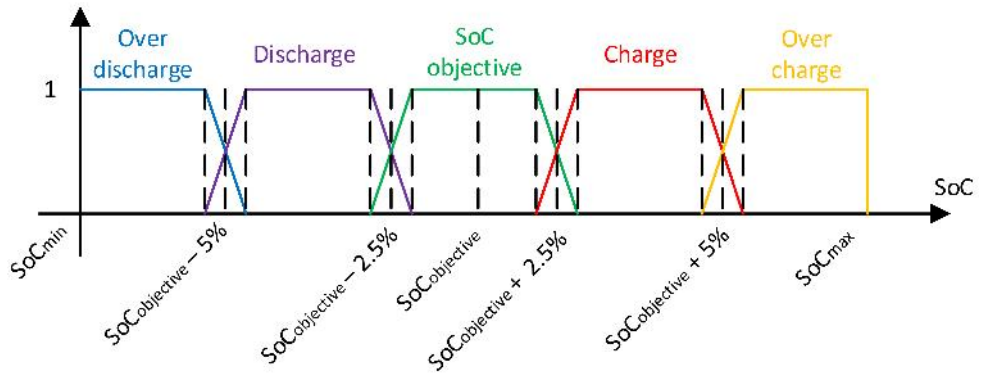

Figure 84. Membership functions : Battery SoC

The membership functions are divided into 5 functions:
- *Over discharge*: the battery SoC is below the range of the SoC objective, hence the battery has to be charged;
- *Discharge*: the battery SoC is low in relation to the SoC objective. The battery is used economically;
- *SoC objective*: the battery SoC is close to the SoC objective; both sources are used to propel the vehicle;
- *Charge*: the battery SoC is above the SoC objective. The battery is used in the all electric mode;
- *Over charge*: the battery is over the range of the SoC objective; the vehicle works in the all electric mode.

ICE timer membership function

The second input of the controller is the ICE timer which is shown in FIGURE. 85. The goal of this function is to avoid switching off the ICE untimely. Once it is turned on, it has ICE has to work for at least 25 seconds. 25 seconds is considered to be the minimum to reach the rate power of the ICE.

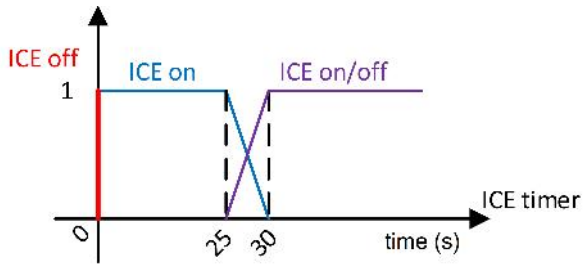

Figure 85. Membership function : ICE timer

The membership functions are three:
– *ICE off*: the ICE is turned off at *t-1* and can be turned on at *t*;
– *ICE on*: the ICE is on at *t-1* and can be turned off at *t*;
– *ICE on/off*: the ICE is turned on at *t-1* and can continue to be used or not;

Drive cycle power membership functions

The last input of the controller is the drive cycle power which is presented in FIGURE. 86. The membership functions are built according to the iso-efficiency curves shown in FIGURE. 87.

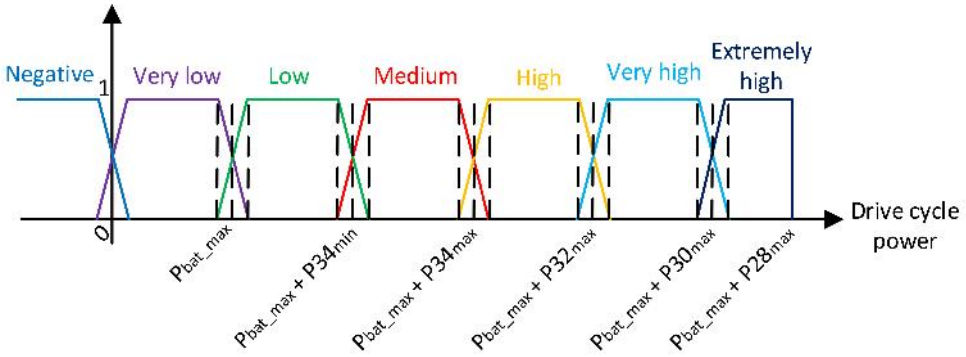

Figure 86. Membership function : Drive cycle power

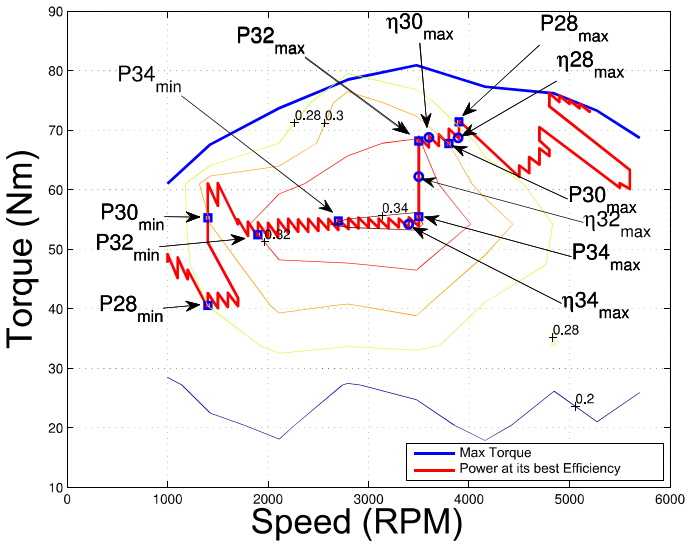

Figure 87. ICE map

The membership functions use the extracted data of the ICE map. Values which are extracted are for each iso-efficiency curve (η_{34}, η_{32}, η_{30} and η_{28}): the minimum power ($P34_{min}$, $P32_{min}$, $P30_{min}$ and $P28_{min}$) and the maximum power ($P34_{max}$, $P32_{max}$, $P30_{max}$ and $P28_{max}$).

According to these values and the maximum battery power the drive cycle power membership functions are constructed. These functions are divided into 7:

- *Negative Power*: the PHEV is in regenerative braking mode;
- *Very low Power*: only the battery is used to propel the vehicle;
- *Low Power*: the battery itself is not enough to supply the electric motor. The ICE has to be turned on at its best efficiency to help the battery to supply the electric motor;
- *Medium Power*: the battery power and the ICE at 34 % efficiency meet the drive cycle load;
- *High Power*: The battery power and the ICE at 32 % efficiency meet the drive cycle load;
- *Very high Power*: The battery power and the ICE at 30 % efficiency meet the drive cycle load;
- *Extremely high Power*: The battery power and the ICE at 28 % efficiency meet the drive cycle load.

4.4.2 *Output membership functions:* P_{ICE}

The fuzzy logic controller output is the ICE power. The ICE power membership functions are presented in FIGURE. 88. Its membership functions are built similarly as the drive cycle power membership functions using the ICE iso-efficiency curve (FIGURE. 87). The last extracted values from the ICE iso-efficiency map is the best efficiency point for each iso-efficiency curve ($\eta 34_{max}$, $\eta 32_{max}$, $\eta 30_{max}$ and $\eta 28_{max}$).

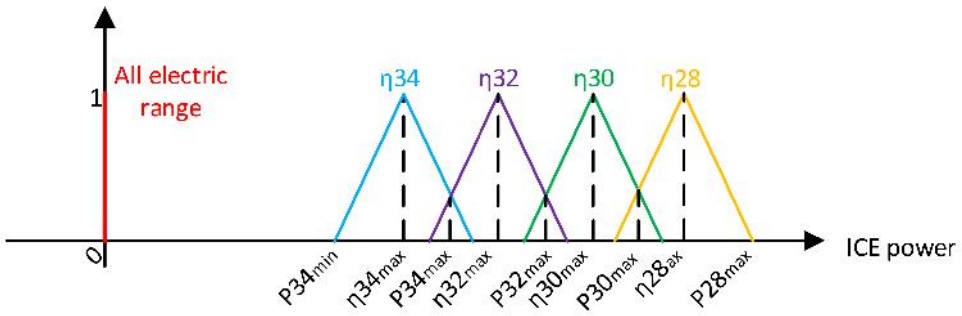

Figure 88. Output membership functions: P_{ICE}

The output membership functions are divided into 5:
- *All Electric range*: The ICE is off and the PHEV is in the all electric mode;
- η_{34}: the ICE works in the η_{34} iso efficiency curve (between 34 % and maximum efficiency);
- η_{32}: the ICE works in the η_{32} iso efficiency curve (between 32 % and 34 % efficiency);
- η_{30}:the ICE works in the η_{30} iso efficiency curve (between 30 % and 32 % efficiency);
- η_{28}: the ICE works in the η_{28} iso efficiency curve (between 28 % and 30 % efficiency).

The next section deals with rules witch link the inputs to the output.

4.4.3 *Rules*

FIGURE. 89 presents the rules when the decision is made to stay in "off" mode or switch "on" the ICE. FIGURE. 90, shows the rule when the ICE has to stay in "on" mode.

In the first case, the ICE is either on or off due to the low drive cycle demand. The ICE is only used when the battery is discharged. When the demand is high, irrepective of the level of the battery SoC, the ICE is turned on due to the limitation of the battery ($\mathtt{Pdischarge}_{\max}$).

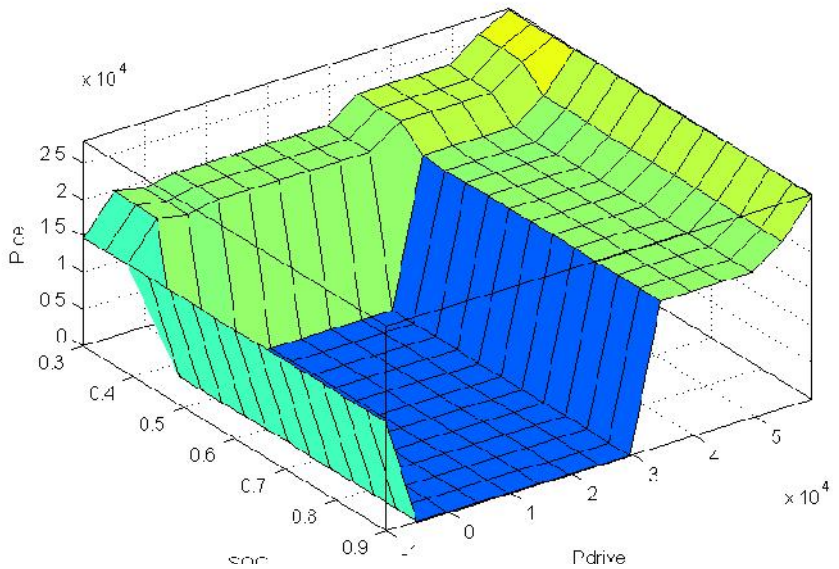

Figure 89. Rules when the ICE can be either switched "on" or stay in the "off" mode

In the second case, when the ICE has to be "on", the priority is to use the ICE at its best efficiency, except when the demand is too high.

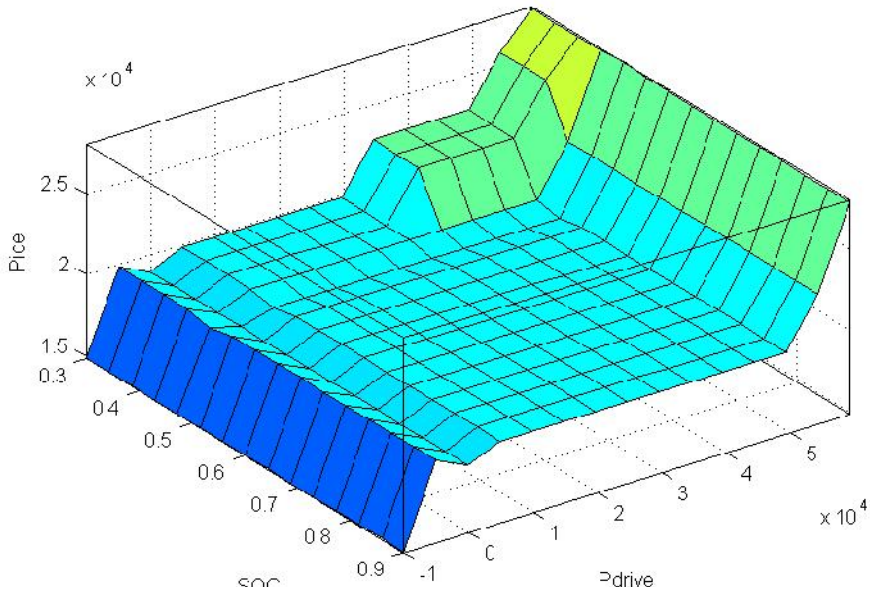

Figure 90. Rules when ICE has to be turned "on"

The priority of the PHEV controller is to reduce the fuel consumption, and to avoid untimely turning on and off the ICE, which can damage it.

The two controllers located in the house and the PHEV are adaptable according to the micro-grid system parameter: the ICE, the battery and the battery charger. The SoC objective is a parameter that is calculated everyday, which updates the PHEV fuzzy logic controller.

The battery SoC objective is described in the next section. The battery SoC is the link between the two controllers. Indeed, the battery SoC appears in both controllers.

4.5 SOC OBJECTIVE

The SoC objective is used to parameter the PHEV controller. The SoC objective parameter is needed to build the SoC membership function as shown in section 4.4.1. At the end of the travel, the battery SoC has to be at least at the SoC objective value within a window of $\pm$ 5 %. FIGURE. 91 presents the algorithm used to calculate this SoC. The 5 % window can be optimized.

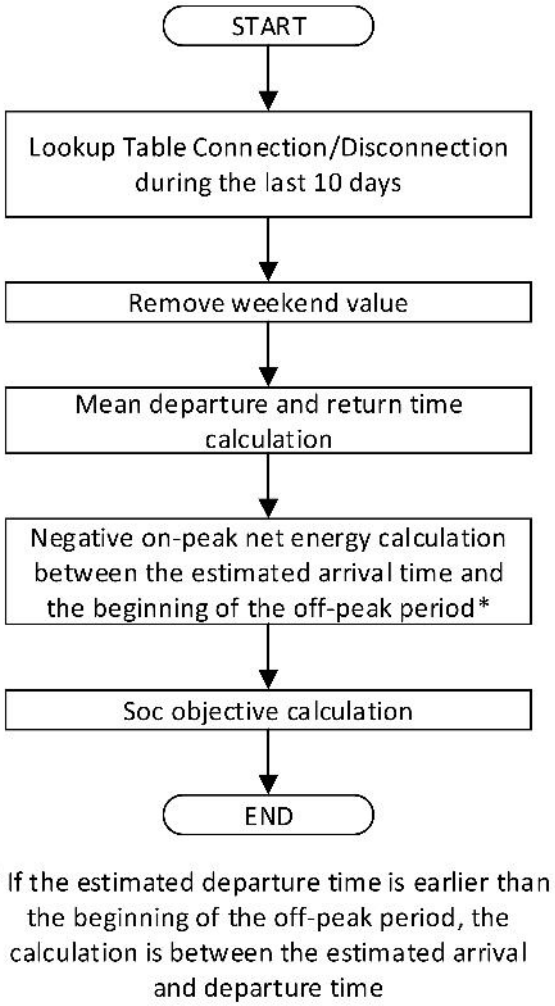

Figure 91. SoC objective algorithm

The home controller records the last 10 days of energy consumption and production and the time departure and arrival of the PHEV. The 10 days includes at least 5 consecutive working days. This study assumes that the PHEV is connected to the micro-grid, when the vehicle gets home. In addition, if the PHEV is connected/disconnected more than once in a day, the controller records only the first disconnection and the last connection.

The controller calculates the average net power (4.4), the average of departure and arrival time of the last 10 days excluding the weekend days.

$$P_{net} = P_{solar} - P_{load} \tag{4.4}$$

The negative on-peak net energy (4.5) is calculated using the average dynamic net power limited by the average arrival time of the last 10 days and, at the beginning of the off-peak period. The average dynamic net power

is the negative part of the average power of the 10 last days, minus the mean of the power between the arrival time and the start of the off-peak period. This energy calculation allows to take into account the power peaks between the estimate time of the vehicle connection (when the driver reaches home) and the beginning of the off-peak period.

$$E_{\text{on-peak}} = \int_{Arrival\,time}^{off-peak\,period\,starts} P_{net}(t) - \overline{P}_{net}(t)\,dt \mid (P_{net}(t) - \overline{P}_{net}(t)) < 0 \tag{4.5}$$

Finally the SoC objective is given in equation (4.6) where the SoC_{min} is the minimum SoC objective. $E_{\text{on-peak}}$ is the negative on-peak net energy between the mean arrival time and the beginning of the off-peak time, and $E_{battery}$ is the total battery energy.

$$SoC_{objectif} = SoC_{min} - \frac{E_{\text{on-peak}}}{E_{battery}} \tag{4.6}$$

The maximum and minimum SoC objective has to be at least 5 % over/under than the minimum/maximum battery SoC due to the 5 % window. Therefore, in this study, the maximum SoC objective is 85 % and the minimum is 35 %.

FIGURE. 92 and FIGURE. 93 show the variation of the SoC objective according to the estimated arrival time of the PHEV, for the summer and the winter cases respectively.

More the estimated arrival time of the PHEV is early higher is the SoC objective value due to the energy calculation (4.5).

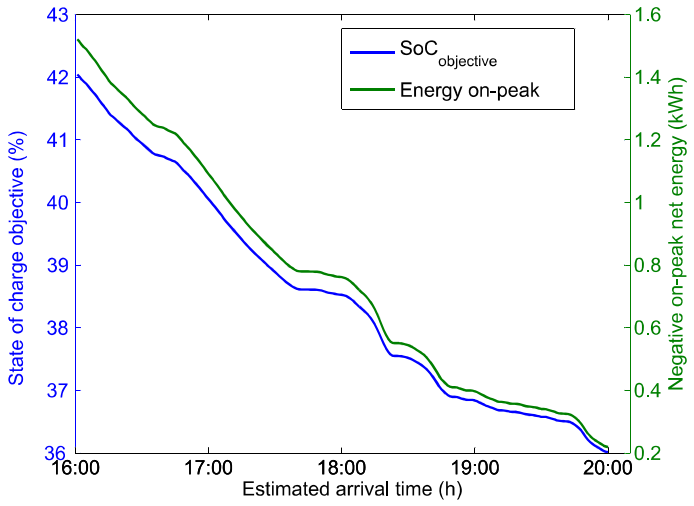

Figure 92. SoC objective variation for the summer case

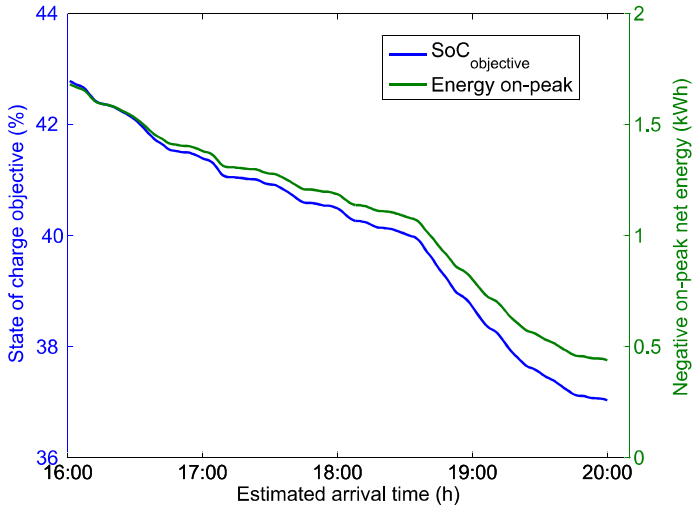

Figure 93. SoC objective variation for the winter case

The next sub section presents the online results and the comparison between the offline and the online results.

4.6 RESULTS AND COMPARISON WITH OFFLINE RESULTS

First, the SoC objective results for both summer and winter scenario are presented. Secondly, the results of the same scenario and sub scenario of the previous section, are presented.

4.6.1 *SoC objective*

To calculate the SoC objective, the departure and the arrival time of the last 10 days is necessary. TABLE. 12 shows these times and their mean time for the summer and winter cases. To calculate the mean, departure and arrival times, weekend values are removed.

In both scenario, the real departure time is 8:00 AM and the driver comes back at 5:23 PM whereas the predicted departure time is 8:00 AM for the winter case and 8:01 AM for the summer case. The predicted arrival time is 5:39 PM for the winter case and 5:30 PM for the summer case. The results, in the next section using the estimated departure and arrival times. Using these values and the last 10 days of production and consumption data, the winter SoC objective is about 55 % and the summer SoC objective is about 38 %. The winter SoC objective is higher than the summer one, due to the higher household loads and lower solar production in winter. Indeed, the battery has to help the grid more to supply the household loads during winter than in summer time.

	Departure time	Arrival time
D-1	7:58 AM	5:38 PM
D-2	8:10 AM	5:40 PM
D-3	7:51 AM	5:41 PM
D-4	8:20 AM	5:55 PM
D-5	7:45 AM	5:45 PM
D-6	7:55 AM	5:58 PM
D-7	7:40 AM	5:20 PM
D-8	8:15 AM	5:12 PM
D-9	8:00 AM	5:20 PM
D-10	7:55 AM	5:18 PM
Mean time (January 17^{th})	8:00 AM	5:39 PM
Mean time (June 22^{nd})	8:01 AM	5:30 PM

Table 12. The departure and arrival time for the calculation of the SoC objective

4.6.2 *Summer Case*

The summer case (June 22^{nd}), is divided into three sub cases: a fully charged battery at the beginning of the simulation, the battery is fully discharged and the battery is fully charged but the solar energy is not installed.

Fully charged battery: SoC = 80 %

FIGURE. 94, FIGURE. 95, FIGURE. 96 and FIGURE. 97 show the battery SoC, the power involved in the micro-grid system, the four PHEV drive cycle and the ICE operations respectively.

The battery discharges in the morning before the driver goes to work, then the PHEV works in the all electric mode except on the way back of the third drive cycle, as shown in FIGURE. 96 where the ICE helps the battery to provide the required power (FIGURE. 94).

When the PHEV is connected to the house, during the on-peak period, the battery helps the grid only when peak power occurs. When the load demand is low, the battery charges due to the low SoC. During this period, the battery is in the charge sustaining mode. When the off-peak period appears, the battery starts to charge, to prepare for the next day.

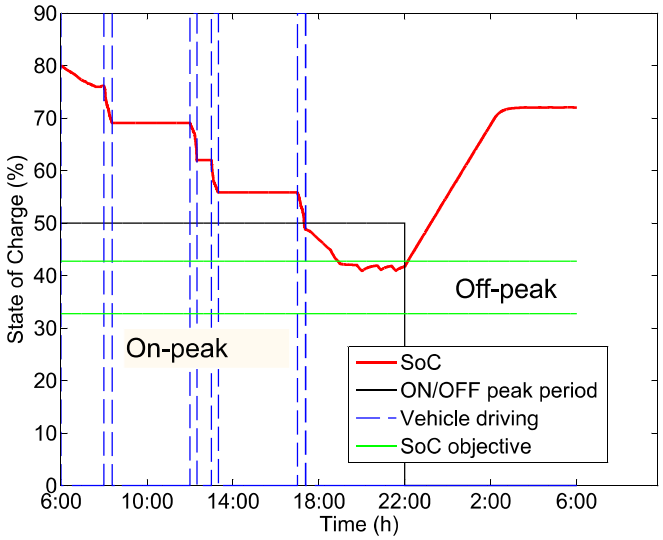

Figure 94. FL: SoC profile for the summer case with an initial SoC of 80 %

As shown in FIGURE. 95, during the on-peak period, the battery works in peak shaving mode. Then, when the off-peak period appears the battery charges in two steps. First, the battery is charged at its maximum charging current up to 2 AM, the charging power is decreased to reach a SoC of 72 %. The battery stops to charge at 3 AM.

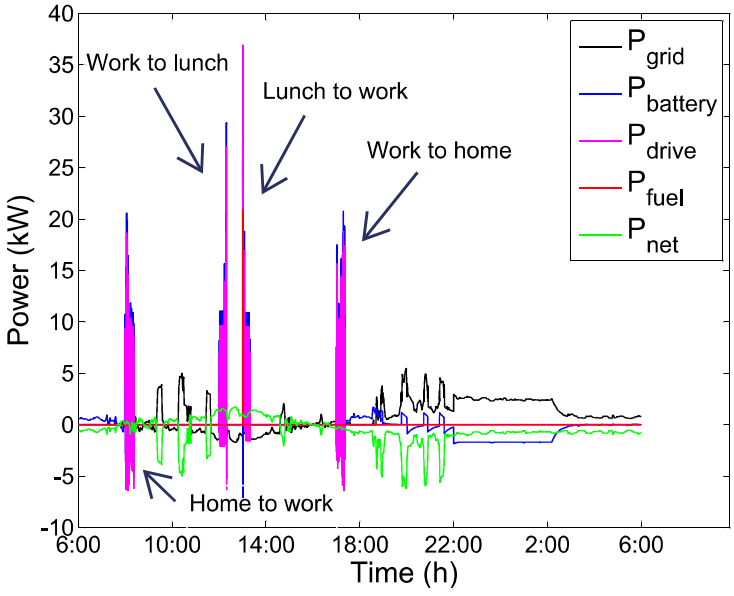

Figure 95. FL: power profile for the summer case with an initial SoC of 80 %

FIGURE. 96 is a zoom in of the four drive cycles. The only moment where the ICE is used, is when the battery power is not enough to supply the drive cycle power. At this time the ICE works in its best efficiency during the minimum time of 25 seconds.

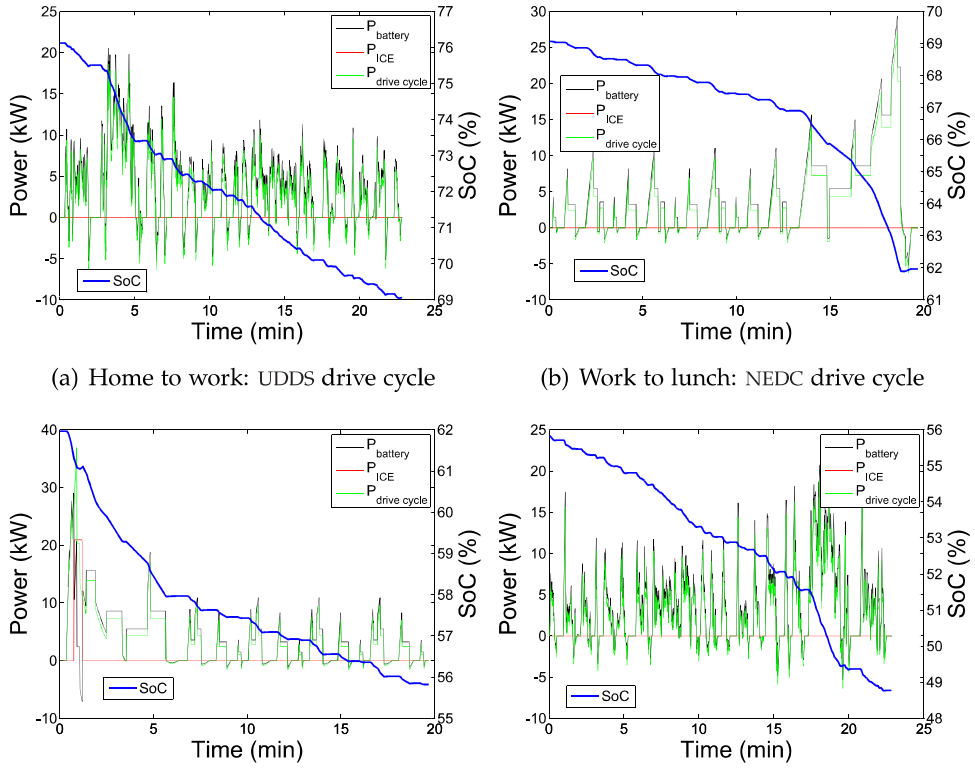

(a) Home to work: UDDS drive cycle

(b) Work to lunch: NEDC drive cycle

(c) Lunch to work: reverse NEDC drive cycle

(d) Work to home: reverse UDDS drive cycle

Figure 96. FL: travel drive cycle for the summer case with an initial SoC of 80 %

TABLE. 13 presents the financial situation between the conventional system, the online and the offline micro-grid system.

	Conventional system	Micro-grid system (online)	Micro-grid system (offline)
Grid cost	1.92 €	2.38 €	2.41 €
Fuel cost	4.68 €	0.08 €	0.11 €
Total cost	6.60 €	2.46 €	2.52 €

Table 13. FL summer result with a fully charged battery

The online simulation has a lower gain due to the battery charging. Indeed, in offline simulation, the battery is charged up to 80 % of its SoC, whereas in

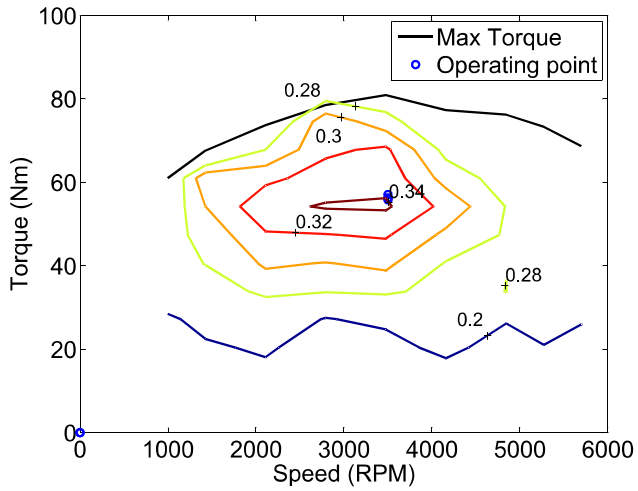

Figure 97. FL: ICE operation for the summer case with an initial SoC of 80 %

the online simulation the battery charges is up to 72 %. Taking into account the remaining cost of the battery, the total grid cost becomes 2,63 € and the total cost becomes 2,69 €. Therefore, the cost reduction is about 60 %. This reduction is close to that calculated in the offline simulation.

FIGURE. 98 compares the battery SoC in both simulation: offline and online.

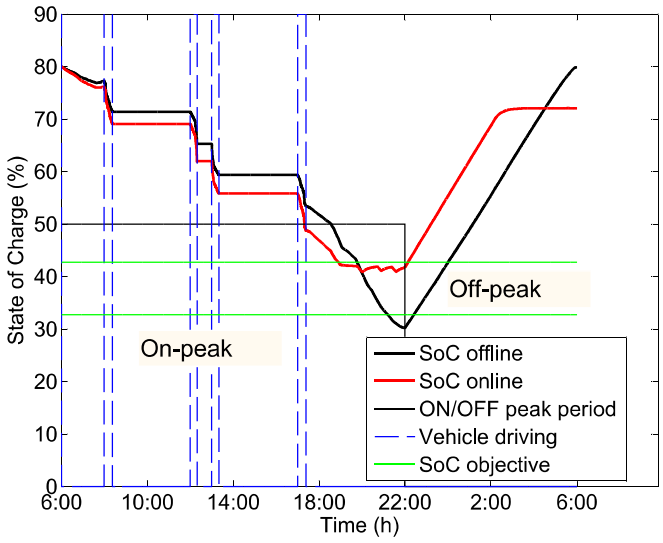

Figure 98. SoC profile comparison between the online and the offline simulation for the summer case with an initial SoC of 80 %

From 6 AM to the PHEV disconnection time, the battery behavior is similar in both simulations. Once the PHEV is connected, in offline simulation, the battery helps the grid to meet the loads, whereas in online simulation, the battery is used during peak power, and the battery charges when the household loads are low. The battery is in the charge sustaining mode.

It is important to notice that the offline simulation uses the full SoC range (until 30 % SoC), whereas the online simulation limits the SoC at 43 %.

Afterwards, in both simulations, during the off-peak period, the battery is charged. In online simulation, it is acceptable to use the battery the next day thought it is not fully charged.

The next sub case deals with a simulation which starts with a discharged battery.

Battery discharged: SoC = 35 %

FIGURE. 99, FIGURE. 101, FIGURE. 100 and FIGURE. 102 present the battery SoC, the ICE operations, the power involved in the micro-grid system and the four PHEV drive cycles respectively.

As shown in FIGURE. 99, the battery charges at the beginning of the run to prepare the PHEV before it leaves due to the low battery SoC.

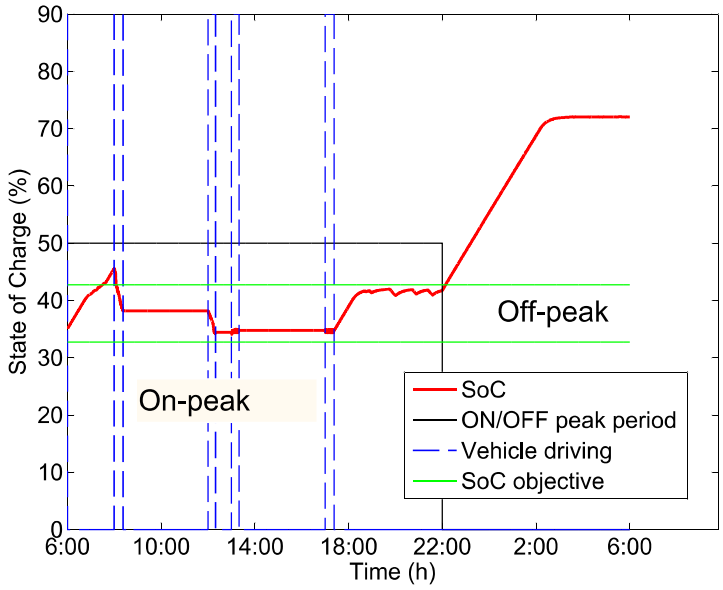

Figure 99. FL: SoC profile for the summer case with an initial SoC of 35 %

During the first trip, the battery is in the all electric mode whereas in the second drive cycle, the battery works in the first half in the all electric mode, and the last half in the charge sustaining mode. The last two drive cycles work in the charge sustaining mode ensuring the SoC objective window. Once the PHEV is connected to the house, due to the low load demand and the

level of the SoC, the battery charges until the first peak occurs, where it works in the peak shaving mode until the off-peak period starts. Around 2 AM the battery reaches 72 % SoC and stops charging. The battery is charged enough for the next day.

As shown in FIGURE. 100, the battery is discharged at the beginning of the simulation, then charged for 10 % (FIGURE. 99) before the PHEV leaves home. In addition, at this time, the household loads are low and smooth, which does not impact the grid supply. As in the previous case, and as presented in FIGURE. 102, the battery uses the all electric mode in the first trip and in the first half of the second drive cycle. In the rest of the travel, the battery works in the charge sustaining mode due to the SoC objective. Indeed, at the end of the first trip the battery SoC is entered in the SoC objective window.

Afterwards, in the evening, when the PHEV is connected, the battery charges due to the low loads. Once peak power occurs the battery switches to the peak shaving mode. Then, in the off-peak period, the battery charges at its maximum power and at 2 AM the battery charging stops. The battery is ready for the next day.

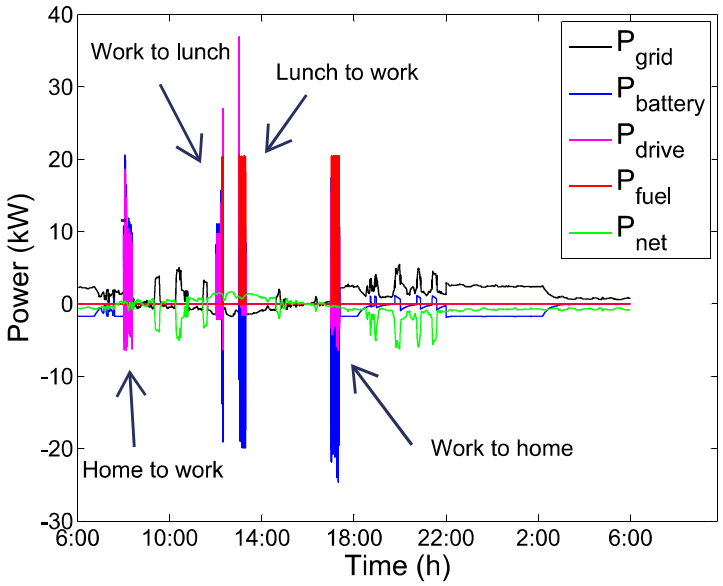

Figure 100. FL: power profile for the summer case with an initial SoC of 35 %

FIGURE. 101 shows that the ICE is working in the best iso-efficiency contour.

TABLE. 14 presents the cost summary between the conventional system, the online and offline micro-grid systems.

The system shows a cost reduction of 15 % compared to the conventional system. In addition, the cost difference between the online and the offline simulations, is the dwell in the battery charging at the beginning of the simulation. Indeed, in online simulation, the battery charging is lower than the offline simulation, which gives enough energy to propel the PHEV in all

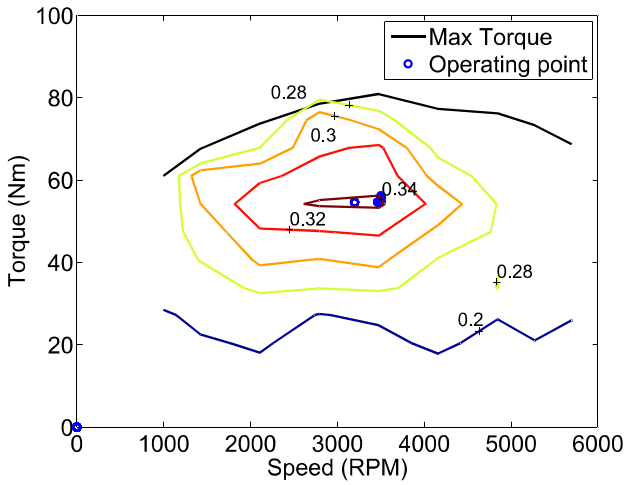

Figure 101. FL: ICE operations for the summer case with an initial SoC of 35 %

the electric mode. However, in online simulation, the battery is not charged enough before the driver leaves home, and then the ICE is switched on which induces a higher cost.

	Conventional system	Micro-grid system (online)	Micro-grid system (offline)
Grid cost	1.92 €	3.34 €	3.95 €
Fuel cost	4.68 €	2.26 €	0.12 €
Total cost	6.60 €	5.60 €	4.07 €

Table 14. FL summer result with a fully discharged battery

If 80 % charged battery is taken into account in the off-peak period, the cost reduction becomes 13 % due to the 8 % SoC remaining. However 72 % SoC is enough for the next day.

FIGURE. 103 presents the battery SoC comparison between the online and offline simulation. The main difference is the battery charging in the morning before the PHEV is disconnected. Indeed in the offline simulation, the SoC increases by 25 %, whereas in the online simulation by 8 %. Therefore, in the offline simulation, the battery is used in the charge depleting mode until to the minimum SoC, whereas in the online simulation, the battery works in the charge sustaining mode until it is fully charged during the off-peak period.

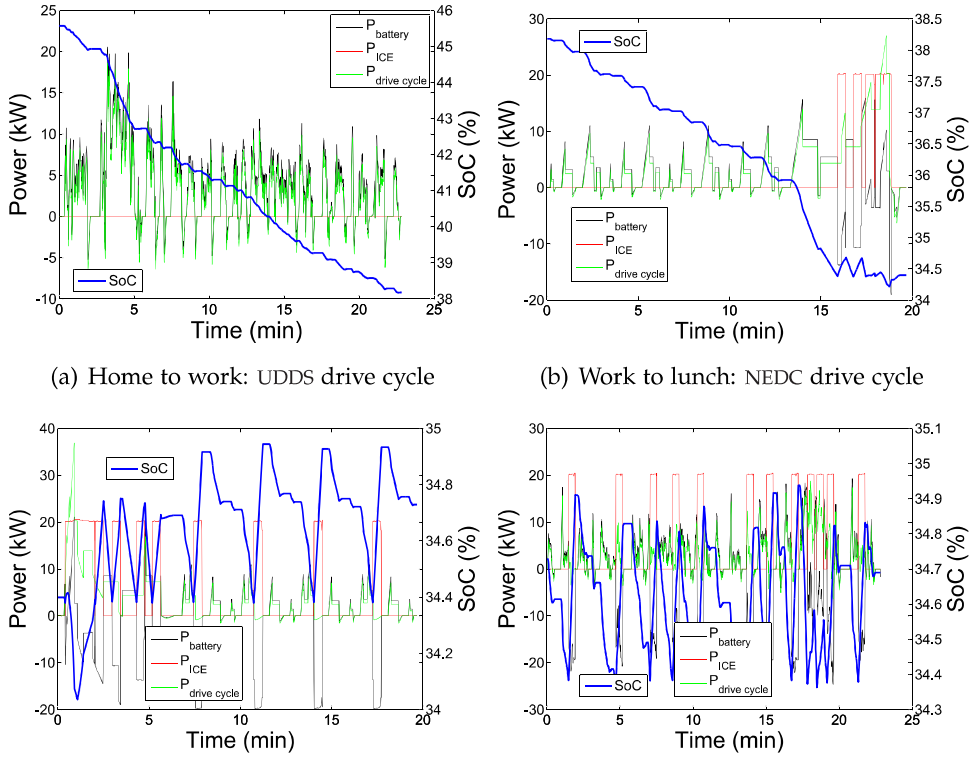

(a) Home to work: UDDS drive cycle

(b) Work to lunch: NEDC drive cycle

(c) Lunch to work: reverse NEDC drive cycle

(d) Work to home: reverse UDDS drive cycle

Figure 102. FL: travel drive cycle for the summer case with an initial SoC of 35 %

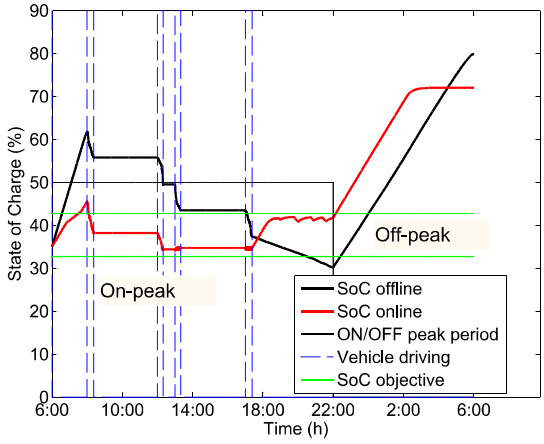

Figure 103. SoC profile comparison between the online and the offline for the summer case with an initial SoC of 35 %

The next case starts with a battery SoC of 80 % and without solar energy.

Without renewable energy sources

The case presents the micro-grid system behavior when the battery is fully charged and the local renewable energy sources are not installed. FIGURE. 104, FIGURE. 105, FIGURE. 106 and FIGURE. 107 represents the battery SoC behavior, powers involved in the system, the power involved in the four drive cycle and the ICE operation mapping when the ICE is used.

The battery SoC has similar behavior as when a battery is fully charged and the local solar energy is installed. Indeed, the battery works in the charge depleting mode when the PHEV is used and when the PHEV is connected to the house during the on-peak period. When the on-peak period starts, the battery starts to charge as well.

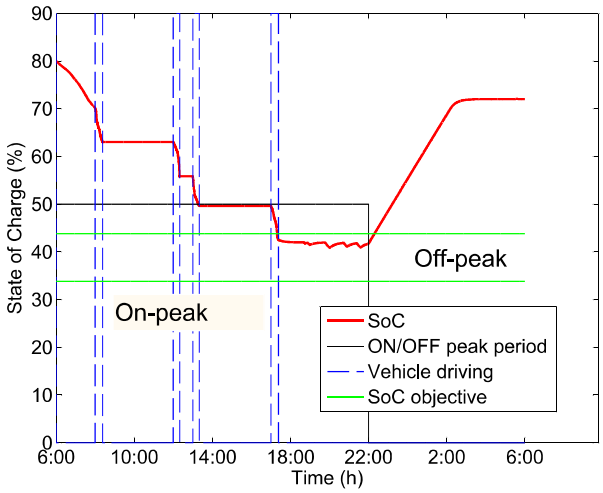

Figure 104. FL: SoC profile for the summer case with an initial SoC of 80 % and without RES

FIGURE. 105 presents the powers involved in the micro-grid system. The battery power starts with a fully battery. In the morning before the PHEV disconnects, the battery supplies the household load. Then during the four trips the battery works in the charge depleting mode as shown in FIGURE. 106. In the evening, when the PHEV is back at home, at on-peak period, the PHEV works in the charge sustaining mode. Finally, at off-peak period the battery is in charging mode until 3 AM.

As in the sub cases, where the battery start with 80 %, the ICE is used only when the battery cannot supply the required drive cycle power due to the battery limitation. This happens in the third trip from lunch to work.

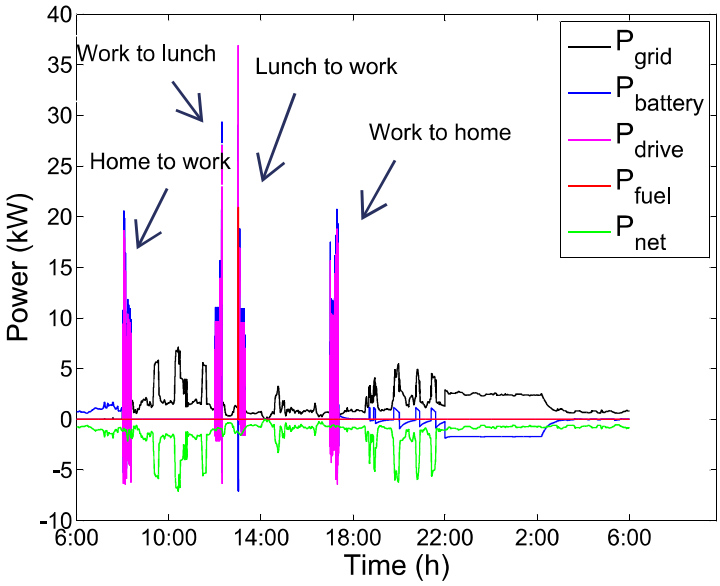

Figure 105. FL: power profile for the summer case with an initial SoC of 80 % and without RES

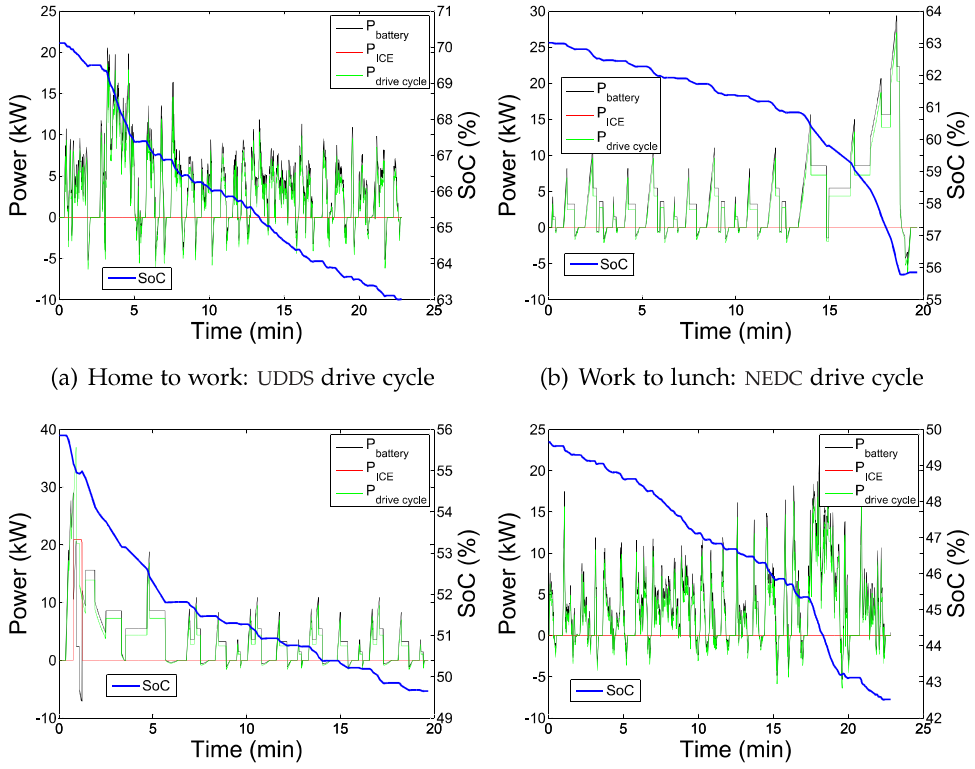

(a) Home to work: UDDS drive cycle

(b) Work to lunch: NEDC drive cycle

(c) Lunch to work: reverse NEDC drive cycle

(d) Reverse NEDC drive cycle

Figure 106. FL: travel drive cycle for the summer case with an initial SoC of 80 % and without RES

FIGURE. 107 shows that the energy control strategy plays properly role, since the ICE is working at its best efficiency which reduce the losses.

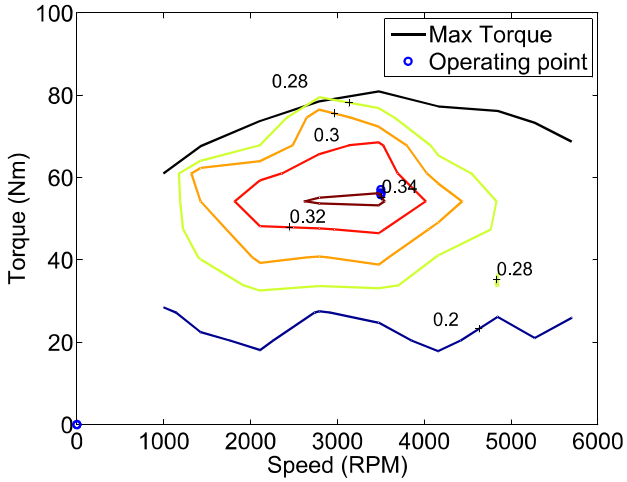

Figure 107. FL: ICE operation for the summer case with an initial SoC of 80 % and without RES

TABLE. 15 summarizes the cost of the three systems: conventional, micro-grid system online and offline.

	Conventional system	Micro-grid system (online)	Micro-grid system (offline)
Grid cost	4.16 €	4.63 €	4.65 €
Fuel cost	4.68 €	0.08 €	0.11 €
Total cost	8.84 €	4.72 €	4.76 €

Table 15. FL summer result during summer case with an initial SoC = 80 % and without RES

The results shows that the online simulation is cheaper than the offline simulation due to the fact that in, the online simulation, the battery is not fully charged. The battery is charged up to 72 %. Adding the remaining cost of a fully charge battery, the total energy cost becomes 4.88 € which gives a reduction of 45 % compared to the conventional system.

FIGURE. 108 shows the comparison of the battery SoC between the online and offline simulations.

During the day, the battery behavior is similar. The battery works in the charge depleting mode. However, when the PHEV is connected to the home, the offline simulation continues to use the battery in the charge depleting mode, whereas the online simulation uses the battery in the peak shaving

mode. When the off-peak period appears in both simulations, the battery is in the charge mode.

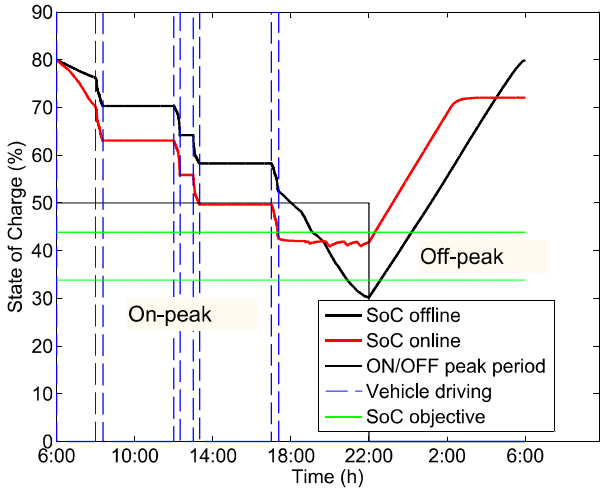

Figure 108. SoC comparison between online and offline results during summer case with an initial SoC = 80 % and without RES

This section has presented the summer case, where all the sub cases show, a cost reduction when the battery is fully charged at the beginning of the simulation, and with or without solar energy, or with a discharged battery when the simulation starts. The next section presents the winter case.

4.6.3 *Winter case*

Similar to the summer case, the winter case is divided into three sub cases: where the simulation starts with a fully charged battery, a fully discharged battery and without solar energy.

Battery charged: SoC = 80 %

FIGURE. 109, FIGURE. 110, FIGURE. 112 and FIGURE. 111 present the battery SoC behavior, powers involved in the system, the power involved in the four drive cycles and the ICE operation map when it is used.

As in the previous case, the battery supplies the household loads, due to the high level of SoC. Then, during the four drive cycle in the first two trips, the battery is used in the all electric mode, whereas in the last two trips the battery switches to the charge sustaining mode, due to the SoC objective window. When the PHEV is back home, the battery first helps the grid to meet the loads. Secondly, due to the low SoC, the battery uses the charge sustaining mode for smoothen the peak consumption until the off-peak period occurs. Finally, in the off-peak period, the battery is in the charging mode.

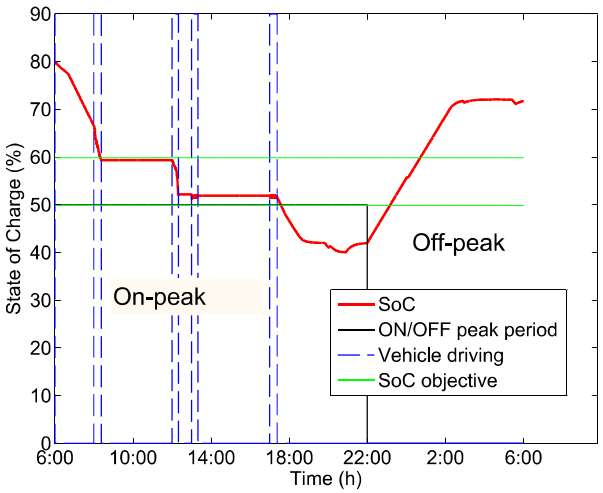

Figure 109. FL: SoC profile for the winter case with an initial SoC of 80 %

As shown in FIGURE. 110, in the morning, the battery supplies the full household loads. When the PHEV disconnects from the house, the grid takes over. In the evening, at on-peak period: first the battery helps the grid to meet the household loads. Secondly, the battery is used in the peak shaving mode. Afterwards, at the off-peak period, the battery charges until 2 AM to reach 71 % SoC.

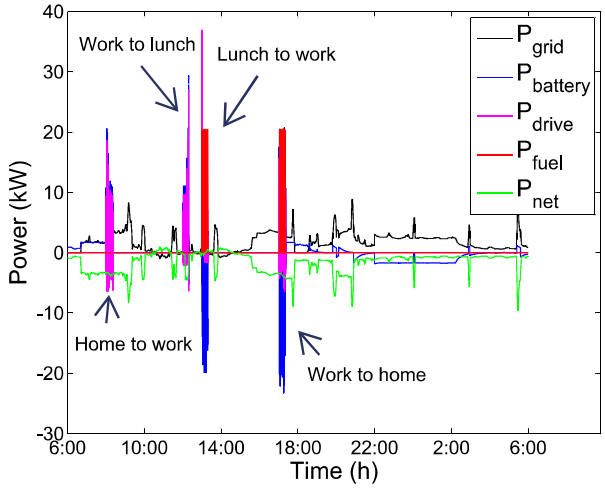

Figure 110. FL: power profile for the winter case with an initial SoC of 80 %

FIGURE. 111 presents the ICE operation. In this case the ICE works only in its best efficiency contour, and more at its best efficiency point ($\eta 34_{max}$).

FIGURE. 112 shows the four trips. In the first two trips, the battery is in

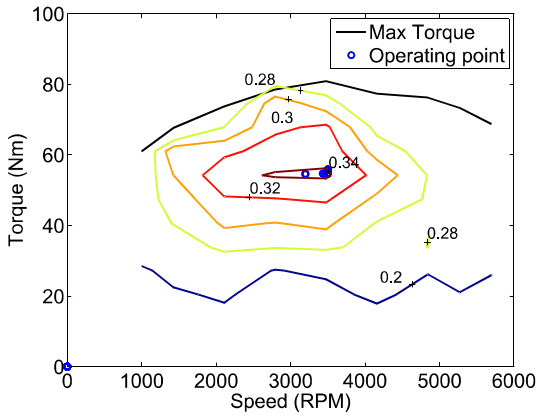

Figure 111. FL: ICE operations for the winter case with an initial SoC of 80 %

the all electric mode whereas in the last two ones, it works in the charge sustaining mode.

TABLE. 16 presents the financial situation between the conventional system, the online and the offline micro-grid systems.

Even if the battery is not fully charged at the end of the simulation (71 %), the online simulation reduces the energy cost by 29 %, and if the remaining battery charge is taken into account, the reduction becomes 27 %. Indeed, if the remaining energy to fully charged the battery (80 %), the grid cost becomes 5.69 €, giving a total cost of 7.40 €.

	Conventional system	Micro-grid system (online)	Micro-grid system (offline)
Grid cost	5.41 €	5.50 €	5.90 €
Fuel cost	4.68 €	1.71 €	0.11 €
Total cost	10.09 €	7.21 €	6.01 €

Table 16. FL winter result with a fully charged battery

FIGURE. 113 presents the SoC comparison between the offline and the online simulations. The battery behavior is similar in the morning, before the PHEV is disconnected. However, in the offline simulation, the battery discharges to a lower level than in the online simulation. That allows the battery to work in all electric mode. In the offline simulation, the battery operates in the charge depleting mode to reach 30 % SoC. However, in the online simulation, the battery does not go below 40 %. Finally, both simulations charge the battery at the off-peak period.

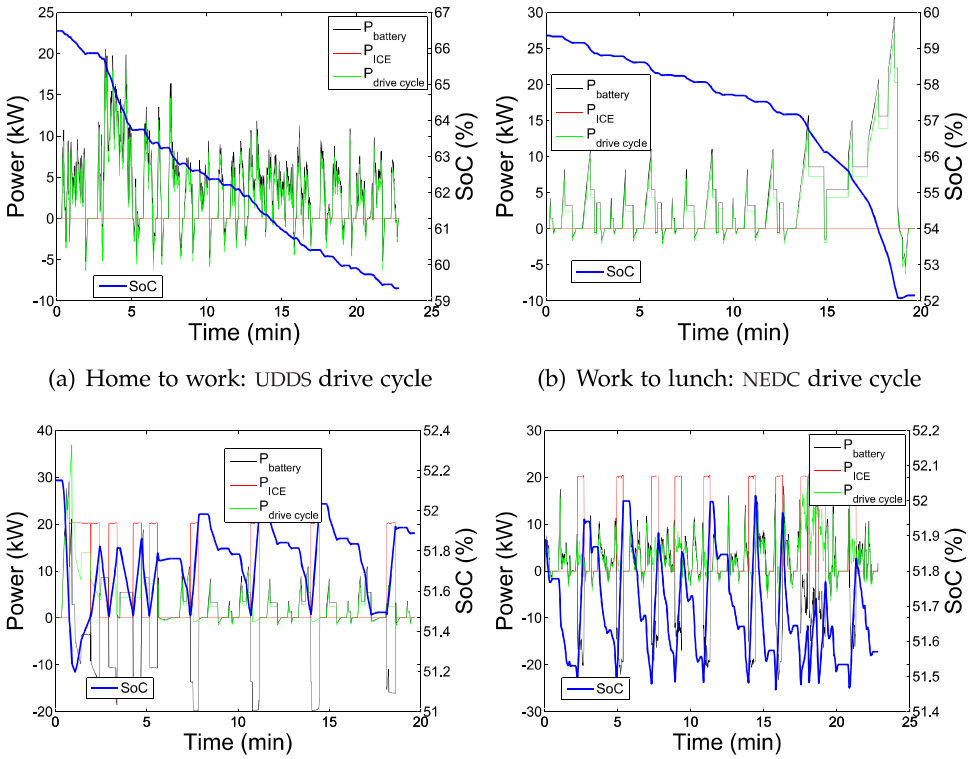

(a) Home to work: UDDS drive cycle

(b) Work to lunch: NEDC drive cycle

(c) Lunch to work: reverse NEDC drive cycle

(d) Work to home: reverse UDDS drive cycle

Figure 112. FL: travel drive cycle for the winter case with an initial SoC of 80 %

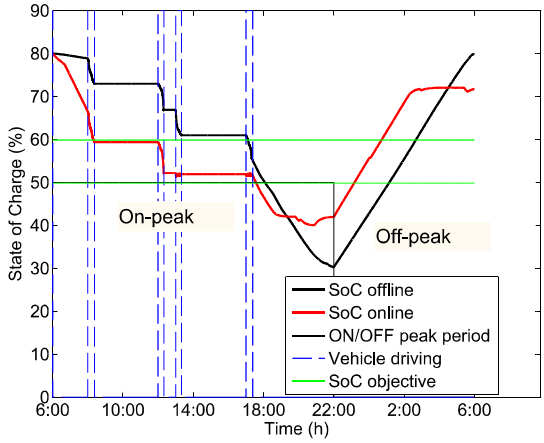

Figure 113. SoC profiles comparison between online and offline for the winter case with an initial SoC of 80 %

In the next sub case, the simulation starts with a discharged battery.

Battery discharged: SoC = 35 %

FIGURE. 114, FIGURE. 115, FIGURE. 117 and FIGURE. 116 represent the battery SoC behavior, powers involved in the system, the power involved in the four trips and the ICE operation map when it is used respectively.

As shown in FIGURE. 114, at the beginning of the simulation, the household loads are low, which the battery allows to charge. Afterwards, the household loads increase, therefore the battery stops to charge (FIGURE. 115) due to its SoC level.

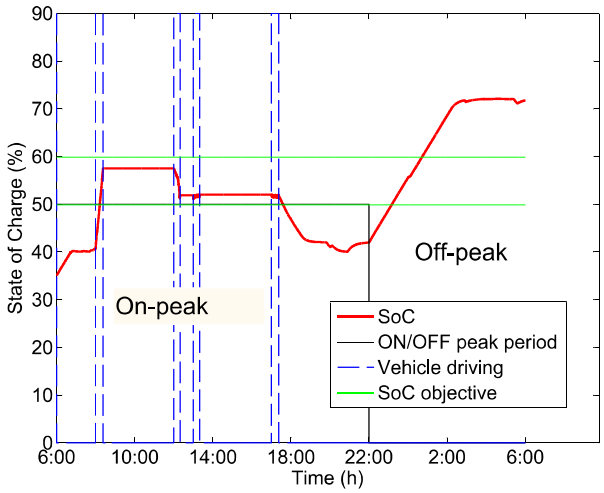

Figure 114. FL: SoC profile for the winter case with an initial SoC of 35 %

Once the PHEV is disconnected, in the first trip, the battery works in the charging mode. At the end of this trip, the SoC increases by 18 % reaching the SoC objective window. In the second trip, the battery works 90 % of the time in the all electric mode, and finishes in the charge sustaining mode. In the last two trips, the battery operates also in the charge sustaining mode.

Moreover the ICE works in its best efficiency contour and at the second contour nearby at its best efficiency point.

Once the PHEV connects to the house, the battery helps the grid to meet the household loads. When these loads are low, the battery switches to charging mode in low power. Afterwards, at off-peak period the battery charges until 2 AM and at the end of the simulation the battery works in peak shaving mode.

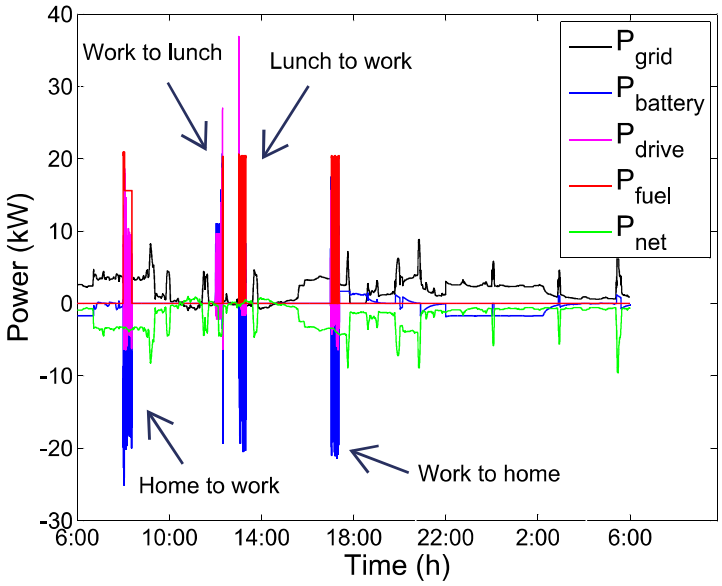

Figure 115. FL: power profiles for the winter case with an initial SoC of 35 %

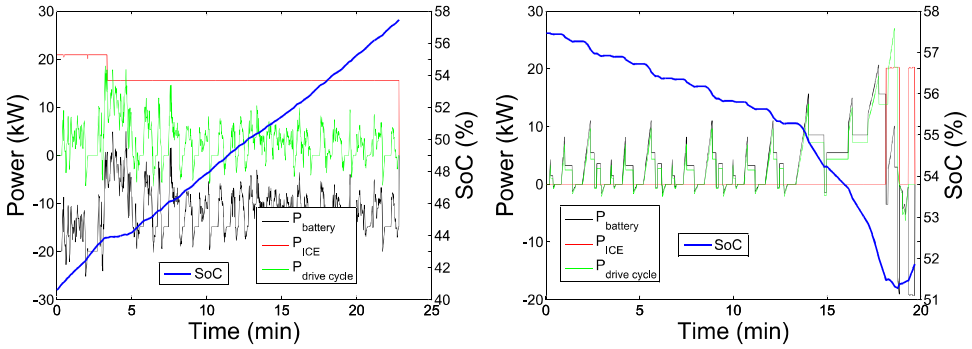

(a) Home to work: UDDS drive cycle

(b) Work to lunch: NEDC drive cycle

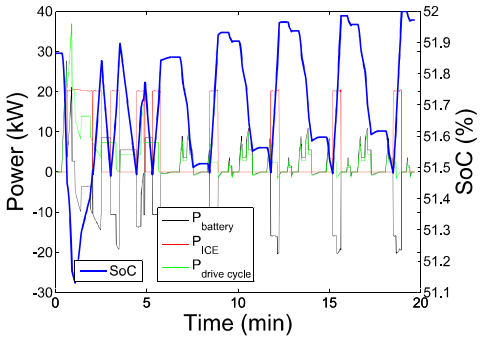

(c) Lunch to work: reverse NEDC drive cycle

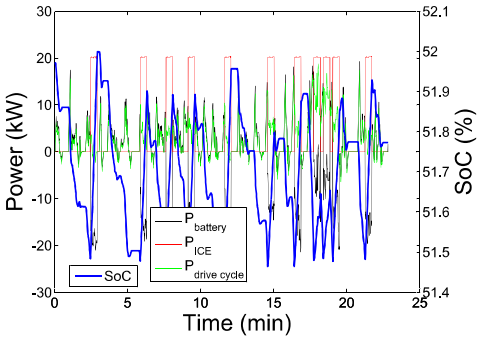

(d) Work to home: reverse UDDS drive cycle

Figure 117. FL:travel drive cycle for the winter case with an initial SoC of 35 %

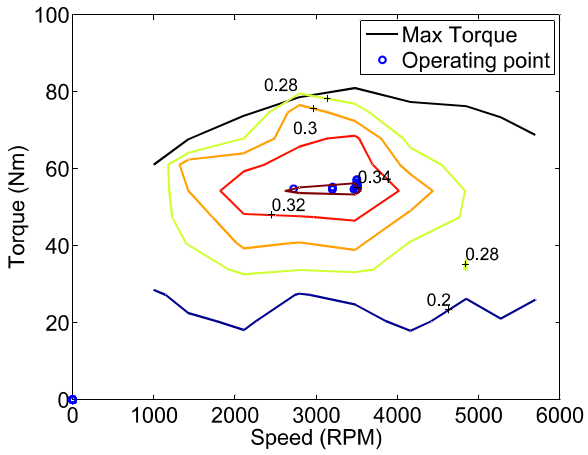

Figure 116. FL: ICE operations for the winter case with an initial SoC = 35 %

TABLE. 17 presents the financial situation between the conventional system, the online and offline micro-grid system.

	Conventional system	Micro-grid system (online)	Micro-grid system (offline)
Grid cost	5.41 €	6.10 €	7.45 €
Fuel cost	4.68 €	5.08 €	0.12 €
Total cost	10.09 €	11.18 €	7.57 €

Table 17. FL winter result with a fully discharged battery

The offline simulation is the highest than in the other simulations. The cost increases by 10 %. However, this situation is mitigated if the driver connects the vehicle every evening. Moreover, in summer there is a general reduction cost (13 %), and it is only in this winter sub case that the micro-grid system becomes more expensive.

FIGURE. 118 shows the comparison between the online and the offline simulations. The battery behavior at the beginning of the simulation is critical for the next four trips. Indeed, in the offline simulation the battery works in the all electric mode whereas, in the online simulation, one trip charges the battery, then the battery works in the all electric mode and for the last two, it works in the charge depleting mode. Afterwards, at on-peak period, the battery works in the charge depleting mode, and at off-peak period, it charges.

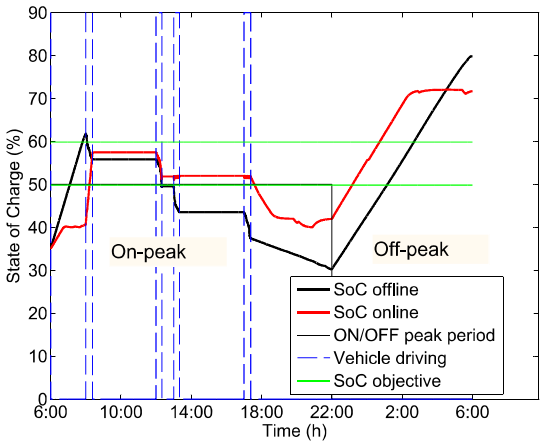

Figure 118. SoC profiles comparison between online and offline for the winter case with an initial SoC of 35 %

The last sub case starts with a fully charged battery and without solar energy.

Without renewable energy sources

FIGURE. 119, FIGURE. 120, FIGURE. 121 and FIGURE. 122 present the battery SoC behavior, powers involved in the system, the power involved in the four trips and the ICE operation map when it is used respectively.

At the beginning, the battery discharges to supply the household loads (FIGURE. 119).

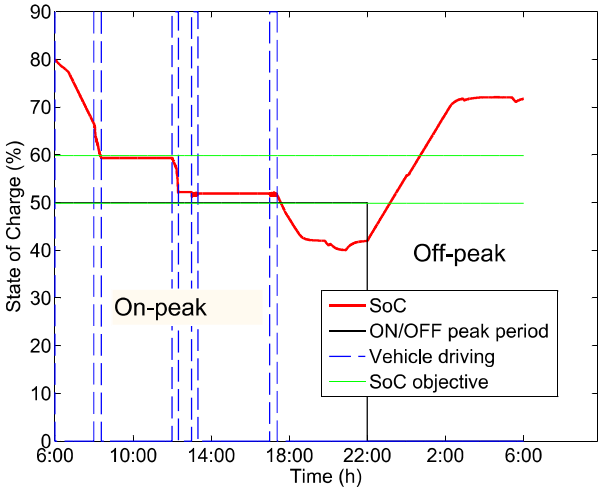

Figure 119. FL: SoC profile for the winter case with an initial SoC of 80 % and without RES

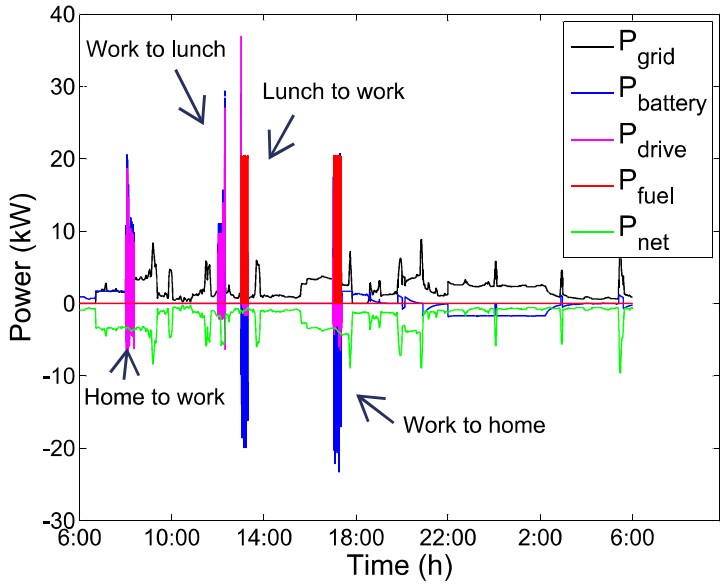

Figure 120. FL: power profile for the winter case with an initial SoC of 80 % and without RES

Afterward, FIGURE. 121 a zoom in of the four trips; in the first two trips, the battery works in the all electric mode and the two last trips, the battery works in the charge sustaining mode due to the SoC objective window. Then, at on-peak period and when the the battery is connected to the house, the battery is in the peak shaving mode when P_{net} is high and in opposite, when P_{net} is low, the battery charges at low power.

As in previous case the ICE works in its best efficiency contour, as presented in FIGURE. 122.

TABLE. 18 summarizes the cost of the three systems. It shows a reduction of 26 % between the conventional and the online systems. If a fully charged battery is taken into account (charge until 80 % as opposed to 72 %) the reduction becomes 25 %.

	Conventional system	Micro-grid system (online)	Micro-grid system (offline)
Grid cost	6.32 €	6.41 €	6.81 €
Fuel cost	4.68 €	1.71 €	0.11 €
Total cost	11.00 €	8.12 €	6.92 €

Table 18. FL summer results for the winter case with an initial SoC of 80 % and without RES

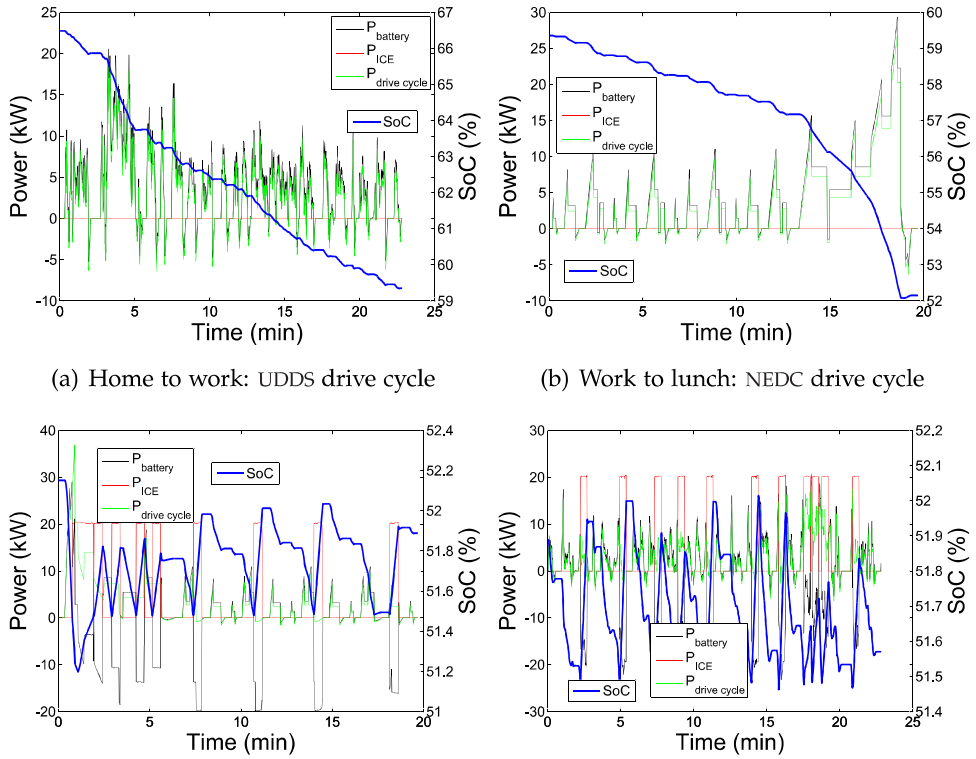

(a) Home to work: UDDS drive cycle

(b) Work to lunch: NEDC drive cycle

(c) Lunch to work: reverse NEDC drive cycle

(d) Work to home: reverse UDDS drive cycle

Figure 121. FL: travel drive cycle for the winter case with an initial SoC of 80 % and without RES

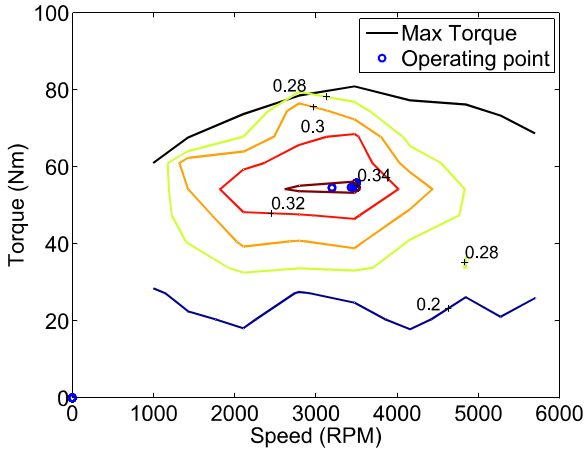

Figure 122. FL: ICE operations for the winter case with an initial SoC of 80 % and without RES

FIGURE. 123 compares the online and offline battery behavior. The behavior

until the driver connects the PHEV to the house is similar. Then in offline simulation, the battery continues to be in the charge depleting mode whereas in the online simulation the battery starts its charge sustaining mode. At the end, both simulations charge the battery at the off-peak period.

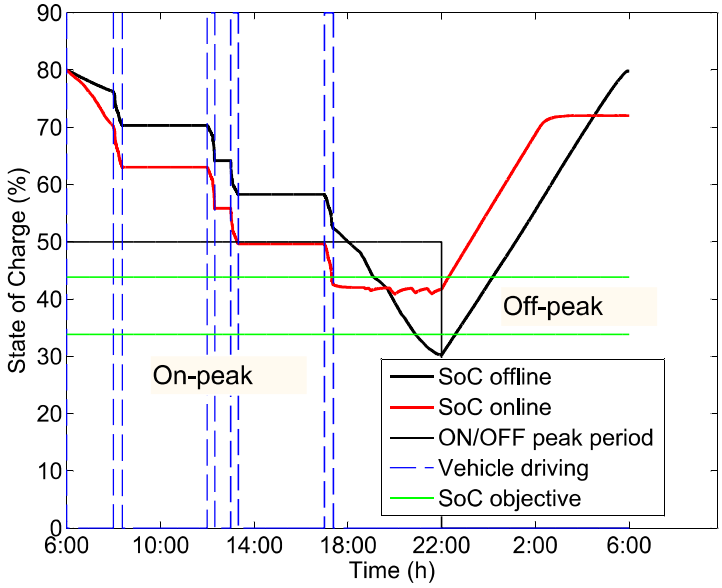

Figure 123. SoC comparison between online and offline results during winter case with an initial SoC of 80 % and without RES

This section has presented the results of a winter case which includes three sub cases. The micro-grid system presents a cost reduction when the simulation starts with a fully charged battery. However, in the winter case, when the battery is discharged at the beginning of the simulation, the energy cost increases by 10 % but this case should be rare, if the driver connects the vehicle everyday.

4.6.4 *Conclusion*

As summarized in FIGURE. 124, except for the winter case when the simulation starts with a fully discharged battery, the micro-grid system presents a cost significant reduction. Indeed, the saving comes from the reduced usage of the ICE by allowing the PHEV to operate in the all electric mode. This meets transportation requirements for the studied trip.

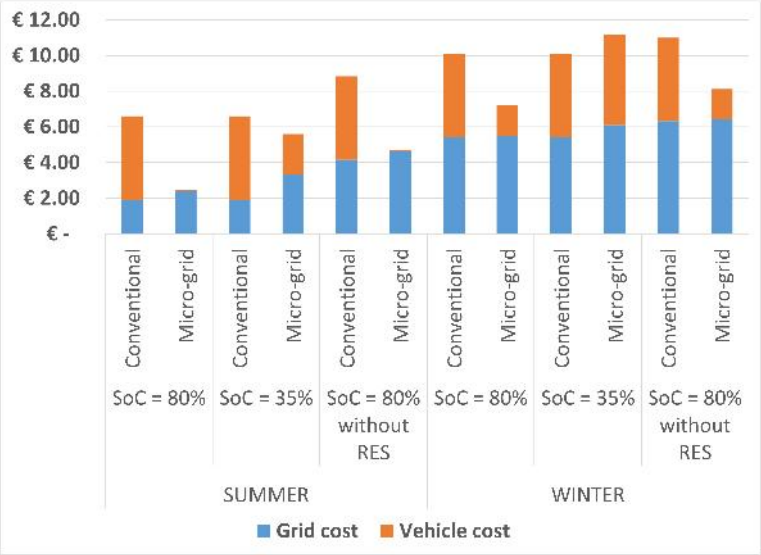

Figure 124. FL: 6 cases comparison

The other saving is from the storage of cheaper energy in the off-peak period, that is later used for peak shaving during on-peak period, when the grid cost is higher. These simulation studies have shown that, the energy costs can be reduced by optimizing the charging and the usage of the PHEV battery.

The next section presents the average monthly savings.

4.6.5 *Monthly results*

The same method as in the dynamic programming simulation, a trimmed average is applied on the household loads and the solar production, to be able to find the average cost of a day, and for a month. Every simulation starts with a fully charged battery. FIGURE. 125 shows this results where the highest saving is in June. For the whole year, about 42 % savings is made, which is comparable to the dynamic programming results (46 %).

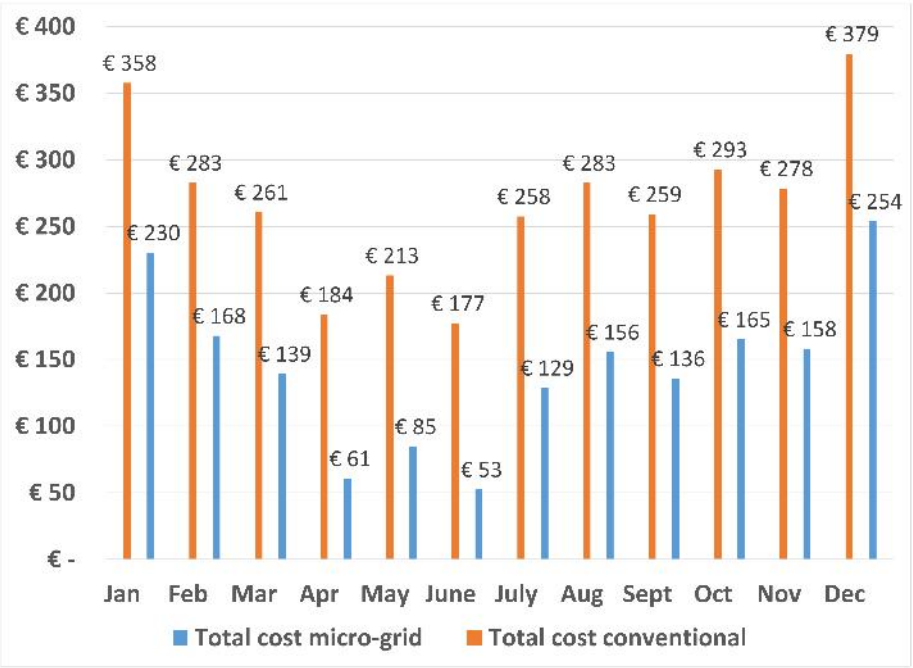

Figure 125. FL: monthly cost comparison

However, the result is encouraging although the installation cost of the solar energy, the cost of the PHEV and the installation cost of the bidirectional battery charger are not taken into account.

4.7 CONCLUSION

This chapter has presented the full energy control strategy of the micro-grid system. The two controllers in the house and in the PHEV using the fuzzy logic control, have been presented. Indeed, the construction of the controllers was detailed: the PHEV controller is build according to the ICE size and the maximum battery power. This controller is updated everyday according to the calculated SoC objective. The house controller is built according to the battery charger size and the electricity price.

The results were divided into two sections. The first one considered two cases: summer and winter. Each case was then divided into three sub cases: where the battery is fully charged at the beginning of the simulation; with or without renewable energy sources and where the battery is fully discharged at the beginning of the simulation. As in dynamic programming the micro-grid system shows the results are repeatable in winter and in summer and is flexible: renewable energy sources can be installed or not.

In addition, it has been shown that in the winter case, where the battery is fully discharged at the beginning of the simulation, the micro-grid system is more expensive than the conventional system. This situation occurs if the

driver forgets to plug the PHEV. To avoid this situation, a wireless battery charger can be used. According to [68], the wireless battery charger presents lower efficiency than the wired battery charger, but the driver does not have to remember to plug in the vehicle.

The second result shows the overall monthly gain. Using the trimmed average method, the simulation shows an overall reduction of 44 % compared to the conventional system. This is comparable to the dynamic programming algorithm which has a reduced of 46 %.

As noticed in the dynamic programming algorithm, the electricity price using the on and the off-peak period, allows to control the battery charging. This means that if the schedule change of the on and off peak price, the charging of the battery also change accordingly.

This control strategy us validated by an experimental set up in the next chapter. The last chapter will present the experiment set-up of the fuzzy logic energy control strategy.

5

EXPERIMENT

The last step of this research, after finding the minimum energy cost, though the energy control strategy either in the PHEV and in house, is to implement the two controllers. Due to the battery limitation the set-up is scaled to a quarter as presented in FIGURE. 126. Labview® is used to implement the two fuzzy logic controllers.

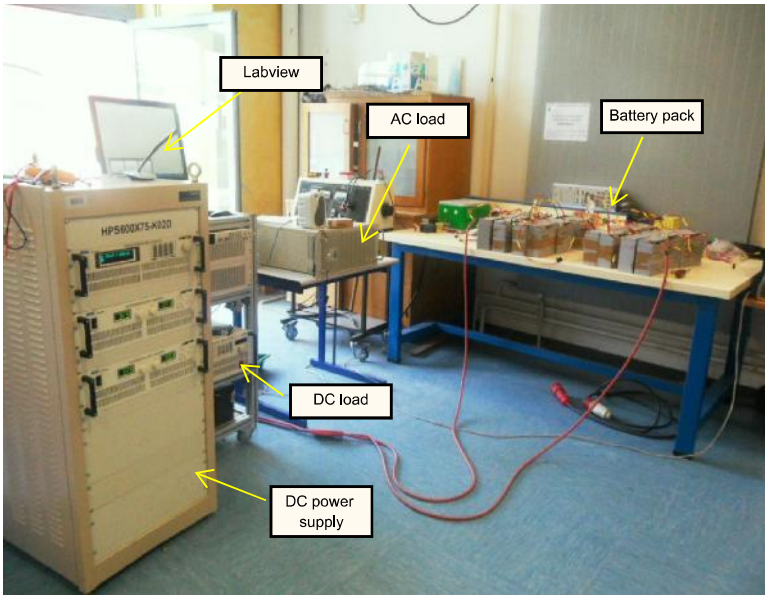

Figure 126. Set-up picture

The Labview program is divided into two windows: the front panel and the diagram. Both windows are described in this chapter. An active load emulates the solar energy as well as the drive cycle power. The DC active load is composed of the power supply SPSe and the load PLW36K-400-1200, and is connected to Labview® via a General Purpose Interface Bus (GPIB) communication.

The AC loads is also controlled from Labview® via a GPIB communication. This load emulates the household loads.

The battery used in this set-up is a lead acid battery which has the same characteristic than in the simulation parts.

The last part presents the experimental results of the two cases: summer and winter with a fully charged battery at the beginning of the run.

5.1 LABVIEW®

The two controllers: home and PHEV are imported from Matlab® into Labview®. Before running the experiment, the scenario has to be created. Indeed a preprocessing is done using the previous Matlab® interface to create the scenario and the two controllers according to the input parameters.

This section presents the Labview® interface and diagram.

5.1.1 *Front panel*

The front panel is composed of 5 parts: the DC active load limitation in term of current and voltage, the displays (SoC, $P_{battery}$, battery voltage and DC active power), the stop button, the options for saving data and the 3 graphs displaying the scenario, the power profile and the total cost.

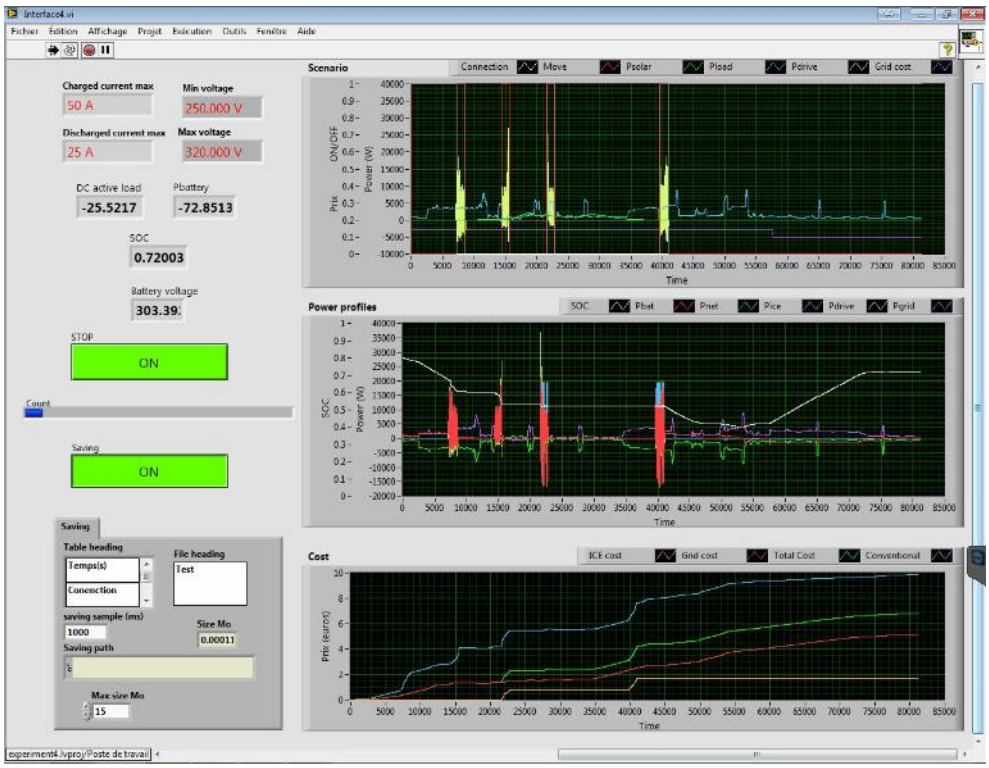

Figure 127. Labview® user interface

DC active load limitation

The DC active load limitations prevent the over-voltage and over-current in the battery. The voltage, and discharged and charged current are linked with the battery limitation.

Displays

The displays show in real time the battery SoC, the battery voltage, the DC active load reference and the battery power.

Stop buttons

The two stop buttons are used: for stopping the run and the data saving.

Data saving option

The data saving option provides the table heading, the name of the file, the file path, the sample time and the maximum file size.

Graphs

The graphs show the running scenario, the SoC, the battery power, the net power, the grid power and the last graph presents the different cost of the micro-grid system; such as the cost linked to the ICE, the grid cost and the total micro-grid cost. The last graph also includes the conventional system which includes the conventional car and the grid supply.

5.1.2 *Diagram*

FIGURE. 128, shows the Labview® program, showing the two fuzzy logic controllers imported from Matlab®. It also shows in the scenario data from the preprocessing interface created under Matlab®.

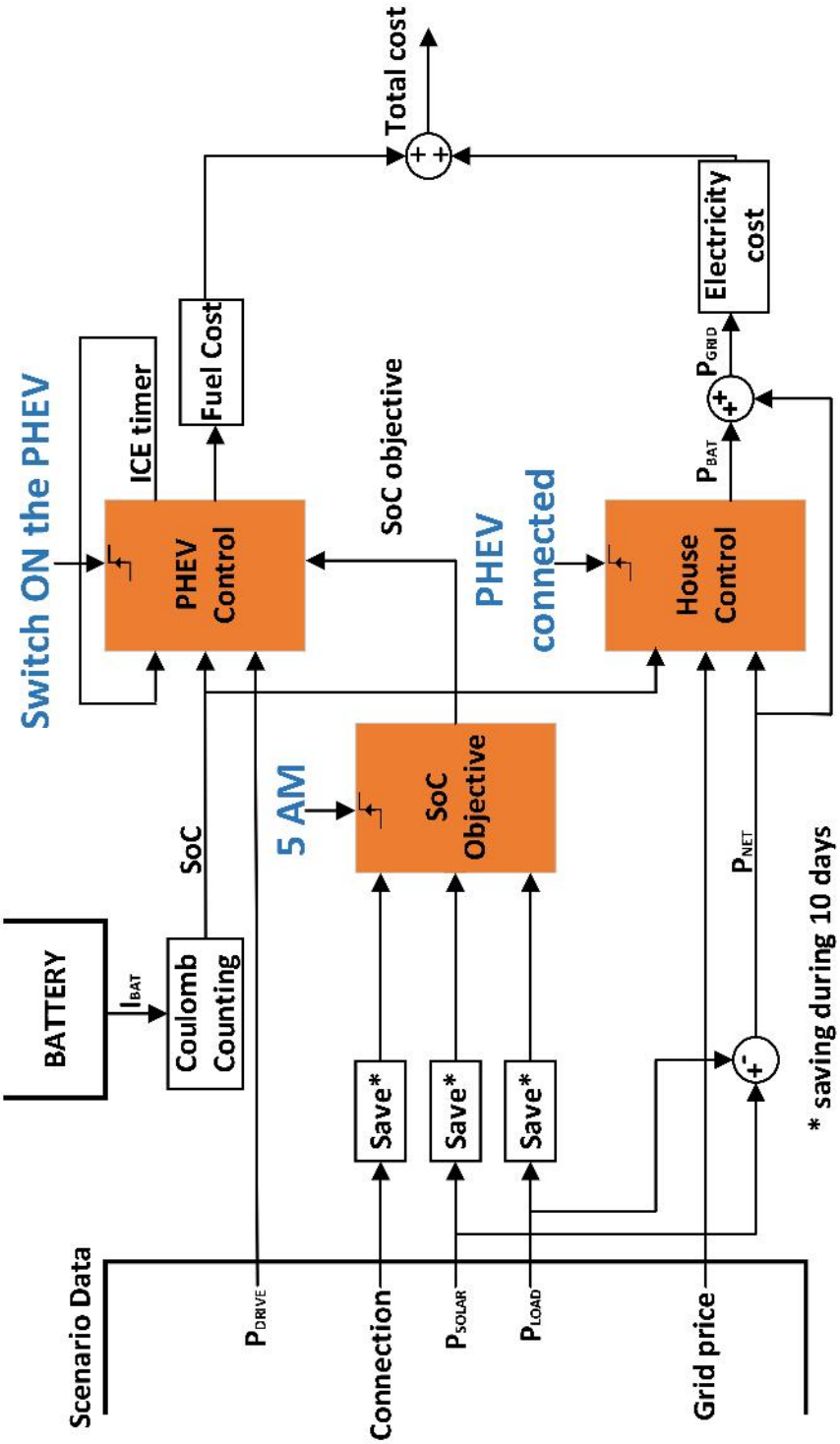

Figure 128. Real Time diagram

The DC active load which emulate the solar energy and the drive cycle power, is described in the next section.

5.2 DC ACTIVE LOAD PROGRAM AND COMMUNICATION PROTOCOL

The DC active load is divided into two devices: the power supply and the load. The SPSe power supply from AMREL® is used when the power is negative and the PLW36K-400-1200 load from AMREL® when the power is positive.

FIGURE. 129 describes the algorithm which is divided into three parts depending of the reference power:

- when the reference power is positive, the DC power supply is switched off and the DC load measure the voltage, calculates the reference current and send the value;
- when the reference power is zero, both DC load and DC power supply are switched off;
- when the reference power is negative, the DC is switched off and the DC power supply work in constant voltage mode to charge the battery.

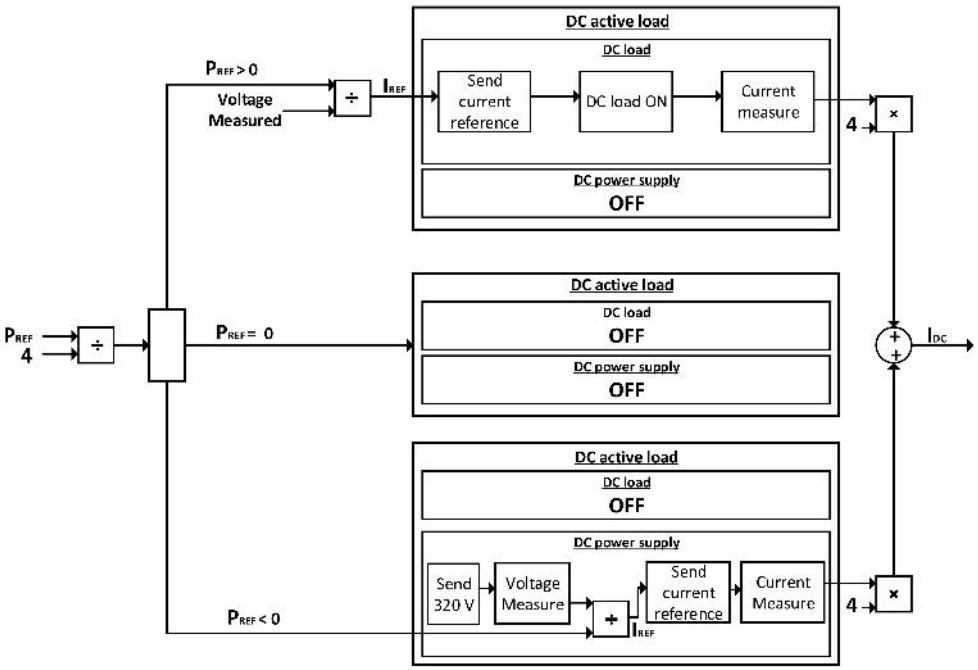

Figure 129. DC active load algorithm

The battery charging mode is working in the constant voltage mode. The constant voltage mode maintains nearly the same input voltage to the battery throughout the charging process, regardless of the battery SoC. Constant-

voltage chargers provide a high initial current to the battery because of the greater potential difference between the battery and charger.

The communication between Labview® and the DC active load is done with GPIB protocol. This protocol is also know as IEEE-488 interface bus, is an 8 bit wide byte serial, bit parallel interface system which incorporates:

- 5 control lines
- 3 handshake lines
- 8 bi-directional data lines.

The two GPIB ports (DC load and DC power supply) are connected to the Agilent 82350 PCI-GPIB interface card. Labview® integrates the GPIB communication using visa toolkit via the Agilent® card, as shown in FIGURE. 130. The four commands used in the DC active load are: on/off power, measurement of the voltage and current and the current reference. The respective command are indexed in TABLE. 19 where xx is the reference value.

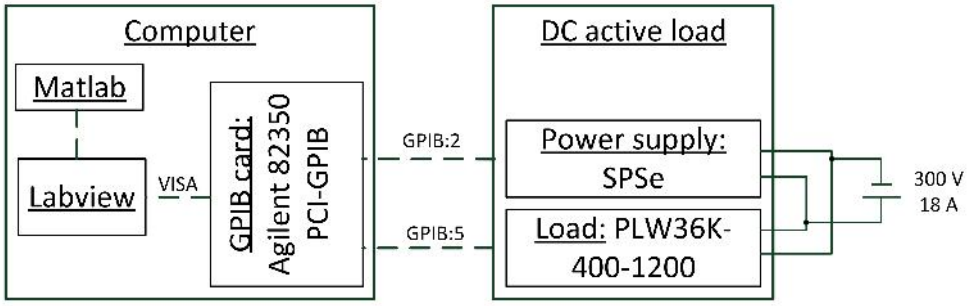

Figure 130. Experiment diagram

	DC power supply	DC load
Current measurement	MEAS;CURR?1	;MEAS:CURR?
Voltage measurement	MEAS:VOLT?1	;MEAS:VOLT?
Switch on	OUTP 1 OFF	ENABLE VISA
Set current reference	CURR 1 xx	MOD CURR;:CURR xx

Table 19. GPIB commands

The next section presents the summer and winter results with a fully charged battery at the beginning of the run.

5.3 RESULTS AND COMPARISON WITH SIMULATIONS

This section presents two case studies: one in summer and one in winter. These two case studies start with a fully charged battery at the beginning of the run. In addition, a SoC comparison of the two simulations (offline and online) as well as the experiment are presented.

5.3.1 *Summer case*

FIGURE. 131, FIGURE. 132 and FIGURE. 133 show the SoC comparison,the cost evolution during the day and comparison between the controllers and the battery power respectively.

FIGURE. 131 shows the SoC comparison between offline, online simulation and experiment. The experimented follows the online curve except at the beginning of the run and at end of the charging.

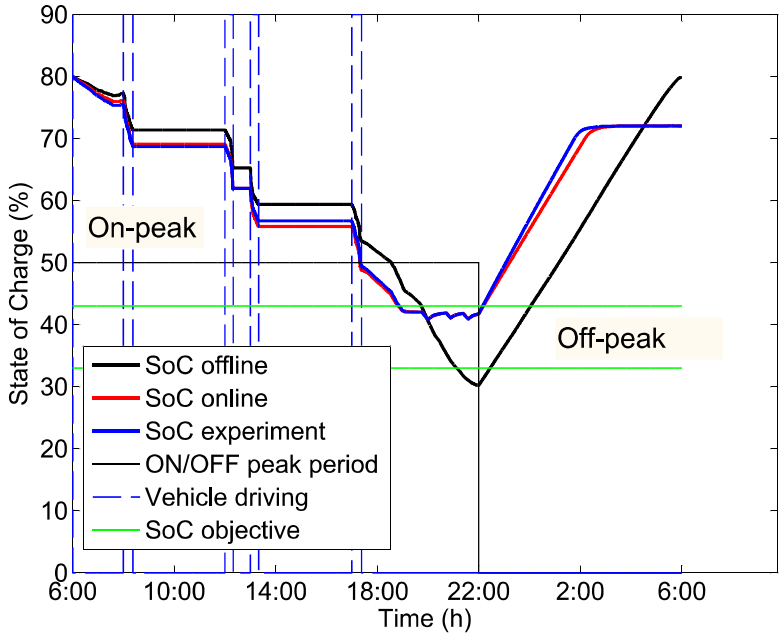

Figure 131. SoC profile comparison between the online, the offline simulation and experiment for the summer case with an initial SoC of 80 %

The morning difference is due to the inaccuracy of the DC load. Indeed the DC load is set for a large power range (until 36 kW) and the the power dissipate in the DC load is a quarter of 700 W as shown in FIGURE. 133 (b)

The charging difference (FIGURE. 133 (e)) is due to the charging method used. In this experiment the constant voltage method is used and the house controller gives the maximum power that the battery should get, whereas in the online simulation, the house controller gives exactly the power required

to charge the battery.

During the trips the battery power follows the reference due to the high power as shown in FIGURE. 133 (c). In addition, in the evening, during on-peak period, the reference and the battery power is similar as depicted in FIGURE. 133 (d).

FIGURE. 132 shows the evolution of the cost for the conventional and the micro-grid systems. The cost of the micro-grid system is divided into two costs: the ICE cost and the grid cost.

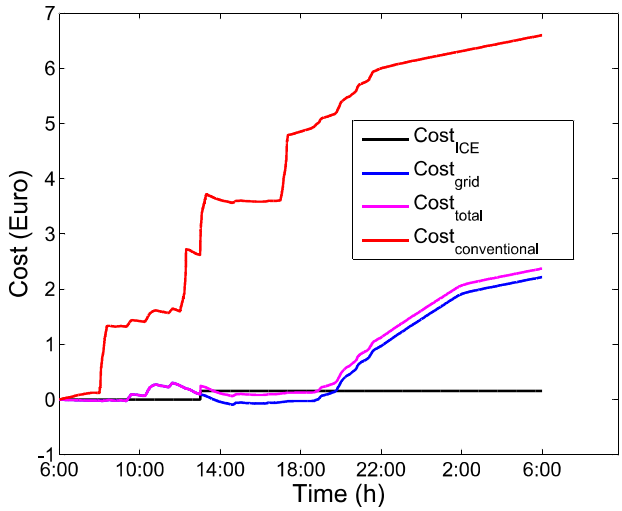

Figure 132. Energy cost (conventional, ICE, grid and total micro-grid) for the summer case with an initial SoC of 80 %

TABLE. 20 presents the cost comparison between the convention system, the two simulations offline and online and the experiment. It has been shown that the cost reduction in offline case is 62 %, in online case is 60 % and in experiment case 64 %. The experiment result is higher than the offline simulation due at the inaccuracy between the reference and the battery power in the morning. Indeed, the difference is sold to the grid. In addition the selling price is higher than the buying price, that explains the difference cost.

	Conventional system	Micro-grid system (online)	Micro-grid system (offline)	Micro-grid system (experiment)
Grid cost	1.92 €	2.55 €	2.41 €	2.22 €
Fuel cost	4.68 €	0.08 €	0.11 €	0.16 €
Total cost	6.60 €	2.63 €	2.52 €	2.38 €

Table 20. Experimental summer results for a fully charged battery

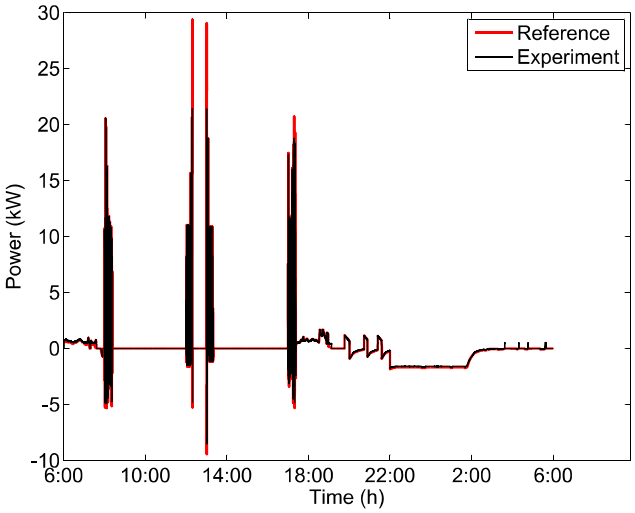

(a) Full comparison between reference and battery power

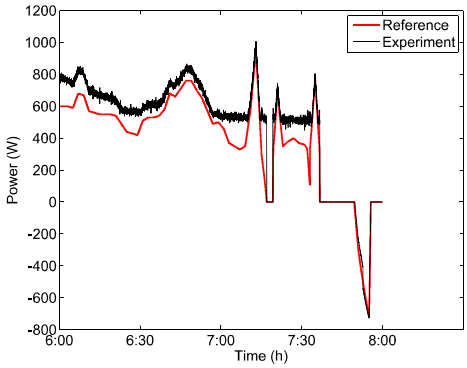

(b) Morning zoom in

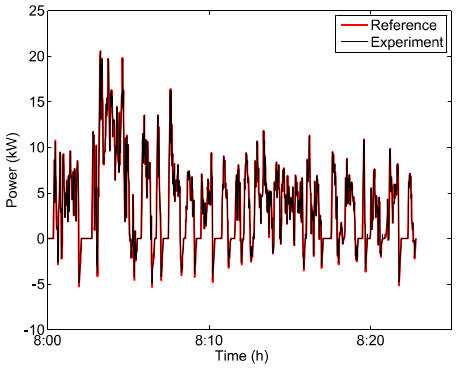

(c) 1st trip zoom in

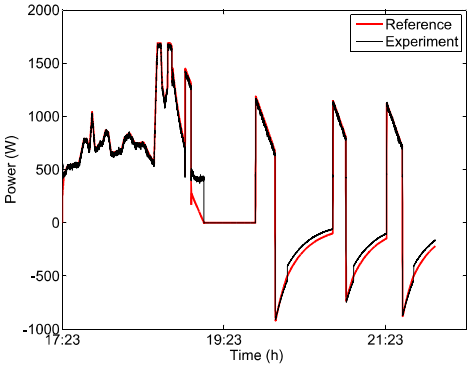

(d) On-peak zoom in

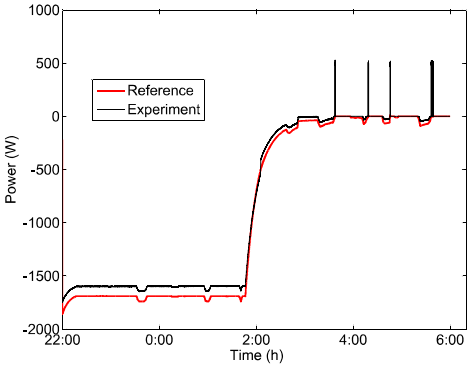

(e) Off-peak zoom in

Figure 133. Comparison between reference and battery power for the summer case with an initial SoC of 80 %

The next section presents the winter case where the battery is fully charged at the beginning of the run.

5.3.2 *Winter case*

FIGURE. 134, FIGURE. 135 and FIGURE. 136 shows the SoC comparison, the cost evolution during the day and comparison between the controllers and the battery power respectively.

FIGURE. 134 shows the SoC comparison between the offline and online simulation and the experiment. The experiment SoC is between the offline and the online SoC. Indeed, in the morning the battery helps the grid to meet the household loads. The difference is due to the accuracy of the battery model which calculates the voltage and the current, whereas in the experiment the battery voltage and current are directly measured.

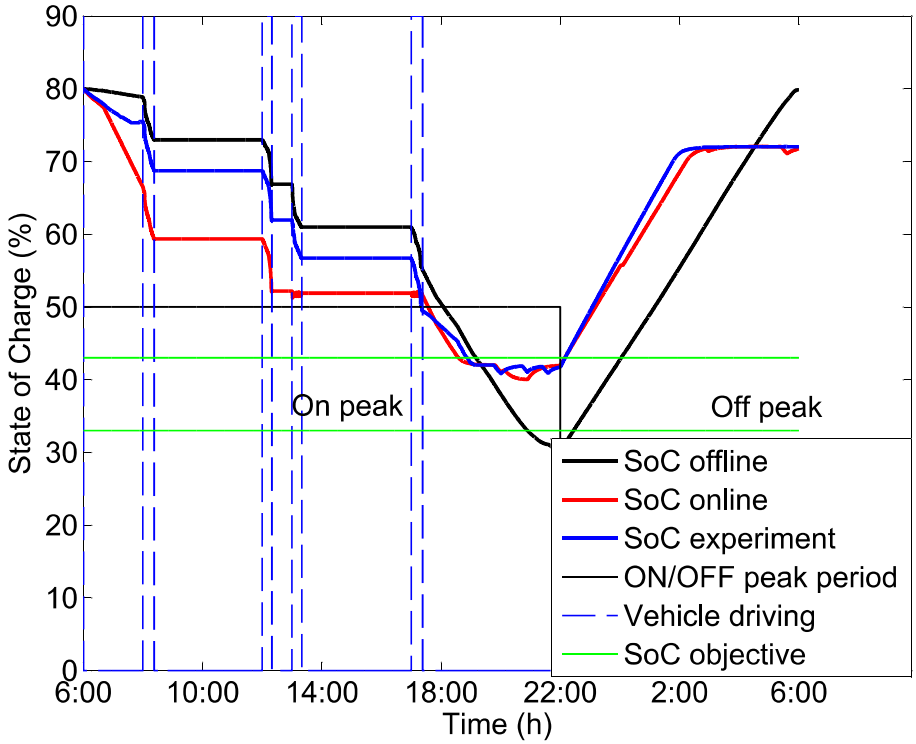

Figure 134. SoC profile comparison between the online, the offline simulation and experiment for the winter case with an initial SoC of 80 %

FIGURE. 135 shows the cost evolution of the convention and micro-grid system (total cost) including the ICE and grid cost in this system. The ICE has been used in the second and third trip which impacts the total energy cost of the micro-grid system.

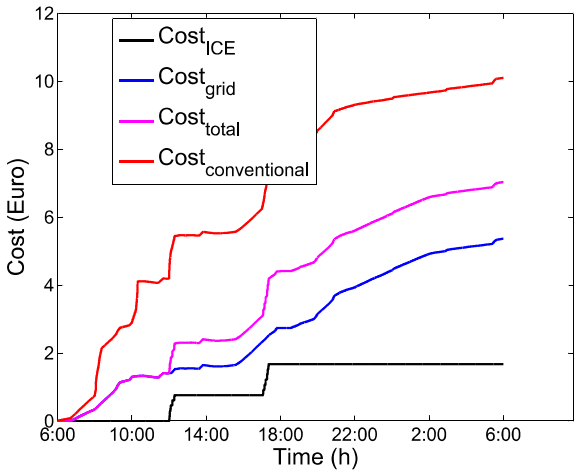

Figure 135. Energy cost (conventional, ICE, grid and total micro-grid) for the winter case with an initial SoC of 80 %

TABLE. 21 presents the total cost of the conventional, online, offline and experiment systems. It shows that the offline simulation reduces the cost by 40 % whereas the online simulation reduces it by 27 %. The experiment reduces the total cost by 29 % compared to the conventional system.

	Conventional system	Micro-grid system (online)	Micro-grid system (offline)	Micro-grid system (experiment)
Grid cost	5.41 €	5.69 €	5.90 €	5.54 €
Fuel cost	4.68 €	1.71 €	0.11 €	1.67 €
Total cost	10.09 €	7.40 €	6.01 €	7.21 €

Table 21. Experimental winter results for a fully charged battery

FIGURE. 136 shows that the battery power is similar to the reference given by the controllers. The same problem as in the previous case appears at off-peak period as presented in FIGURE. 136 (c), the battery charging takes into account the constant voltage method to charge the battery.

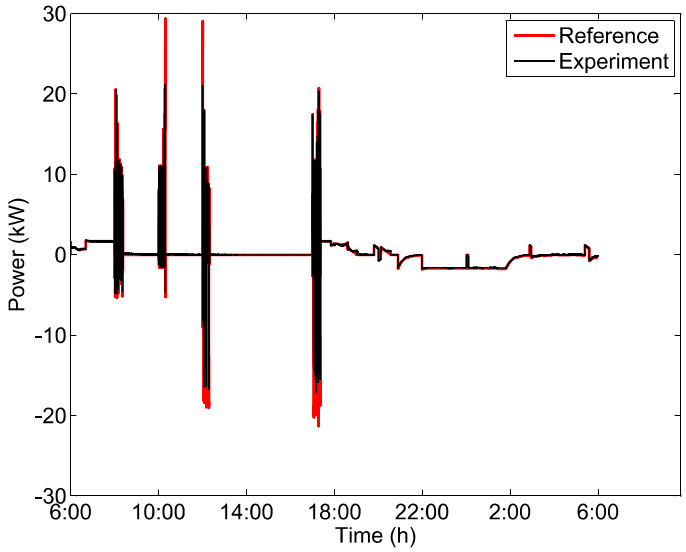

(a) Full comparison between reference and battery power

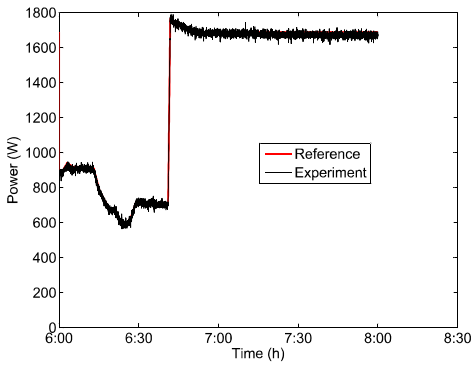

(b) Morning zoom in

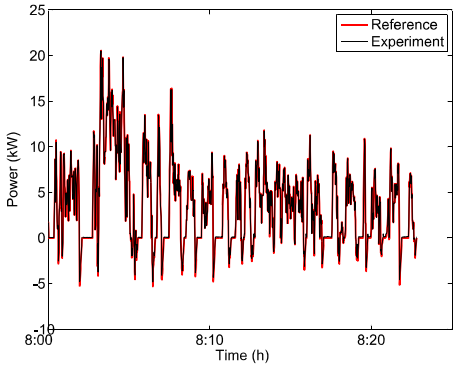

(c) 1st trip zoom in

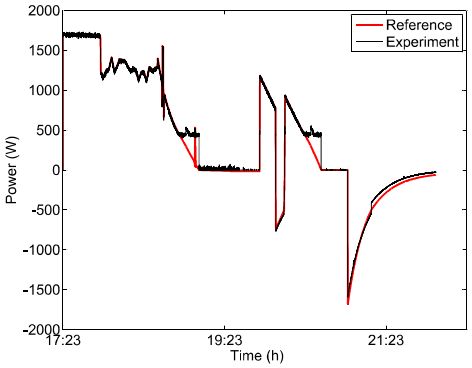

(d) On-peak zoom in

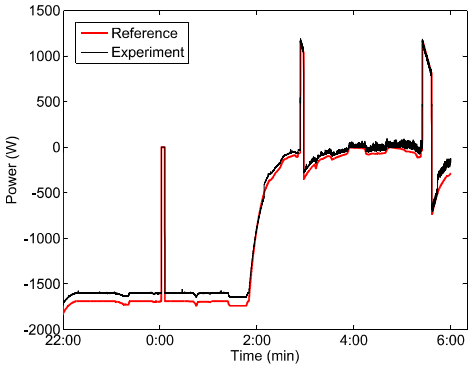

(e) Off-peak zoom in

Figure 136. Comparison between reference and battery power for the winter case with an initial SoC of 80 %

This section has presented two case studies: in sumer and in winter

where the runs start with a fully charged battery. The results show that the experimental SoC is very similar to the online simulation. A significant cost reduction is presented: in summer the cost reduction is 65 % whereas in winter the cost reduction is 29 %.

5.4 CONCLUSION

This chapter has presented the test set-up that was used to validate the two controllers : house and PHEV. A Labview® program was implemented to manage the DC active load using the GPIB communication protocol. User interface was designed to display the scenario, the power and the SoC profiles and the cost in real time.

Summer and Winter cases have been presented and compared to the two previous simulations: online and offline. It has been shown that the cost reduction for the summer case is 64 % and the for the winter case is 29 %. In addition, it has been shown that the two controller references and the battery power are similar and give acceptable results.

CONCLUSION AND FUTURE WORK

This research presented a need for a solution to the problem of climate change, by integrating PHEV and EV with the grid. Indeed, the energy production increases day-by-day, and with the introduction of EV/PHEV as a new load; battery does not solve the problem during peak consumption. However, it can be used as an external storage, which can help the grid to meet the household loads by decreasing the peak loads.

The objective was to minimize the energy cost of a real household including local renewable energy sources and a PHEV. This objective was part of a larger NSERC project entitled "Smart Net-Zero Energy Buildings Strategic Research Network".

The first step was to find a global optimization to find the minimum cost of a day using the NZEH named ÉcoTerra. Chapter 3 presented the dynamic programming algorithm which was used to find the reference cost. The objective and constraints were described. Summer and winter cases were discussed using three sub cases: the simulation starts with a fully charged battery with and without renewable energy sources and, where it starts with a fully discharged battery with renewable energy sources. It has be shown that the cost reduction over an year is about 46 % using the micro-grid system.

The second step was to build two controllers, one located in the house and the other in the PHEV. The two controllers are linked with the SoC objective value, which calculated the required battery SoC in the evening when the PHEV is connected. The controllers are based on fuzzy logic algorithm and the full control was presented in chapter 4. The PHEV controller is based on the ICE size and the battery limitations, whereas the house controller parameters are the bidirectional charger size and the electricity price system. The simulation result shows that over a year the micro-grid system reduces the cost by 44 %.

The last step was to implement the two controllers in a test set-up. Chapter 5 presented the set-up and it showed a similar cost reduction as the online simulation. This cost reduction for the summer case is about 64 % for the experiment versus 60 % for the online simulation and for winter case the cost reduction is about 29 % for experiment versus 27 % for the online simulation.

In conclusion, the micro-grid system reduced the energy cost of a household. However this study has not taken into account the cost installation of renewable energy sources, the bidirectional battery charger and the PHEV cost. In addition, it has been shown that the smart-grid system is adaptable according to the number or renewable energy sources. Moreover, the architecture of the PHEV (series, parallel or complex) does not make a difference to the house controller. However, the PHEV controller has to be adapted.

The plug-in wired charging method was assumed in this research. However, a wireless charger is recommended, which ensures the connection of the vehicle to the micro-grid when the PHEV is at home.

Contributions

The contributions of this thesis to the PHEV and micro-grid control strategy field are:

- *Adaptive PHEV controller*: the PHEV is built according to the ICE operation map and the battery limitations, then it can be adapted with different ICE and battery,

- *Include the V2H capability*: the PHEV controller includes the V2H capability by using the SoC objective value and then, the PHEV controller parameter has to be updated every day according this value,

- *Micro-grid control strategy*: a full energy control strategy including local renewable energy sources, PHEV has been designed and validated on a test bench,

- *Battery charging according to on and off peak period*: a real time control strategy taking into account the battery charging during off-peak time,

- *Adaptive house controller*: the house controller is adaptive according the battery charger, the number of local renewable energy sources.

Publications

The contributions of this research has been presented in several publications:

- *Book chapter contribution:*

  Chapter 9, **EV's and PHEVs for Smart Grid Application** in the book **Energy Management Strategies for Electric and Plug-in Hybrid Electric Vehicles,** Sheldon S. Williamson, Springer, 2013

- *International Conference with proceeding:*

  M. Kabalo, F. Berthold, B. Blunier, D. Bouquain, S. Williamson, A. Miraoui, **Efficiency Comparison of Wire and Wireless Battery Charging: Based on Connection Probability Analysis**, *IEEE Transportation Electrification Conference and Expo (ITEC14)*, 2014

  S. Rao, F. Berthold, K. Pandurangavittal, B. Blunier, D. Bouquain, S. Williamson, A. Miraoui, **Plug-in Hybrid Electric Vehicle energy system using Home-to-Vehicle and Vehicle-to-Home: Optimization of power converter operation**, *IEEE Transportation Electrification Conference and Expo (ITEC13)*, 2013

F. Berthold, B. Blunier, D. Bouquain, S. Williamson, A. Miraoui, **Offline and Online Optimization of Plug-in Hybrid Electric Vehicle Energy Usage (Home-to-Vehicle and Vehicle-to-Home)**, *IEEE Transportation Electrification Conference and Expo (ITEC12)*, 2012

F. Berthold, B. Blunier, D. Bouquain, S. Williamson, A. Miraoui, **PHEV Control Strategy Including Vehicle-to-Home (V2H) and Home-to-Vehicle (H2V) functionalities**, *Vehicle Power and Propulsion Conference (VPPC11)*, 2011

– *Canadian Conference with proceedings:*

F. Berthold, B. Blunier, D. Bouquain, S. Williamson, Y. Chen, A Athienitis, A. Miraoui, **Optimization of a Battery Charging Schedule in a Net Zero Energy House using Vehicle-to-Home functionality**, *eSim14*, 2014

F. Berthold, B. Blunier, D. Bouquain, S. Williamson, A. Miraoui, **Household Cost Optimization (Grid, Battery, Vehicle-to-Home and Home-to-Vehicle)**, *Cimate Change Technology conference (CCTC13)*, 2013

C. Desai, F. Berthold, S. Williamson, **Plug-in Hybrid Electric Transit Bus Parameters Sizing Using Multi-Objective Genetic Algorithm**, *Electrical Power and Energy Conference (EPEC10)*, 2010

– *French Conference with proceedings:*

F. Berthold, B. Blunier, D. Bouquain, S. Williamson, A. Miraoui, **Gestion d'énergie d'un véhicule hybride rechargeable connecté à une maison**, *Young researcher Seminar (IngéDoc11)*, 2011

F. Berthold, B. Blunier, D. Bouquain, S. Williamson, A. Miraoui, **Gestion d'énergie d'un véhicule hybride rechargeable intégrant les fonctionnalités d'achat (grid/home to vehicle) et de revente (vehicle to grid/home) de l'énergie**, *Électrotechnique du Futur (EF11)*, 2011

Future work

The future work is divided into two categories: improvement of the experimented set up,and adding features to the micro-grid system.

Experiment

1. A bidirectional AC/DC converter has to be implemented to complete the experiment set-up. The converter chosen is ZEMIS-PM3AC10-11, which links the grid to the battery and is available at the laboratory in UTBM.

2. The interface which generates the scenario can be modified to add the weekly feature. Indeed, to test the micro-grid system on a daily scenario is not enough. A weekly scenario would allow the verification of the battery behavior.
3. A Battery Management System (BMS) has to be implemented to improve the SoC accuracy calculation and also to equalize the cells. The BMS is under development at laboratory in UTBM. Cell balancing improves the life of the battery. The battery lifetime can be used as a parameter in the control strategy. Evaluating the SoH is difficult because of the number of losses. As presented in [47], the losses can be reversible or irreversible due to aging and cycling. Since the battery is expensive, the SoH has to be added as new membership function in the fuzzy logic controllers: in the house and in the PHEV to extend the lifetime.

Micro-grid system

1. Optimized the SoC objective window. Indeed, in this research a $\pm 5\,\%$ window has been assumed, but this value can be optimized to have better results in terms of cost especially in winter.
2. The micro-grid system can be improved by shifting some household loads. Indeed, e.g. the washer, dryer, dishwasher load can be optimal shifted to smoothen the energy demand. A new energy controller has to be designed to manage these high energy appliances. Moreover, a priority appliance list can be set to optimally manage the energy according to the comfort of the household.
3. Another improvement is on the electricity price. In fact, in this research only a on and off peak period has been taken into account. However, the electricity cost vary during the day depending on the energy mix. For instance, according to [69], in 2010, 56.42 \$ US/MWh, 286 \$ US/MWh and 90.20 \$ US/MWh, are the cost of generating nuclear, solar power and onshore wind power respectively for utility generation.
4. The battery charging at work place or market place can be added to the control strategy, to have a higher level of SoC, when the PHEV reaches home and a new topology has to be designed to allow this new feature.
5. Energy storage systems such as hydrogen can be added to the micro-grid system. Indeed, as shown in the results, the solar energy is only available when the PHEV is not connected. The solar energy is transfered to the grid instead of being sold during on-peak periods. This energy can also be transformed into hydrogen and used later in a fuel cell vehicle. This makes the micro-grid more autonomous and "greener". This aspect is studied in the MobyPost project [49] at UTBM.
6. A new feature can be added during outage, that allows the micro-grid to be isolated. Then, the battery can supply the household loads by priority, that ensures the comfort of occupants. The utility can warn the controller that an outage will happen, then the PHEV controller changes its mode to be able to supply the household loads. In this case, the

objective is not to reduce the cost, but to have a full battery when the PHEV reaches home.

7. The next step is to develop a smart grid system, by linking several micro-grids. According to IEEE a smart grid is "the next generation electrical power system that is typified by the increased use of communication and information technology in the generation, delivery and consumption of electrical energy". Therefore, the smart-grid system has to be implemented in a larger scale and communication between each micro-grid system has to be developed. Indeed, the results presented in this research, show that battery charging is controlled by the off peak price. Then, if in a same zone, every micro-grid system has the same, that means all available EV/PHEV will be charging at the same time which create a new peak. Therefore, there is a need to ensure smooth the global energy consumption in the smart-grid system. Moreover, the off-peak period can be adapted daily by communication of each other to optimize the battery charging schedule of each micro-grid system.

BIBLIOGRAPHY

[1] Développement durable Environnement Faune et Parcs, "Inventaire québécois des émissions de gaz à effet de serre en 2010 et évolution depuis 1990." (Cited on page 1.)

[2] European Environment Agency, "Distribution by sources of CO2 emissions in france in 2009." (Cited on pages ix and 1.)

[3] CITEPA/SECTEN, "CO2 emissions by method of transport in metropolitan france." (Cited on pages ix and 1.)

[4] K. Clement-Nyns, E. Haesen, and J. Driesen, "The impact of charging plug-in hybrid electric vehicles on a residential distribution grid," *IEEE Transactions on Power Systems*, vol. 25, no. 1, pp. 371 –380. (Cited on page 2.)

[5] "2013 chevy volt electric car." (Cited on pages 2 and 15.)

[6] International Energy Agency, "Energy production world." (Cited on pages ix and 3.)

[7] EDF, "L'utilisation de l'eau dans les centrales nucléaires," (Cited on page 3.)

[8] International Energy Agency, "Energy production france." (Cited on pages ix and 3.)

[9] International Energy Agency, "Energy production canada." (Cited on pages ix and 4.)

[10] Ressources naturelles et Faune, "Production d'électricité." (Cited on page 4.)

[11] Hydro Québec, "Hydro-québec en bref." (Cited on pages ix and 4.)

[12] Ministère de l'écologie, du Développement durable et de l'énergie, "Prix de vente moyens nationaux des carburants du 01/01/1990 au 31/12/2012," (Cited on pages ix and 5.)

[13] S. Merceron and M. Theulière, "Les dépenses d'energie des ménages depuis 20 ans : Une part en moyenne stable dans le budget, des inégalites accrues." (Cited on page 5.)

[14] International Energy Agency, "Technology roadmap: Electric and plug-in hybrid electric vehicles." (Cited on pages ix and 6.)

[15] International Energy Agency, "Energy technology perspectives 2011." (Cited on page 7.)

[16] J. Gireldez, R. Roche, S. Suryanarayanan, and D. Zimmerle, "A linear programming methodology to quantify the impact of PHEVs with v2g capabilities on distribution systems," in *2013 IEEE Green Technologies Conference*, pp. 8–15. (Cited on page 7.)

[17] K. Morrow, D. Karner, and J. Francfort, "Plug-in hybrid electric vehicle charging infrastructure review." (Cited on pages 7 and 29.)

[18] P. Denholm and W. Short, "An evaluation of utility system impacts and benefits of optimally dispatched plug-in hybrid electric vehicles," (Cited on page 7.)

[19] S. Wang, N. Zhang, Z. Li, and M. Shahidehpour, "Modeling and impact analysis of large scale v2g electric vehicles on the power grid," in *IEEE Innovative Smart Grid Technologies - Asia (ISGT Asia)*, pp. 1–6. (Cited on page 7.)

[20] M. Yilmaz and P. Krein, "Review of the impact of vehicle-to-grid technologies on distribution systems and utility interfaces," *IEEE Transactions on Power Electronics*, vol. 12, no. 28, pp. 5673–5689. (Cited on page 7.)

[21] A. K. Srivastava, B. Annabathina, and S. Kamalasadan, "The challenges and policy options for integrating plug-in hybrid electric vehicle into the electric grid," *The Electricity Journal*, vol. 23, no. 3, pp. 83–91. (Cited on page 7.)

[22] A. Ravey, B. Blunier, and A. Miraoui, "Control strategies for fuel-cell-based hybrid electric vehicles: From offline to online and experimental results," *IEEE Transactions on Vehicular Technology*, vol. 61, no. 6, pp. 2452–2457. (Cited on page 8.)

[23] X. Wu, B. Cao, J. Wen, and Y. Bian, "Particle swarm optimization for plug-in hybrid electric vehicle control strategy parameter," in *IEEE Vehicle Power and Propulsion Conference, 2008. VPPC '08*, pp. 1–5. (Cited on page 8.)

[24] H. Banvait, S. Anwar, and Y. Chen, "A rule-based energy management strategy for plug-in hybrid electric vehicle (PHEV)," in *American Control Conference, 2009. ACC '09.*, pp. 3938–3943. (Cited on page 8.)

[25] D. Bouquain, B. Blunier, and A. Miraoui, "A hybrid fuel cell/battery wheelchair - modeling, simulation and experimentation," in *IEEE Vehicle Power and Propulsion Conference, 2008. VPPC '08*, pp. 1–6. (Cited on page 8.)

[26] S. Li, S. Sharkh, F. Walsh, and C. Zhang, "Energy and battery management of a plug-in series hybrid electric vehicle using fuzzy logic," *IEEE Transactions on Vehicular Technology*, vol. 60, no. 8, pp. 3571–3585. (Cited on pages 8 and 81.)

[27] S. M. T. Bathaee, A. Gastaj, S. R. Emami, and M. Mohammadian, "A fuzzy-based supervisory robust control for parallel hybrid electric vehicles," in *Vehicle Power and Propulsion, 2005 IEEE Conference*. (Cited on pages 8 and 81.)

[28] A. Piccolo, A. Vaccaro, and D. Villacci, "Fuzzy logic based optimal power flow management in parallel hybrid electric vehicles," (Cited on page 8.)

[29] F. Khoucha, M. Benbouzid, and A. Kheloui, "An optimal fuzzy logic power sharing strategy for parallel hybrid electric vehicles," in *2010 IEEE Vehicle Power and Propulsion Conference (VPPC)*, pp. 1–5. (Cited on pages 8 and 81.)

[30] N. Li, L. Chen, and S. Low, "Optimal demand response based on utility maximization in power networks," in *2011 IEEE Power and Energy Society General Meeting*, pp. 1–8. (Cited on page 8.)

[31] M. Pedrasa, T. Spooner, and I. MacGill, "Coordinated scheduling of residential distributed energy resources to optimize smart home energy services," *IEEE Transactions on Smart Grid*, vol. 1, no. 2, pp. 134–143. (Cited on page 8.)

[32] K. Mets, T. Verschueren, W. Haerick, C. Develder, and F. De Turck, "Optimizing smart energy control strategies for plug-in hybrid electric vehicle charging," in *Network Operations and Management Symposium Workshops (NOMS Wksps), 2010 IEEE/IFIP*, pp. 293–299. (Cited on page 8.)

[33] Wikipedia, "La jamais contente." (Cited on pages ix and 12.)

[34] A. Moustacchi, "AUTOMOBILE - histoire." (Cited on page 12.)

[35] Wikipédia, "Toyota prius." (Cited on pages ix and 12.)

[36] Renault France, "Gamme véhicules électriques." (Cited on pages xiv and 14.)

[37] A. Emadi, K. Rajashekara, S. Williamson, and S. Lukic, "Topological overview of hybrid electric and fuel cell vehicular power system architectures and configurations," *IEEE Transactions on Vehicular Technology*, vol. 54, no. 3, pp. 763 – 770. (Cited on pages 15 and 17.)

[38] D. Bouquain, "Contribution à la modélisation et à l'optimisation des architectures de vehicules hybrides." (Cited on pages 15, 17, and 39.)

[39] Honda, "Specifications - 2014 honda insight hybrid." (Cited on page 19.)

[40] C. Desai, "Design and optimization of hybrid electric vehicle drivetrain and control strategy parameters using evolutionary algorithms." (Cited on page 20.)

[41] S. Moura, J. Siegel, D. Siegel, H. Fathy, and A. Stefanopoulou, "Education on vehicle electrification: Battery systems, fuel cells, and hydrogen," in *2010 IEEE Vehicle Power and Propulsion Conference (VPPC)*, pp. 1–6. (Cited on pages ix and 21.)

[42] I. Husain, *Electric and Hybrid Vehicles: Design Fundamentals, Second Edition*. CRC Press. (Cited on page 21.)

[43] D. Doerffel and S. Sharkh, "A critical review of using the peukert equation for determining the remaining capacity of lead-acid and lithium-ion batteries," *Journal of Power Sources*, vol. 155, no. 2, pp. 395–400. (Cited on page 21.)

[44] M. Chen and G. Rincon-Mora, "Accurate electrical battery model capable of predicting runtime and i-v performance," *IEEE Transactions on Energy Conversion*, vol. 21, no. 2, pp. 504–511. (Cited on pages 23 and 42.)

[45] M. Ehsani, Y. Gao, and A. Emadi, *Modern Electric, Hybrid Electric, and Fuel Cell Vehicles. Fundamentals, Theory, and Design SECOND EDITION*. CRC Press. (Cited on pages ix, xiv, 23, 28, 39, and 41.)

[46] N. Watrin, R. Roche, H. Ostermann, B. Blunier, and A. Miraoui, "Multiphysical lithium-based battery model for use in state-of-charge determination," *IEEE Transactions on Vehicular Technology*, vol. 61, no. 8, pp. 3420–3429. (Cited on page 24.)

[47] N. Watrin, B. Blunier, and A. Miraoui, "Review of adaptive systems for lithium batteries state-of-charge and state-of-health estimation," in *2012 IEEE Transportation Electrification Conference and Expo (ITEC)*, pp. 1–6. (Cited on pages 24 and 140.)

[48] B. Blunier, "Modélisation de moto-compresseurs en vue de la gestion de l'air dans les systèmes pile à combustible - simulation et validation expérimentale." (Cited on page 25.)

[49] A. Djerdir, "MobyPost: French public-private project to utilize solar produced hydrogen in postal delivery vehicles - IEEE transportation electrification initiative web portal," (Cited on pages 26 and 140.)

[50] I. Husain, *Electric and hybrid vehicles*. CRC Press. (Cited on page 26.)

[51] M. Daugherty and K. Leonard, "Ultracapacitors for renewable energy storage.". (Cited on pages ix and 26.)

[52] "Four-stroke engine." (Cited on pages ix and 27.)

[53] Alternative Energy, "Wind turbines - kinetic wind energy generator technology." (Cited on pages ix and 31.)

[54] "NSERC smart net-zero energy buildings strategic research network - accueil." (Cited on page 35.)

[55] "Smartgrid.gov." (Cited on page 36.)

[56] S. CMHC, "Equilibrium maison saine pour un environnement sain." (Cited on pages ix, 37, and 39.)

[57] Natural Resources Canada, "The r-2000 standard." (Cited on page 37.)

[58] M. Barnes, A. Athienitis, V. Delisle, J. Ayoub, and B. Berneche, "Net zero energy homes of the future: A case study of the écoterra house in canada," in *Renewable Energy Congress, Glasgow, Scotland*, p. 112. (Cited on pages ix and 38.)

[59] O. Tremblay, L.-A. Dessaint, and A.-I. Dekkiche, "A generic battery model for the dynamic simulation of hybrid electric vehicles," in *IEEE Vehicle Power and Propulsion Conference, VPPC 2007*, pp. 284–289. (Cited on page 42.)

[60] L. Gao, S. Liu, and R. Dougal, "Dynamic lithium-ion battery model for system simulation," *IEEE Transactions on Components and Packaging Technologies*, vol. 25, no. 3, pp. 495–505. (Cited on page 42.)

[61] J. An, B. Huang, Q. Kang, and M. Zhou, "PSO-based method to find electric vehicle's optimal charging schedule under dynamic electricity price," in *10th IEEE International Conference on Networking, Sensing and Control (ICNSC)*, pp. 913–918. (Cited on pages 45 and 86.)

[62] S. Rao, K. Pandurangavittal, F. Berthold, B. Blunier, D. Bouquain, S. S. Williamson, and A. Miraoui, "Plug-in hybrid electric vehicle energy system using home-vehcile and vehicle-to-home: Optimization of power converter operation," (Cited on page 52.)

[63] X. Liu, Y. Wu, and J. Duan, "Power split control strategy for a series hybrid electric vehicle using fuzzy logic," in *IEEE International Conference on Automation and Logistics, ICAL 2008*, pp. 481–486. (Cited on pages 55 and 81.)

[64] K. Çağatay Bayindir, M. Gözüküçük, and A. Teke, "A comprehensive overview of hybrid electric vehicle: Powertrain configurations, powertrain control techniques and electronic control units," *Energy Conversion and Management*, vol. 52, no. 2, pp. 1305–1313. (Cited on pages 55 and 81.)

[65] S. Wirasingha and A. Emadi, "Classification and review of control strategies for plug-in hybrid electric vehicles," *IEEE Transactions on Vehicular Technology*, vol. 60, no. 1, pp. 111–122. (Cited on pages 55 and 81.)

[66] O. Sundstrom and L. Guzzella, "A generic dynamic programming matlab function," in *Control Applications,(CCA) & Intelligent Control,(ISIC), 2009 IEEE*, pp. 1625–1630. (Cited on pages 55 and 57.)

[67] Q. Yan, I. Manickam, M. Kezunovic, and L. Xie, "A multi - tiered real - time pricing a lgorithm for electric vehicle charging stations," in *2014 IEEE Transportation Electrification Conference and Expo (ITEC)*. (Cited on page 86.)

[68] M. Kabalo, F. Berthold, B. Blunier, D. Bouquain, S. S. Williamson, and A. Miraoui, "Efficiency comparison of wire and wireless battery charging: Based on connection probability analysis." (Cited on page 122.)

[69] International Energy Agency and OECD Nuclear Energy Agency, *Projected costs of generating electricity*. International Energy Agency, Nuclear Energy Agency, Organisation for Economic Co-operation and Development. (Cited on page 140.)